Redox Properties of Sorbed Natural Organic Matter

Dissertation

der Mathematisch-Naturwissenschaftlichen Fakultät

der Eberhard Karls Universität Tübingen

zur Erlangung des Grades eines

Doktors der Naturwissenschaften

(Dr. rer. nat.)

vorgelegt von

Lic. Edisson Reinaldo Subdiaga Rondon

aus Tovar Stadt, Venezuela

Tübingen

2018

Gedruckt mit Genehmigung der Mathematisch-Naturwissenschaftlichen Fakultät der
Eberhard Karls Universität Tübingen.

Tag der mündlichen Qualifikation:	<u>24</u> . <u>10</u> . <u>2018</u>
Dekan:	Prof. Dr. Wolfgang Rosenstiel
1. Berichterstatter:	Prof. Dr. Stefan B. Haderlein
2. Berichterstatter:	Dr. Silvia Orsetti

To Dilcia and Reinaldo…

Acknowledgments

Abstract

Natural organic matter (NOM) is a complex mixture that originates from the decay of organic residues from plants and microbial sources. NOM, typically present in sorbed state as mineral coating or in particulate form rather than in solution, plays a key role in biogeochemical processes, i.e., electron shuttling between redox active minerals and bacteria. The main goal of this work was to investigate the influence of sorption of NOM on its redox properties (namely, electron exchange capacities (EEC) and redox state). Given the inherent heterogeneity of NOM, sorption of natural organic matter to mineral surfaces might induce changes in the redox properties of NOM fractions (sorbed vs. aqueous). Moreover, the electron transfer between redox active moieties in NOM and mineral surfaces might also alter its redox properties.

Batch sorption experiments with standard humic acids (HA) isolates at defined redox states and redox-inert sorbents (Al_2O_3 and DAX-8 resin) were conducted. Mediated electrochemical approaches were applied to determine the Electron -Accepting (EAC) and -Donating (EDC) Capacities of HA fractions (dissolved, aqueous and in suspension). Adsorption of native HA onto Al_2O_3 resulted in large decreases in EEC of HA filtrates, while the EDC of sorbed HA increased significantly. These findings are consistent with preferential sorption of redox active components (e.g., quinone/hydroquinone, phenols) in HA. The increase in EDC of sorbed HA might be linked to: i) conformational changes of HA moieties on the Al_2O_3 surface or/and ii) surface catalyzed polymerization of polyphenol compounds under oxidizing conditions. The latter hypothesis was confirmed by up to 50% increase in EDC of a polyphenolic compound sorbed to Al_2O_3. Sorption of HA to DAX-8 had little effects on the EEC of HA fractions. Furthermore, sorption of electrochemically reduced HA to Al_2O_3 led to slightly lower EEC of HA in suspensions. Strong depletion of aromatic components in aqueous fractions of reduced HA caused large decreases in EEC.

In addition to mediated electrochemical approaches, molecular scale (high-field Fourier Transform Ion Cyclotron Resonance Mass Spectrometry; FT-ICRMS) methods were applied to investigate the changes in electrochemical properties and the concomitant changes in chemical composition of HA fractions upon sorption. FT-ICRMS analysis provided clear evidence of preferential sorption of tannin-like compounds (rich in polyphenolic groups) onto Al_2O_3.

Moreover, sorption of Pahokee Peat HA standard isolate (PPHA) on Na-saturated montmorillonite (Na-SWy-2) was studied at pH 7. While the EEC of PPHA in aqueous phase after sorption decreased up to 60 % compared to PPHA stock solution, the adsorbed fraction became more oxidized (up to 70 % lower EDC). This was associated to preferential sorption of redox active functional groups and/or electron transfer between Fe(III) in Na-SWy-2 and electron donor groups in PPHA.

This study demonstrates that sorption of NOM considerably influences its redox properties to various degrees depending on the characteristics of the sorbent and the occurrence of electron transfer reactions. These effects can be related to molecular scale processes at the NOM-mineral interface. Considering that NOM in soil and groundwater is usually present in sorbed state, these findings are fundamental for an improved understanding of biogeochemical processes involving NOM. Additional work is needed to confirm the effects of sorption of NOM on its redox properties as well as the additivity of changes in EEC of NOM upon sorption to Fe-bearing minerals.

Zusammenfassung

Natürliches organisches Materie (NOM) ist ein komplexes Gemisch, das durch den Abbau organischer Überreste von Pflanzen und mikrobiellem Material entsteht. NOM liegt überwiegend in sorbiertem Zustand als Mineralüberzug oder in partikulärer Form und nur ein kleiner Anteil in gelöster Form vor. Es spielt eine Schlüsselrolle in biochemischen Prozessen wie z.B. beim Elektronentransfer zwischen redoxaktiven Mineralen und Bakterien. Das Ziel der vorliegenden Arbeit war, den Einfluss von Sorption von NOM auf seine Redoxeigenschaften (d.h. Elektronenaustauschkapazität (EEC) und Redoxzustand) zu untersuchen. Angesichts der Heterogenität von NOM könnte die Sorption an Mineraloberflächen Änderungen der Redoxeigenschaften der sorbierten bzw. der wässrigen NOM-Fraktionen hervorrufen. Außerdem könnte auch der Elektronentransfer zwischen Mineraloberflächen und redoxaktiven Bestandteilen in NOM dessen Redoxeigenschaften ändern.

Es wurden Batch-Sorptionsexperimente mit Isolaten von Standardhuminsäuren (HA) mit definierten Redoxzuständen und redox-inerten Sorbentien (Al_2O_3 und DAX-8-Harz) durchgeführt. Die Elektronenakzeptor und –donorkapazität (EAC bzw. EDC) der HA-Fraktionen (gelöst, wässrig und in Suspension) wurde mit Hilfe der „Mediated Electrochemical Analysis" quantifiziert. Bei der Adsorption von natürlicher HA an Al_2O_3 verringerte sich die EEC der HA-Filtrate stark, während sich die EDC der sorbierten HA signifikant erhöhte. Diese Ergebnisse stehen im Einklang mit der bevorzugten Sorption von redoxaktiven Komponenten in HAs (z.B. Chinon/Hydrochinon, Phenole). Der Anstieg der EDC von sorbierten HA hat zwei mögliche Ursachen: i) konformative Änderungen von HA-Bestandteilen auf der Al_2O_3-Oberfläche und/oder ii) oberflächenkatalysierte Polymerisierung von Polyphenolbestandteilen unter oxidierenden Bedingungen. Bei der Sorption eines polyphenolische Modellverbindung auf Al_2O_3 wurde ein Anstieg der EDC um bis zu 50 % beobachtet, wodurch die zweite (ii) Hypothese bestätigt wurde.

Die Sorption von HA auf DAX-8-Harz hatte nur geringe Effekte auf die EEC der HA-Fraktionen. Die Sorption von elektrochemisch reduzierten HA auf Al_2O_3 führte zu leicht verringerter EEC der HA in Suspension. Durch starke Abreicherung von aromatischen Bestandteilen in der wässrigen Fraktion der reduzierten HA wurde eine große Abnahme der EEC hervorgerufen.

Zusätzlich zu der „Mediated Electrochemical Analysis" wurden auch Analysemthoden auf der molkularen Skala (high-field Fourier Transform Ion Cyclotron Resonance Mass Spectrometry; FT-ICRMS) verwendet, um die durch Sorption hervorgerufenen Änderungen der elektrochemischen Eigenschaften und die einhergehenden Veränderungen in der chemischen Zusammensetzung der HA-Bestandteile zu untersuchen. Die Analyse mittels FT-ICRMS weist klar auf bevorzugte Sorption von Tannin-ähnlichen Bestandteilen (reich an Polyphenol-Gruppen) auf Al_2O_3 hin.

Die Sorption von Pahokee Peat Huminsäure (PPHA) auf Na-gesättigtem Montmorillonit (Na-SWy-2) wurde bei pH 7 untersucht. Während die EEC von PPHA in wässriger Phase nach der Sorption im Vergleich zur PPHA-Stammlösung um 60 % abnahm, wurde die adsorbierte Fraktion oxidierter (bis zu 70 % niedrigere EDC). Dies hing mit der bevorzugten Sorption von redoxaktiven funktionellen Gruppen und/oder Elektronentransfer zwischen Fe(III) in Na-SWy-2 und elektronenabgebenden Gruppen in der PPHA zusammen.

Die vorliegende Studie zeigt, dass die Sorption von NOM deren Redoxeigenschaften, abhängig von den Eigenschaften der Sorptionsmaterialien und dem Auftreten von Elektronentransferreaktionen, unterschiedlich stark beeinflussen kann. Diese Effekte können mit molekularen Prozessen an der Grenzfläche in Zusammenhang gebracht werden.

Da NOM in Böden und dem Grundwasser üblicherweise in sorbiertem Zustand vorkommt, sind die Ergebnisse dieser Arbeit fundamental für ein verbessertes Verständnis der biogeochemischen Prozesse bei denen NOM eine Rolle spielt. Weiterführende Studien sind nötig, um die Effekte der Sorption von NOM auf ihre Redoxeigenschaften und die Additivität der Änderung der EEC bei der Sorption von NOM auf Fe enthaltende Minerale zu bestätigen.

Table of Contents

List of Figures

fractions of oxygen and sulfur atoms involved in the π-bond structures of the molecule.[60]

Figure SI1. Emission-Excitation Fluorescence Spectra (EEM) of Elliott Soil Humic Acid (ESHA) for: a) native ESHA stock solution (^{nat}ESHA$_{stock}$), b) reduced ESHA stock solution (^{red}ESHA$_{stock}$), c) native ESHA in aqueous phase (^{nat}ESHA$_{aq}$) after ~ 50%

List of Tables

Chapter 1.

1. Introduction

1.2 Background

Natural Organic Matter (NOM) originating from the decomposition of organic biomolecules from plants and microbial sources[1-3] is ubiquitous in soils, sediments and aquifers. The structure and physicochemical properties of NOM are determined by its source, formation history, and climatic conditions.[4-5] NOM exhibit different biogeochemical relevant functions in the environment such as electron shuttling in microbial processes, fate and transformation of pollutants, nutrient sorption and metal mobility as reported in many studies.[6-10] Most of these studies investigated the implications of the presence of NOM in comparison with NOM free systems; however, neither its redox properties (namely, electron exchange capacities and redox state) nor its speciation (sorbed vs. dissolved) have been investigated so far.

In soils, sediments and groundwater, a major fraction of the organic carbon is typically present in sorbed state as mineral coating or in particulate state rather than in aqueous phase. It has been reported that the formation of organo-mineral interactions might be crucial for NOM stabilization.[11-14] Even though many studies focused on the effect of environmental factors on NOM sorption onto minerals and other solid phases are available, very limited research can be found regarding the potential for alterations in redox properties of NOM as consequence of NOM sorption to mineral phases. This PhD thesis has been designed to systematically investigate: i) the effects of redox state of NOM on its sorption behavior, ii) alterations in redox properties and speciation of NOM as a result of sorption to redox inert sorbents, iii) the effects of NOM sorptive fractionation on its redox properties, and iv) the influence of the intrinsic electron transfer characteristics of the sorbent (inert vs. active) on the redox properties of NOM.

1.3 Redox properties of NOM

NOM is comprised of heterogeneous mixture of countless polyfunctional organic compounds present in soils, sediments and aquifers.[1, 15-18] Its composition and structure is defined by the ecosystem history, implying a certain uniqueness of each NOM sample.[19-22] Owing to its particular chemical complexity, diverse classes of organic

compounds (e.g., black carbon, nucleic acids, amino acids, carboxylic acids, carbohydrates, condensed aromatics, lipids, lignin and tannins) have been identified in various NOM isolates.[19,23-24] Humic substances (HS) derived from terrestrial and aquatic plants comprise up to 50% of the dissolved organic carbon in NOM.[25-26] Humic substances are operationally divided into different sub-fractions, according to their pH-dependent aqueous solubility including: (i) fulvic acid (FA), which is soluble in the entire pH range, (ii) humic acid (HA), which is insoluble at low pH containing highly aromatic carboxylic acid and phenolic moieties, and (iii) humin, which is insoluble at any pH given its high molecular weight (**Fig. 1a**).
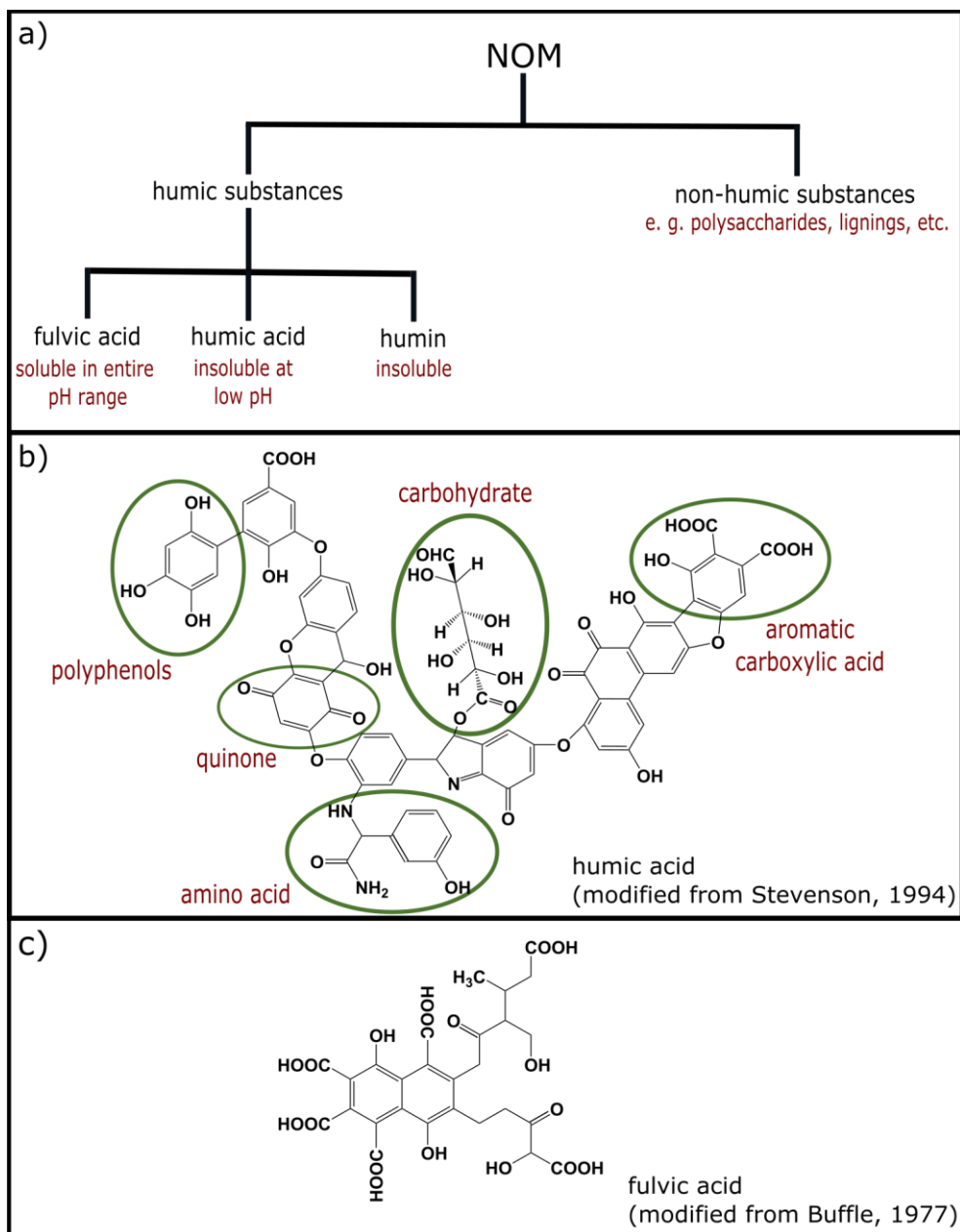
Figure 1. a) Operational classification of humic substances; **b)** proposed generic structure of Humic Acid (HA, modified from ref. 19); **c)** proposed generic structure of Fulvic Acid (FA, modified from ref. 27).

26

Due to its inherent heterogeneity, the redox potential (E^0_H) of a NOM sample is not a discrete value rather it covers a distribution of potentials; for humic acids, their E^0_H has been reported to range from + 150 mV to – 300 mV vs. SHE.[28-29] The redox activity within purified NOM has been ascribed primarily to quinone-hydroquinone groups (**Fig. 2**) and polyphenols.[30-36] Due to their prominent redox activity, humic substances have important biogeochemical functions such as redox buffering in microbial respiration processes[37-39] and redox transformation of organic pollutants.[8,10] The prominent redox activity of NOM in biogeochemical processes has generated great interest in the scientific community to determine the electron -accepting (EAC) and -donating (EDC) capacities of NOM (e.g., the amount of electrons that NOM can either accept or donate per weight unit). The sum of the EAC and EDC values of a given NOM sample corresponds to the total electron exchange capacities (EEC = EAC + EDC), which is a measure of the total number of redox active sites in the sample (**Fig. 2**).
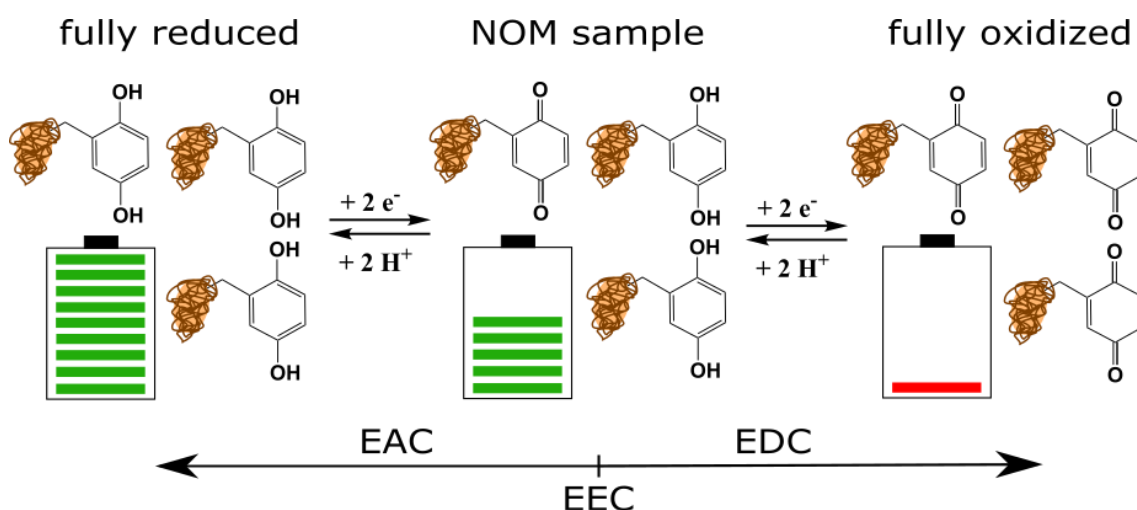
Figure 2. Electron -accepting (EAC) and -donating capacities (EDC) of a NOM sample depicted by the reversible redox reaction of hydroquinone/quinone couples, along with analogy to charging and discharging of a battery in terms of EDC. The total electron exchange capacities (EEC = EAC + EDC) correspond to the sum of capacities to accept and donate electrons.

The electron exchange capacities of HS can be determined by applying several approaches. Traditional methods to measure the EAC and EDC of HS rely on indirect quantification by wet chemical redox reactions (redox titrations) after sample treatments with reductants or oxidants (e.g., Zn^0, H_2S, H_2/Pt, hexacyanoferrate, etc.).[32, 40-42] Besides on depending on indirect measurements, the electron transfer associated to such reductants-oxidants is pH dependent, very time consuming, destructive and not versatile regarding measured redox potential. Another critical issue associated to these treatments is that they might induce side reactions, making the outcome susceptible to artifacts that diminish the accuracy, robustness and comparability of such indirect approaches.[43] These limitations can be overcome by using recent mediated electrochemical techniques, which offer quick, effective and pH-independent electron transfer reactions to and from HS mediated by radical compounds and, most important, direct characterization, since the

amount of electrons transferred is tracked by chronocoulometry.[43] Given the potential of mediated electrochemical analyses to assess the effect of NOM sorption on its redox properties throughout this PhD work, a detailed description of this technique is provided in section 1.4.

1.4 Mediated Electrochemical Analysis

Mediated electrochemical analysis provides an advantageous approach to quantify the electron exchange capacities and redox state of relevant organic geochemical phases and minerals (e. g., NOM isolates, iron-bearing clay minerals, plant biomass-derived black carbon (biochar), iron (oxyhydr-)oxides and clay-rich sediments).[29,35,43-53] In these electrochemical experiments, redox active compounds (redox mediators) are added to the electrochemical cell in solution to enhance the electron transfer from/to the redox active functional groups in NOM or metal-bearing minerals to/from the working electrode at defined reaction potentials. In order to generate accurate and robust results, the redox mediators must provide: i) fast and reversible redox reaction and equilibration with the working electrode, ii) well-defined standard reduction potentials, iii) well-known electron and proton (H^+) stoichiometry upon reduction-oxidation reactions, iv) pH-independent redox potentials, and v) high solubility in aqueous solutions and stability during the whole course of the experiment.[43,52,54] There are several suitable redox mediators (**Table 1**) used to quantify the electron exchange capacities of biogeochemical phases, including the apparent standard reduction potential ($E_H^{0'}$) of such mediators at pH 7. In these techniques, two systematic procedures are followed: mediated electrochemical reduction (MER) and mediated electrochemical oxidation (MEO), which provide direct quantification of the EAC and EDC capacities of such biogeochemical phases, respectively. The MER-MEO methodologies consist of using three electrode set-ups, which include an inert glassy carbon crucible working electrode that also serves as reaction cell, a silver/silver chloride (Ag/AgCl) reference electrode and a platinum (Pt) wire as auxiliary electrode immersed in buffered solution (**Fig. 3a**).

The amount of transferred electrons to and from the analyte can be quantified as reductive or oxidative current peaks. The EAC and EDC are calculated by integration of the baseline-corrected current peak of reductive current responses in MER (for EAC) or oxidative current peak in MEO (for EDC) and normalization to mass of the redox active analyte by using equation 1, where I_{MER} and I_{MEO} are the reductive and oxidative currents peaks (baseline-corrected) in MER and MEO, which give the amount of electrons transferred to/from the analyte after integration, F corresponds to the Faraday constant (F = 96485 s*A*mol^{-1}e$^-$), and $m_{analyte}$ is the mass of analyte spiked into the cell.

$$EAC = \frac{\int I_{MER}\, dt}{F * m_{analyte}} \qquad or \qquad EDC = \frac{\int I_{MEO}\, dt}{F * m_{analyte}} \tag{1}$$

By applying a constant reductive potential between the working and the reference electrodes ($E_H = -0.49$ V vs. SHE), in MER for instance, initially oxidized redox mediators

spiked to the electrochemical cell become reduced (e.g., $DQ^{2+} \rightarrow DQ^{\cdot+}$). Upon current equilibration over time, a small volume of the analyte is spiked into the reaction cell, and the previously reduced mediator rapidly reduces all redox active functional groups in the analyte, generating a stoichiometric amount of oxidized redox mediator (DQ^{2+}), which is readily re-reduced in the electrochemical cell, resulting in a current peak that is monitored between the working and the auxiliary electrodes with a potentiostat (**Fig. 3b**). The inverse redox mediation mechanism can be described in terms of MEO.

Table 1. Oxidized-reduced chemical structure, apparent standard reduction potential ($E_H^{0'}$) vs. standard hydrogen electrode (SHE), number of transferred electrons (e-) and protons (H^+) at pH 7 of suitable redox mediators used in mediated electrochemical analyses of relevant biogeochemical phases (NOM, plant biomass-derived black carbon (biochar), clay minerals, iron (oxyhydr-)oxides and clay-rich sediments). Modified from ref. 52.

Redox Mediator	Oxidized species	Reduced species	$E_H^{0'}$ [V]	e-	H^+
2,2′-azino-bis(3-ethylbenzothiazoline-6-sulfonic acid) (ABTS.+ / ABTS)			+ 0.70	1	0
Dimethylaminomethyl ferrocene			+ 0.59	1	0
Ferrocence monocarboxylic acid			+ 0.51	1	0
1,4-Naptoquinone			+ 0.09	2	2
Cyanoviologen			- 0.14	1	0
1,10-Ethylene-2,20-bipyridiniumdibromide monohydrate (Diquat)			- 0.30	1	0
4,4′-Bipyridinum-1,1′-bis(2-ethylsulphonate))			- 0.38	1	0
1,1′-trimethylene-2,2′-bipyridyl dibromide (Triquat)			- 0.54	1	0
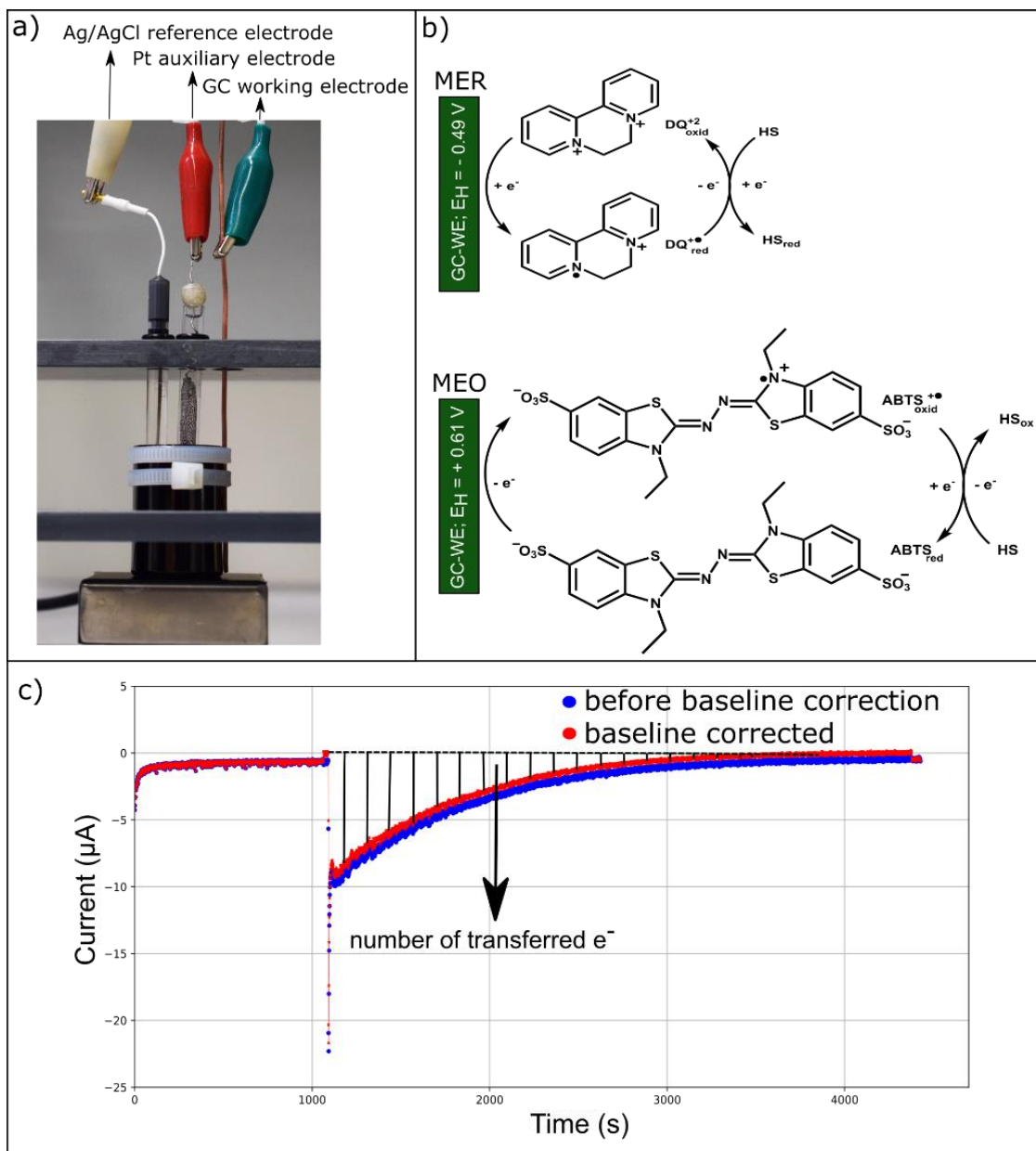
Figure 3. a) Typical set-up used for mediated electrochemical reduction (MER) or oxidation (MEO) techniques, consisting of a glassy carbon as working electrode and reaction cell (GC-WE), silver / silver chloride (Ag/AgCl) reference electrode and platinum (Pt) wire auxiliary electrode, b) Schematic representation of redox transfer mediation by the organic radicals Diquat (DQ) in MER and ABTS in MEO to enhance electron transfer reaction between biogeochemical phases (humic substances (HS), clay minerals, etc.) and the glassy carbon working electrode (modified from Ref 43), c) example of generated data (including baseline correction) to calculate number of transferred electrons from/to NOM to/from working electron either in oxidative/reductive mode.

1.5 Adsorption of NOM to mineral surfaces

NOM readily adsorbs from solution to many mineral surfaces[55-56] as a result of numerous processes with distinct energetic contributions, including ligand exchange, cation bridges, anion and cation exchange, non-specific van der Waals interactions and the hydrophobic effect.[57-64] Sorbent and system properties (pH, ionic strength, etc.) often cause selective NOM adsorption, which alters the chemical composition of the remaining NOM fraction in aqueous phase.[65-71] Therefore, it would be expected that fractionation induced by selective sorption processes would likely cause changes in the electron exchange capacities of the non-sorbed as well as the sorbed NOM fractions. Furthermore, electron transfer between NOM and mineral surfaces might occur at sorbents with intrinsic redox activity (e.g., iron or manganese (hydr-)oxides or Fe-containing clay minerals). Detailed description of these systems is required in order to understand the possible effect of NOM adsorption onto either redox inert or redox active sorbents.

1.5.1 Adsorption of NOM to redox inert sorbents

Adsorption of NOM onto redox inert sorbents (TiO_2, Al_2O_3, SiO_2, etc.) and clays is a subject of major relevance in environmental science and geochemistry since adsorption protects NOM from degradation and plays a key role on carbon transport in soils and aquifers.[12-14, 72] Typically, in adsorption experiments, NOM subfractions like HA or FA are studied.[73,74] The adsorption of NOM often follows a saturation-type Langmuir isotherm and usually decreases with increasing pH.[62,75,76] NOM fractionation upon adsorption to either polar or non-polar sorbents is expected to induce different effects on the redox properties of NOM (both sorbed and in aqueous phase). Considering the distribution of redox potentials (E^0_H) of a NOM sample,[28-29] selective as well as non-selective sorption processes are plausible to trigger alterations in the E^0_H of the NOM fraction left in aqueous phase (non-sorbed) as well as the NOM fraction with higher affinity for the sorbent (**Fig. 4**). Furthermore, due to conformational changes the availability of redox active groups in NOM might change upon sorption to redox inert sorbents. The changes in 3D-conformation of NOM supramolecular arrangements are closely related to the specific type and extent of interactions between NOM and the sorbents. Highly energetic interactions such as electrostatics and ligand exchange at the polar metal oxide surface[77] or non-specific van der Waals forces of low energy at hydrophobic surfaces such as synthetic resins, would be expected to lead to different 3D-conformational states of the NOM molecules, therefore resulting in plausible alterations in the redox properties of sorbed NOM. This description does not exclude additional alterations/reactions that might be caused by the presence of the sorbent (e.g., transformation of organic compounds).
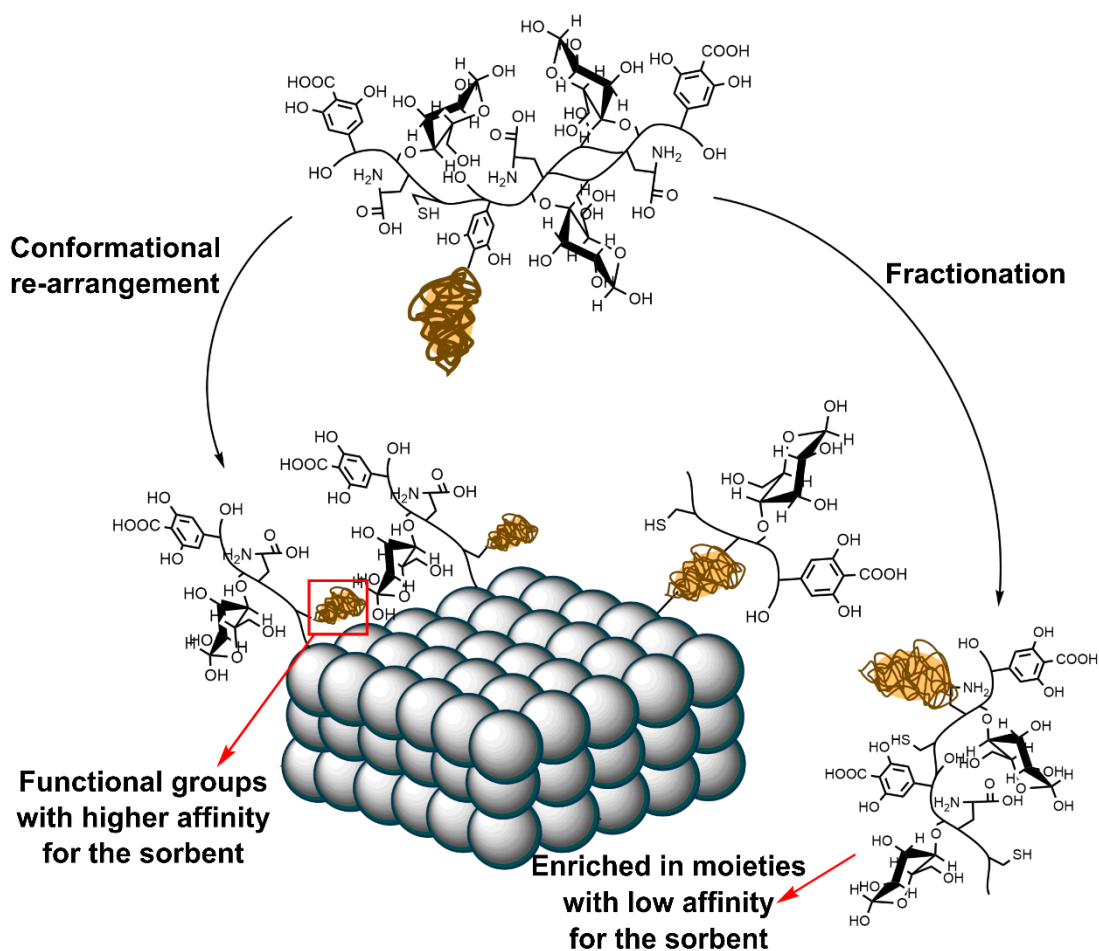
Figure 4. Illustration of processes to occur upon NOM adsorption onto redox inert sorbents. The structures of NOM and sorbent intend to represent only models to assess possible effects of NOM adsorption on its redox properties.

1.5.2   Adsorption of NOM to iron bearing clays.

Redox active minerals are ubiquitous in the environment and play a major role in the fate and transformation of organic and inorganic pollutants in soils and groundwater.[78-79] Among the redox active minerals, some clays contain structural iron (Fe) that is usually involved in biogeochemical redox reactions such as transformation of heavy metals, radionuclides and organic pollutants, and as electron acceptor in microbial processes.[80-84] It is important to note that the structural Fe(III) present in such sorbents can be reduced without being released into the solution, which makes them suitable model sorbents to explore the effects of sorption of NOM onto redox active surfaces on its redox properties (**Fig. 5**). Several studies reporting both selective as well as non-selective NOM sorption onto Fe-bearing clays are available.[85-87] Furthermore, electron transfer between iron present in minerals and hydroquinone model compounds have been reported.[88] Thus, besides alterations in NOM redox properties caused by selective fractionation and conformational changes upon adsorption, electron exchange between NOM and redox active Fe in clays might also play a major role.
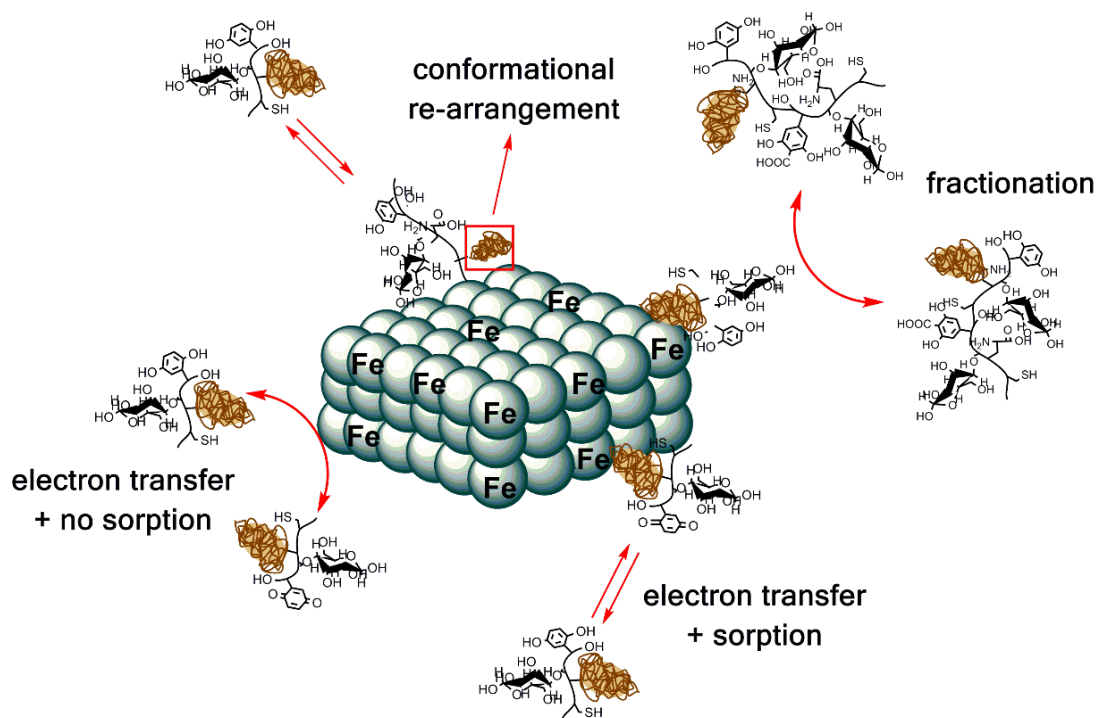
Figure 5. Illustration of processes occurring upon adsorption of NOM onto iron bearing clays. The structures of NOM and sorbent intend to represent only models to assess possible effects of NOM adsorption on its redox properties. Note the oxidation of hydroquinone moieties after electron transfer with Fe(III) at the surface in the presence or absence of sorption.

2. Objectives

This PhD work aims to systematically investigate the overall effects of NOM adsorption on its redox properties (i.e., electron exchange capacities and redox state). Electrochemical characterization of organic matter in different forms (dissolved, suspensions in the presence of mineral particles and filtrates after sorption) is required in order to better understand how NOM adsorption controls biogeochemical functions of NOM in environmental settings.

The specific objectives of this PhD work are:

i)   To explore how the redox state of NOM influences its sorption behavior to redox inert sorbents. Electrochemically pre-reduced NOM samples will be prepared in order to systematically assess the sorption of NOM at different redox states (i.e., native vs. reduced NOM).

33

ii)   To investigate how sorption of NOM to redox inert surfaces (aluminum oxide and a hydrophobic resin, DAX-8) influences its redox properties.

iii)   To determine the physicochemical processes (fractionation, conformational re-arrangements, etc.) that lead to changes in redox properties of NOM upon sorption in aqueous phase and in sorbed state. High-field Fourier Transform Ion Cyclotron Resonance Mass Spectrometry (FTICR-MS) will be used to characterize NOM samples in aqueous phase, therefore the selective sorption pathways causing changes in redox properties of NOM upon sorption will be provided.

iv)   To study how the electron transfer between redox active functional groups in NOM and iron at the sorbent influence the redox properties of sorbed NOM.

3.   Thesis Organization

Chapter 1 presents a general introduction of this research work, including some background and fundaments of techniques relevant to the study and objectives.

Chapter 2 comprises a systematic characterization of changes in redox properties of HA standard isolates upon sorption to redox active sorbents. Sorption of three IHSS humic acid standards (in native redox state) to aluminum oxide (Al_2O_3) and a hydrophobic resin, DAX-8 was studied at pH 7 in batch experiments for several HA/sorbent ratios. Results from Electron Accepting and Donating Capacities (EAC and EDC, respectively) measurements for both the suspensions and the filtrates (0.45 µm fraction) are presented. Likewise, reduced HA was prepared using direct electrochemical reduction, and the effect of redox state of NOM on its sorption was assessed.

Chapter 3 investigates how changes in the redox properties of humic acid upon sorption to redox inert sorbents can be explained by studying chemical features of the humic acid left in aqueous phase. High-field Fourier transform ion cyclotron resonance mass spectrometry (FTICR-MS) data describes the occurrence of sorptive fractionation processes in the context of redox inert sorption processes.

Chapter 4 is a preliminary assessment of the effect of NOM sorption to Fe-bearing clays on its redox properties. Sorption of standard HA isolate to Fe(III)-montmorillonite was studied at pH 7. EAC and EDC results for HA in suspensions and filtrates are compared to HA stock solution.

Chapter 5 provides general conclusions and future research directions.

4. References

1. Suffet, I. H.; MacCarthy, P. Aquatic Humic Substances and Their Influence on the Fate and Treatment of Pollutants. In *Aquatic Humic Substances.* Advances in Chemistry, Vol. 219. American Chemical Society: Washington, DC, **1988**.

2. Ghabbour, E. A.; Davies, G. *Understanding Humic Substances: Advanced Methods, Properties and Applications.* The Royal Society of Chemistry: Cambridge, UK, **1999**.

3. D'Andrilli, J.; Foreman, C. M.; Marshall, A. G.; McKnight, D. M. Characterization of IHSS Pony Lake fulvic acid dissolved organic matter by electrospray ionization Fourier transform ion cyclotron resonance mass spectrometry and fluorescence spectroscopy. *Org. Geochem.*, **2013**, 65, 19-28.

4. Qualls, R.G.; Haines, B.L.; Swank, W.T. Fluxes of dissolved organic nutrients and humic substances in a deciduous forest. *Ecology*, **1991**, 72, 254–266.

5. Fimmen, R. L.; Cory, R. M.; Chin, Y. P.; Trouts, T. D.; Mcknight, D. M. Probing the oxidation-reduction properties of terrestrially and microbially derived dissolved organic matter. *Geochim. Cosmochim. Acta*, **2007**, 71, 3003-3015.

6. Jiang, J.; Kappler, A. Kinetics of microbial and chemical reduction of humic substances: Implications for electron shuttling. *Environ. Sci. Technol.*, **2008**, 42 (10), 3563-3569.

7. Wolf, M.; Kappler, A.; Jiang, J.; Meckenstock, R. U. Effects of Humic Substances and Quinones at Low Concentrations on Ferrihydrite Reduction by Geobacter metallireducens. *Environ. Sci. Technol.*, **2009**, 43 (15), 5679-5685.

8. Dunnivant, F. M.; Schwarzenbach, R. P.; Macalady, D. L. Reduction of substituted nitrobenzenes in aqueous solutions containing natural organic matter. *Environ. Sci. Technol.*, **1992**, 26 (11), 2133-2141.

9. Curtis, G. P.; Reinhard, M. Reductive dehalogenation of hexachlorethane, carbon-tetrachloride and bromoform by anthrahydroquinone disulfonate and humic acid. *Environ. Sci. Technol.*, **1994**, 28 (13), 2393-2401.

10. Kappler, A.; Haderlein, S. B. Natural Organic Matter as Reductant for Chlorinated Aliphatic Pollutants. *Environ. Sci. Technol.,* **2003**, 37 (12), 2714-2719.

11. Jones, D. L.; Edwards, A. C. Influence of sorption on the biological utilization of two simple carbon substrates. *Soil Biol. Biochem.*, **1998**, 30 (14), 1895-1902.

12. Guggenberger, G.; Kaiser, K. Dissolved organic matter in soil: challenging the paradigm of sorptive preservation. *Geoderma*, **2003**, 113, 293-310.

13. Kalbitz, K.; Schwesig, D.; Rethemeyer, J.; Matzner, E. Stabilization of dissolved organic matter by sorption to the mineral soil. *Soil Biol. Biochem.*, **2005**, 37, 1319-1331.

14. Kaiser, K.; Guggenberger, G. The role of DOM sorption to mineral surfaces in the preservation of organic matter in soil. *Org. Geochem.*, **2000**, 31, 711-725.

15. Meier, M.; Namjesnik-Dejanovic, K.; Maurice, P. A.; Chin, Y.; Aiken, G. R. Fractionation of aquatic natural organic matter upon sorption to goethite and kaolinite. *Chemical Geology*, **1999**, 157, 275-284.

16. Koch, B. P.; Witt, M. R.; Engbrodt, R.; Dittmar, T.; Kattner, G. Molecular formulae of marine and terrigenous dissolved organic matter detected by

electrospray ionization Fourier transform ion cyclotron resonance mass spectrometry. *Geochim. Cosmochim. Acta*, **2005**, 69, 3299-3308.

17. Hertkorn, N.; Frommberger, M.; Witt, M.; Koch, B. P.; Schmitt-Kopplin, P.; Perdue, E. M. Natural organic matter and the event horizon of mass spectrometry. *Anal. Chem.*, **2008**, 80, 8908-8919.

18. Macalady, D. L.; Walton Day, K. Redox Chemistry of Natural Organic Matter (NOM): Geochemist's Dream, Analytical Chemist's Nightmare. In *Aquatic Redox Chemistry*; Tratnyek, P. G., Grundl, T. J. & Haderlein, S. B., Eds.; Oxford University Press: Washington, **2011**; pp 87-111.

19. Stevenson, F. J. *Humus Chemistry: Genesis, Composition, Reactions*, 2nd ed.; John Wiley & Sons: New York, **1994**.

20. McDonald, S.; Bishop, A. G.; Prenzler, P. D.; Robards, K. Analytical chemistry of freshwater humic substances. *Anal. Chim. Acta*, 2004, 527 (2), 105-124.

21. Schumacher, M.; Christl. I.; Vogt, R. D.; Barmettler, K.; Jacobsen, C.; Kretzschmar, R. Chemical composition of aquatic dissolved organic matter in five boreal forest catchments sampled in spring and fall seasons. *Biogeochemistry*, **2006**, 80, 263-275.

22. Hayes, T. M.; Hayes, M. H. B.; Swift, R. S. Detailed investigation of organic matter components in extracts and drainage waters from a soil under long term cultivation. *Org. Geochem.*, **2012**, 52, 13-22.

23. Kim, S.; Kramer, R. W.; Hatcher, P. G. Graphical method for analysis of ultrahigh-resolution broadband mass spectra of natural organic matter, the Van Krevelen diagram. *Anal. Chem.*, **2003**, 75, 5336-5344.

24. Guigue, J.; Harir, M.; Mathieu, O.; Lucio, M.; Ranjard, L.; Leveque, J.; Schmitt-Kopplin, P. Ultrahigh-resolution FT-ICR mass spectrometry for molecular characterisation of pressurised hot water-extractable organic matter in soils. *Biogeochemistry*, **2016**, 128, 307-326.

25. Thurman, E. M.; Malcolm R. L. Preparative isolation of aquatic humic substances. *Environ. Sci. Technol.*, **1981**, 15 (4), 463-466.

26. Thurman, E. M., *Organic Geochemistry of Natural Waters.* 1985.

27. Buffle J. Les substances humiques et leurs interactions avec les ions mineraus. *In Conference Proceedings de la Commission d'Hydrologie Appliquee de l'A.G.H.T.M. L'University d'Orsay*, 1977, 3-10.

28. Nurmi, J. T.; Tratnyek, P. G. Electrochemical properties of natural organic matter (NOM), fractions of NOM, and model biogeochemical electron shuttles. *Environ. Sci. Technol.*, **2002**, 36 (4), 617-624.

29. Aeschbacher, M.; Vergari, D.; Schwarzenbach, R. P., & Sander, M. Electrochemical Analysis of Proton and Electron Transfer Equilibria of the Reducible Moieties in Humic Acids. *Environ. Sci. Technol.*, **2011**, 45 (19), 8385-8394.

30. Macalady, D. L.; Walton Day, K. Redox Chemistry of Natural Organic Matter (NOM): Geochemist's Dream, Analytical Chemist's Nightmare. In *Aquatic Redox Chemistry*; Tratnyek, P. G., Grundl, T. J. & Haderlein, S. B., Eds.; Oxford University Press: Washington, **2011**; pp 87-111.

31. Nurmi, J. T.; Tratnyek, P. G. Electrochemistry of Natural Organic Matter. In *Aquatic Redox Chemistry*; Tratnyek, P. G.; Grundl, T. J.; Haderlein S. B., Eds.; Oxford University Press: Washington, **2011**, pp 129-151.

32. Scott, D. T.; McKnight, D. M.; Blunt-Harris, E. L.; Kolesar, S. E.; Lovley, D. R. Quinone moieties act as electron acceptors in the reduction of humic substances by humics-reducing microorganisms. *Environ. Sci. Technol.*, **1998**, 32 (19), 2984-2989.

33. Klapper, L.; McKnight, D. M.; Fulton, J. R.; Blunt-Harris, E. L.; Nevin, K. P.; Lovley, D. R.; Hatcher, P. G. Fulvic acid oxidation state detection using fluorescence spectroscopy. *Environ. Sci. Technol.*, **2002**, 36 (14), 3170-3175.

34. Struyk, Z.; Sposito, G. Redox properties of standard humic acids. *Geoderma*, **2001**, 102, 329-346.

35. Aeschbacher, M.; Graf, C.; Schwarzenbach, R. P.; Sander, M. Antioxidant properties of humic substances. *Environ. Sci. Technol.*, **2012**, 46 (9), 4916-4925.

36. Bletsa, E.; Stathi, P.; Dimos, K.; Louloudi, K.; Deligiannakis, Y. Interfacial Hydrogen Atom Transfer by nanohybrids based on Humic Acid Like Polycondensates. *J. Colloid Interface Sci.,* **2015**, 455, 163 – 171.

37. Lovley, D. R.; Coates, J. D.; Blunt-Harris, E. L.; Phillips, E. J. P.; Woodward, J. C. Humic substances as electron acceptors for microbial respiration. *Nature*, **1996**, 382 (6590), 445-448.

38. Kappler, A.; Benz, M.; Schink, B.; Brune, A. Electron shuttling via humic acids in microbial iron(III) reduction in a freshwater sediment. *FEMS Microbiol. Ecol.*, **2004**, 47 (1), 85-92.

39. Heitmann, T.; Goldhammer, T.; Beer, J.; Blodau, C. Electron transfer of dissolved organic matter and its potential significance for anaerobic respiration in a northern bog. *Global Change Biol.*, **2007**, 13 (8), 1771-1785.

40. Blodau, C.; Bauer, M.; Regenspurg, S.; Macalady, D. Electron accepting capacity of dissolved organic matter as determined by reaction with metallic zinc. *Chem. Geol.*, **2009**, 260 (3-4), 186-195.

41. Heitmann, T.; Blodau, C. Oxidation and incorporation of hydrogen sulfide by dissolved organic matter. *Chem. Geol.*, **2006**, 235 (1-2), 12-20.

42. Bauer, M.; Heitmann, T.; Macalady, D. L.; Blodau, C. Electron transfer capacities and reaction kinetics of peat dissolved organic matter. *Environ. Sci. Technol.*, **2007**, 41, 139-145.

43. Aeschbacher, M.; Sander, M.; Schwarzenbach, R. P. Novel electrochemical approach to assess the redox properties of humic substances. *Environ. Sci. Technol.,* **2010**, 44 (1), 87-93.

44. Aeschbacher, M.; Brunner, S. H.; Schwarzenbach, R. P.; Sander, M. Assessing the effect of humic acid redox state on organic pollutant sorption by combined electrochemical reduction and sorption experiments. *Environ. Sci. Technol.*, **2012**, 46 (7), 3882-3890.

45. Gorski, C. A.; Aeschbacher, M.; Soltermann, D.; Voegelin, A.; Baeyens, B.; Fernandes, M. M.; Hofstetter, T. B.; Sander, M. Redox properties of structural Fe in clay minerals. 1. Electrochemical quantification of electron-donating and -accepting capacities of smectites. *Environ. Sci. Technol.*, **2012**, 46 (17), 9360-9368.

46. Gorski, C. A.; Kluepfel, L.; Voegelin, A.; Sander, M.; Hofstetter, T. B. Redox properties of structural Fe in clay minerals. 2. Electrochemical and spectroscopic characterization of electron transfer irreversibility in ferruginous smectite, SWa-1. *Environ. Sci. Technol.*, **2012**, 46 (17), 9369-9377.

47. Gorski, C. A.; Kluepfel, L.; Voegelin, A.; Sander, M.; Hofstetter, T. B. Redox properties of structural Fe in clay minerals: 3. Relationships between smectite redox and structural properties. *Environ. Sci. Technol.*, **2013**, 47 (23), 13477-13485.

48. Kluepfel, L.; Piepenbrock, A.; Kappler, A.; Sander, M. Humic substances as fully regenerable electron acceptors in recurrently anoxic environments. *Nat. Geosci.*, **2014**, 7 (3), 195-200.

49. Kluepfel, L.; Keiluweit, M.; Kleber, M.; Sander, M. Redox properties of plant biomass-derived black carbon (biochar). *Environ. Sci. Technol.*, **2014**, 48 (10), 5601-5611.

50. Klein, A. R.; Silvester, E.; Hogan, C. F. Mediated electron transfer between Fe-II adsorbed onto hydrous ferric oxide and a working electrode. *Environ. Sci. Technol.*, **2014**, 48 (18), 10835-10842.

51. Lau, M. P.; Sander, M.; Gelbrecht, J.; Hupfer, M. Solid phases as important electron acceptors in freshwater organic sediments. *Biogeochemistry*, **2015**, 123, 4961.

52. Sander, M.; Hofstetter, T. B.; Gorski, C. A. Electrochemical Analyses of Redox-Active Iron Minerals: A Review of Nonmediated and Mediated Approaches. *Environ. Sci. Technol.*, **2015**, 49, 5862-5878.

53. Hoving, A. L.; Sander, M.; Bruggeman, C.; Behrends, T. Redox properties of clay-rich sediments as assessed by mediated electrochemical analysis: Separating pyrite, siderite and structural Fe in clay minerals. *Chem. Geol.*, **2017**, 457, 149-161.

54. Fultz, M. L.; Durst, R. A. Mediator compounds for the electrochemical study of biological redox systems - a compilation. *Anal. Chim. Acta*, **1982**, 140 (1), 1-18.

55. Sander, S.; Mosley, L. M.; Hunter, K. A. Investigation of interparticle forces in natural waters: Effects of adsorbed humic acids on iron oxide and alumina surface properties. *Environ. Sci. Technol.*, **2004**, 38 (18), 4791-4796.

56. Avena, M. J.; Koopal, L. K. Desorption of humic acids from an iron oxide surface. *Environ. Sci. Technol.*, **1998**, 32 (17), 2572-2577.

57. Murphy, E. M.; Zachara, J. M.; Smith, S. C. Influence of Mineral-Bound Humic Substances on the Sorption of Hydrophobic Organic Compounds. *Environ. Sci. Technol.*, **1990**, 24, 1507-1516.

58. Ochs, M.; Cosovic, B.; Stumm, W. Coordinative and hydrophobic interaction of humic hydrophobic mercury surfaces. *Geochim. Cosmochim. Acta.*, **1994**, 58 (2), 639-650.

59. Gu, B.; Schmitt, J.; Chen, Z. H.; Liang, L. Y.; McCarthy, J. F. Adsorption and desorption of natural organic matter on iron oxide. Mechanisms and models. *Environ. Sci. Technol.*, **1994**, 28 (1), 38-46.

60. Vermeer, A. W.; Koopal, L. K. Adsorption of Humic Acids to Mineral Particles. 2. Polydispersity Effects with Polyelectrolyte Adsorption. *Langmuir*, **1998**, 14, 4210-4216.

61. Kaiser, K.; Zech, W. Release of natural organic matter sorbed to oxides and a subsoil. *Soil Sci. Soc. Am. J.*, **1999**, 63 (5), 1157-1166.

62. Saito, T.; Koopal, L. K.; van Riemsdijk, W. H.; Nagasaki, S.; Tanaka, S. Adsorption of humic acid on goethite: isotherms, charge adjustments, and potential profiles. *Langmuir*, 2004, 20, 689-700.

63. Kang, S. H.; Xing, B. S. Humic acid fractionation upon sequential adsorption onto goethite. *Langmuir*, **2008**, 24 (6), 2525-2531.

64. Armanious, A.; Aeppli, M.; Sander, M. Dissolved Organic Matter Adsorption to Model Surfaces: Adlayer Formation, Properties, and Dynamics at the Nanoscale. *Environ. Sci. Technol.*, **2014**, 48, 9420-9429.

65. Kaiser, K.; Zech, W. Competitive sorption of dissolved organic matter fractions to soils and related mineral phases. *Soil Sci. Soc. Am. J.*, **1997**, 61, 64-69.

66. Meier, M.; Namjesnik-Dejanovic, K.; Maurice, P. A.; Chin, Y. P.; Aiken, G. R. Fractionation of aquatic natural organic matter upon sorption to goethite and kaolinite. *Chem. Geol.*, **1999**, 157, 275-284.

67. Hur, J.; Schlautman, M. A. Molecular weight fractionation of humic substances by adsorption onto minerals. *J. Colloid Interface Sci.*, **2003**, 264, 313-321.

68. Heidmann, I.; Christl, I.; Kretzschmar, R. Sorption of Cu and Pb to kaolinite–fulvic acid colloids: Assessment of sorbent interactions. *Geochim. Cosmochim. Acta*, **2005**, 69 (7), 1675-1686.

69. Claret, F.; Schaefer, T.; Brevet, J.; Reiller, P. E. Fractionation of Suwannee River Fulvic Acid and Aldrich Humic Acid on α-Al2O3: Spectroscopic Evidence. *Environ. Sci. Technol.*, **2008**, 42, 8809-8815.

70. Galindo, C.; Del Nero, M. Molecular Level Description of the Sorptive Fractionation of a Fulvic Acid on Aluminum Oxide Using Electrospray Ionization Fourier Transform Mass Spectrometry. *Environ. Sci. Technol.*, **2014**, 48, 7401-7408.

71. Galindo, C.; Del Nero, M. Chemical fractionation of a terrestrial humic acid upon sorption on alumina by high resolution mass spectrometry. *RSC Adv.*, **2015**, 5, 73058.

72. Lutzow, M. v.; Kogel-Knabner, I.; Ekschmitt, K.; Matzner, E.; Guggenberger, G.; Marschner, B.; Flessa, H. Stabilization of organic matter in temperate soils: Mechanisms and their relevance under different soil conditions - a review. *Eur. J. Soil Sci.*, **2006**, 57, 426−445.

73. Tao, Z. Y.; Chu, T. W.; Du, J. Z.; Dai, X. X.; Gu, Y. J. Effect of fulvic acids on sorption of U(VI), Zn, Yb, I and Se(IV) onto oxides of aluminum, iron and silicon. *Applied Geochemistry*, **2000**, 15 (2), 133-139.

74. Yang, K.; Lin, D. H., Xing, B. S. Interactions of Humic Acid with Nanosized Inorganic Oxides. *Langmuir*, **2009**, 25 (6), 3571-3576.

75. Veith, J. A.; Sposito, G. On the Use of the Langmuir Equation in the Interpretation of "Adsorption" Phenomena. *Soil Sci. Soc. Am. J.*, **1977**, 41, 697-702.

76. Gu, B.; Mehlhorn, T. L.; Liang, L.; McCarthy, J. F. Competitive adsorption, displacement, and transport of organic matter on iron oxide: I. Competitive adsorption. *Geochim. Cosmochim. Acta.*, **1996**, 60, 1943-1950.

77. Schaumann, G. E. Soil organic matter beyond molecular structure Part I: Macromolecular and supramolecular characteristics. *J. Plant Nutr. Soil Sci.*, **2006**, 169 (2), 145-156.

78. Elsner, M.; Schwarzenbach, R. P.; Haderlein, S. B., Reactivity of Fe(II)-Bearing Minerals toward Reductive Transformation of Organic Contaminants. *Environ. Sci. Technol.*, **2003**, 38, (3), 799-807.

79. Amstaetter, K.; Borch, T.; Larese-Casanova, P.; Kappler, A., Redox Transformation of Arsenic by Fe(II)-Activated Goethite (α-FeOOH). *Environ. Sci. Technol.*, **2009**, 44, (1), 102-108.

80. Hofstetter, T. B.; Schwarzenbach, R. P.; Haderlein, S. B. Reactivity of Fe(II) species associated with clay minerals. *Environ. Sci. Technol.*, **2003**, 37, 519-528.

81. Hofstetter, T. B.; Neumann, A.; Schwarzenbach, R. P. Reduction of nitroaromatic compounds by Fe(II) species associated with iron rich smectites. *Environ. Sci. Technol.*, **2006**, 40, 235-242.

82. Neumann, A.; Hofstetter, T. B.; Skarpeli-Liati, M.; Schwarzenbach, R. P. Reduction of polychlorinated ethanes and carbon tetrachloride by structural Fe(II) in smectites. *Environ. Sci. Technol.*, **2009**, 43, 4082-4089.

83. Yang, J.; Kukkadapu, R. K.; Dong, H.; Shelobolina, E. S.; Zhang, J.; Kim, J. Effects of redox cycling of iron in nontronite on reduction of technetium. *Chem. Geol.*, **2012**, 291, 206-216.

84. Dong, H.; Jaisi, D. P.; Kim, J.; Zhang, G. Microbe-clay mineral interactions. *Am. Mineral.*, **2009**, 94, 1505-1519.

85. Feng, X. J.; Simpson, A. J.; Simpson, M. J. Chemical and mineralogical controls on humic acid sorption to clay mineral surfaces. *Org. Geochem.*, **2005**, 36 (11), 1553-1566.

86. Fleury, G.; Del Nero, M.; Barillon, R. Effect of mineral surface properties (alumina, kaolinite) on the sorptive fractionation mechanisms of soil fulvic acids: Molecular-scale ESI-MS studies. *Geochim. Cosmochim. Acta*, **2017**, 196, 1-17.

87. Young, R. B.; Avneri-Katz, S.; McKenna, A. M.; Chen, H.; Bahureksa, W.; Polubesova, T.; Chefetz, B.; Borch, T. Composition-Dependent Sorptive Fractionation of Anthropogenic Dissolved Organic Matter by Fe(III)-Montmorillonite. *Soil. Syst.*, **2018**, 2 (1), 14.

88. Kung, K. H.; McBride, M. B. Electron transfer processes between hydroquinone and hausmannite (Mn_3O_4). *Clays Clay Miner.*, **1988**, 36 (4), 297-302.

Chapter 2.

2. Effects of Sorption on Redox Properties of Natural Organic Matter

2.1   Abstract

A large fraction of natural organic matter (NOM) usually coexists (e.g. sorbed) with minerals in the environment and might influence some of its key biogeochemical functions in natural systems. However, the redox properties of NOM fractions (aqueous phase vs. sorbed) upon sorption remain poorly understood. This work describes systematically the changes in the electron exchange capacities (EEC = total number of transferred electrons from/to working electrode) of sorbed humic acid (HA) at redox inert sorbents (alumina and hydrophobic resin – DAX-8) and the effect of redox state of HA on its adsorption behavior. Native HA adsorption to alumina resulted in an increase of up to 200 % in electron donating capacities (EDC) for suspensions while HA filtrates showed large decreases in EEC, both compared to HA stock solution. Conversely, HA sorption to DAX-8 did not produce significant alterations in its EEC, and the redox state of HA triggered not measurable differences in its sorption. Given the absence of electron transfer between HA and alumina, the enhancements in EDC of HA upon sorption might be not only associated to sorptive fractionation but also to availability of redox active groups (e.g., polyphenols) due to conformational re-arrangements of HA supramolecular assemblies, or most likely due to sorptive catalyzed polymerization of polyphenolic compounds under oxidizing conditions.

2.2   Introduction

Natural Organic Matter (NOM) is ubiquitous in terrestrial and aquatic systems and is made up by a heterogeneous mixture of diverse organic molecules originating from the decay of biomass.[1-3] The chemical composition, structure and physicochemical properties of NOM are closely linked to its origin (terrestrial or aquatic), the type of biomass such plants or microorganisms, as well as the climatic and environmental conditions such as light exposure.[4-6] Important biogeochemical and environmental functions of NOM

include carbon and energy source for heterotrophic organisms, electron shuttling in microbial processes,[7-9] reactant for redox transformation of pollutants,[10-11] absorbent for nutrients, metals and organic pollutants affecting their mobility and bioavailability in soils, sediments and aquifers. Given its inherent heterogeneity, the standard reduction potential ($E_H^{0'}$) of a NOM sample is not a discrete value but covers a range of potentials as demonstrated for terrestrial and aquatic humic acids.[12-13] While quinone moieties are the major electron acceptor functional groups within HS[13-18] polyphenols and hydroquinone moieties make up for most of the electron donor capacity of HS.[18-21] The presence of various electroactive moieties in NOM gives rise to a wide distribution of potential redox states of the very same NOM sample as a function of the prevailing redox potential. As a given NOM sample may be more or less oxidized, other physicochemical properties such as polarity, 3D-conformation or aggregation state may also alter with its redox state. Thus, the degree of oxidation/reduction of NOM may affect not only electron transfer reactions with other substances, but also its complexing properties, proton binding capacity, solubility, particle size or sorption behavior.

The major fraction of natural organic matter in soils, sediments and aquifers is associated with the solid phase rather than present in solution. NOM readily adsorbs from aqueous solution to mineral surfaces,[22-24] as a result of several types of interactions including ligand exchange, anion or cation exchange and van der Waals interactions.[25-30] Adsorption of NOM to particulate soil components has been widely investigated because of its major relevance to NOM stabilization and transport in the subsurface.[31-33] Adsorption frequently leads to preferential sorption of NOM components; depending on the type of adsorbent and solution properties (pH, ionic strength, etc.), selective sorption of certain NOM components is expected to occur.[34-39] In adsorption experiments, typically subfractions of dissolved NOM like humic acids (HA) or fulvic acids (FA) rather than native NOM samples are studied.[40-41] Although a wealth of knowledge on the mechanisms and the effects of environmental factors on the sorption of such humic substances (HS) at minerals and other solid phases is available, studies on the effects of the redox state on sorption of HS or investigations on how sorption of HS may alter their redox properties are missing. Considering the chemical complexity of the HA and the variety of interactions at the HA-mineral interface, sorption-induced fractionation, conformational re-arrangements of HA moieties and further chemical reactions at the surface are plausible, therefore concomitant changes in the redox chemistry of sorbed, non-sorbed and dissolved HA fractions are expected. Such alterations might depend on both the type of sorption mechanism (sorbent/sorbate interaction) and on the extent of sorption. It is hypothesized that HA sorption to either polar or non-polar sorbents trigger alterations in its redox properties and reactivity (both sorbed and in solution), even in the absence of electron transfer with the sorbents.

In the present study, it was investigated if and how redox properties of humic substances (namely total Electron Exchange Capacity (EEC) and redox state) change during sorption to redox inert sorbents. To this end, batch experiments with standard

humic acids isolates (Elliott Soil, Pahokee Peat and Suwannee River HA) at defined redox states and redox-inert sorbents (polar Al_2O_3 and non-polar DAX-8 resins) were conducted under anoxic conditions. The HA materials were selected to cover a range of electrochemical properties[20] and origins, i.e., terrestrial and aquatic. Recently established mediated electroanalytical techniques[12,20,42-54] were applied to determine the Electron Accepting (EAC) and Donating (EDC) capacities of HA fractions (dissolved, aqueous, in sorbed state).

2.3   Materials and methods

Chemicals. Aluminum oxide (Al_2O_3 90% standardized, Merck, Germany; particle size: 70 % between $0.063 - 0.200$ mm, surface area: 133.6 ± 0.3 $m^2 * g^{-1}$), Supelite DAX-8 resin (poly-methylmethacrylate; Sigma-Aldrich Co., USA; particle size: 90 % between $0.250 - 0.420$ mm, surface area: 177 ± 1 $m^2 * g^{-1}$). The Brunauer, Emmett and Teller (BET) method with N_2 adsorption[55] was used to determine the total specific surface area with an ASAP 2000 system (Micromeritics, GA, USA) (data not shown). 1,10-Ethylene-2,20-bipyridiniumdibromide monohydrate (Diquat = DQ, Sigma-Aldrich Co., USA), 2,2′-azino-bis(3-ethylbenzothiazoline-6-sulfonic (ABTS, Sigma-Aldrich Co., USA), 1 M NaOH and 1 M HCl solutions (Titripur; Reag. USP; Merck; Germany), KCl (99+ %; Across Organics; Germany) and KH_2PO_4 (Merck; 99.5 %; Germany). All aqueous solutions were prepared in Millipore® deionized water. Aluminum oxide was used as received whereas the DAX-8 resin was washed up to 5 times with Millipore (MQ) water until the dissolved organic carbon (DOC) content of the washing water was below 1 mg $C*L^{-1}$ (data not shown). Stock suspensions of the sorbents Al_2O_3 and DAX-8 were prepared in 0.1 M KCl. Oxygen sensitive experiments were conducted in an anoxic glovebox ($O_2 < 0.1$ ppm; N_2 atmosphere, M. Braun, Germany). Stock suspensions of the sorbents were purged with N_2 (purity grade > 99.999 %) for 1 hour prior transfer to the glovebox.

Humic Substances (HS). Elliott Soil Humic Acid IV (ESHA; 4S102H), Pahokee Peat Humic Acid (PPHA; 1S103H) and Suwannee River Humic Acid (SRHA; 2S101H) standard materials were used as received from IHSS. Stock solutions of these HAs were prepared in 0.1 M KCl, manually titrated to pH 7 using fresh solutions (1, 0.1 or 0.01 M) of NaOH or HCl and filtered through pre-washed membranes (Whatman™; 0.45 µm; mixed cellulose ester ME25; Germany) to meet the operational DOC definition (particle size < 0.45 µm).[56] The HA stock solutions (250 - 500 mg C/L) were stored in aluminum foiled Schott bottles and were purged with N_2 for 1 hour prior transfer to the glovebox.

Adsorption experiments. Adsorption of native or reduced HAs to Al_2O_3 and DAX-8 was studied in 100 mL serum brown glass bottles with butyl rubber stoppers at pH 7 in 0.1 M KCl in duplicate batch experiments without addition of buffers. The pH of each batch was manually adjusted for up to seven consecutive days until apparent equilibration was achieved. Apparent adsorption equilibrium was achieved after 3-7 days as indicated by constant UV-Vis absorption spectra of filtered (0.45 µm) samples and

constant pH values. These tests were performed in samples with low HA/sorbent mass ratios (data not shown). Adsorption isotherms were obtained at constant total HA concentrations by varying the sorbent concentrations. Aliquots of suspensions were taken and kept inside the glovebox for subsequent electrochemical analyses (see below). Then, the filtrate (Minisart® syringe filter; 0.45µm; regenerated cellulose, Sartorius, Germany) of the remaining suspension was collected for further analyses. Adsorption data were analyzed using linear or Langmuir isotherm models[57] using Python tools and the fitting error was calculated by using the ordinary root-mean-square error (RMSE) approach.

$$HA_{sorb} = \frac{HA_{max}*K_{ads}*HA_{aq}}{1 + K_{ads}*HA_{aq}} \tag{1}$$

The Langmuir model (equation 1; HA_{sorb} = the amount of adsorbed HA per mass of adsorbent; HA_{aq} = aqueous HA concentration; HA_{max} = adsorption capacity and K_{ads} = Langmuir adsorption constant) was applied to guide the eye if saturation type adsorption isotherms were obtained. Even though the conditions to interpret the isotherm parameter values mechanistically are not fulfilled when studying heterogeneous mixtures of solutes such a humic acids, the Langmuir isotherm has been widely applied to parameterize NOM adsorption to mineral surfaces.[58-59]

Characterization of HA. Two independent methods to determine DOC were used; i) after acidification an elemental analyzer (Vario Cube; Elementar; Hanau; Germany) and ii) UV-Vis spectroscopy by using 10 mm quartz cuvettes (Suprasil; Hellma Analytics; Germany) and a photoLab 6600 UV−Vis spectrophotometer (WTW; Germany). Both methods were applied to HA stock solutions. As DOC analysis by UV-Vis in filtrates after sorption could be biased due to fractionation of chromophoric DOC components upon sorption,[37,60] DOC in filtrates from sorption experiments was quantified by TOC analyzer and was used for all calculations done in this work. The specific UV-Vis Absorbance at 254 nm ($SUVA_{254}$ = L*(mg C*m)$^{-1}$) of HS samples was calculated as the measured absorbance using a 10 mm cuvette multiplied by 100 to transform length units to meters and division by DOC concentration (mg C*L^{-1}) ($SUVA_{254}$ = Abs_{254}*100*DOC^{-1}).[61] Excitation-emission-matrix (EEM) fluorescence spectra of suspension filtrates were measured using a Fluoromax® 4 (Horiba, Jobin-Yvon, Japan) spectrofluorometer. If necessary the filtrates were diluted to UV-Vis at 254 nm absorbance values below 0.3 to avoid inner-filter effects.[62] EEM fluorescence spectra were recorded over a range of emission (350 – 600 nm) and excitation (250 - 500 nm) wavelength.[63-64] EEM data is shown in supporting information **Figure SI1**.

Electron Exchange Capacity (EEC) of HA. The redox properties of HA stock solutions, whole HA-sorbent suspensions and HA in filtrates were determined by mediated electrochemical analysis.[42,48] The EAC and EDC of humic acids were determined either in the reduction (MER) or oxidation (MEO) mode. In short, MER and MEO were conducted at pH 7 in the presence of 0.1 M KCl and 0.1M phosphate buffer using a glassy carbon cell (Sigradur G, HTW, Germany) as working electrode, a Pt wire

(0.5 mm; 99.9 %) attached to Pt gauze (52 mesh, 99.9 %), both from Sigma-Aldrich Co., USA as auxiliary electrode and a Ag/AgCl reference electrode (Bioanalytical systems Inc., USA) connected to a potentiostat (1000C Multi-potentiostat, CH Instruments, USA). Diquat and ABTS were used as electron transfer mediators in MER and MEO, respectively. The absence of adsorption of Diquat and ABTS to Al_2O_3 was confirmed by UV-Vis spectroscopy (data shown in Supporting Information **Fig. SI2**). After mediators were spiked to the electrochemical cell polarized to either reductive (MER; E_H(pH 7) = - 0.49 V vs. SHE) or oxidative (MEO; E_H(pH 7) = + 0.61 V vs. SHE) potentials, at least triplicates of each sample were analyzed by recording the current versus time between the working electrode and the auxiliary electrode at a constant potential. The charge transferred from/to the sample via the mediator to/from the electrode was obtained by integrating the current signal after baseline correction using a composite rule as implemented in the SciPy library of Python. EAC, EDC and total Electron Exchange Capacities (EEC = EAC + EDC) were calculated by normalizing the transferred charged to the mass of organic carbon in the sample. This analytical approach was used to characterize EEC of HA samples (native, reduced or oxidized in dissolved, filtrates or in suspension form) for all experiments shown in this work.

Direct Electrochemical Reduction (DER) of ESHA. Bulk electroanalysis of ESHA was carried out in a cup-shaped electrochemical cell ($\sim$ 0.2 L; glassy carbon; Sigradur G, HTW, Germany) at E_H (pH 7) = - 0.59 V until the reductive current signal decreased to $\sim$ 30 µA and no significant change in MER-MEO of withdrawn aliquots sample was measured.[12,42] pH of ESHA bulk solution was kept stable at $\sim$ pH 4.7 during the course of the electroanalysis by manual titration with diluted HCl.

Oxidation of reduced ESHA by O₂. In order to evaluate whether the electrochemically reduced moieties in HA could be reoxidized by O_2, oxidation of electrochemically reduced ESHA stock solutions, filtrates and whole suspensions (after sorption to Al_2O_3 or DAX-8, respectively) was carried out as follows. Within the glovebox, 10 mL of sample were transferred into a 20 mL glass vial, and crimp-sealed with silicone blue/PTFE septa (BGB®, Germany) white septa. After transfer outside the glovebox, the sample was purged with oxygen gas (> 99.999 %) for 15 minutes through the septum using stainless steel needles and kept under O_2 headspace on a shaker for 5 days. Finally, the vials were purged with N_2 (> 99.999 %) for 30 minutes to remove non-reacted O_2 prior to EAC and EDC measurements within the glovebox. The DOC concentration of suspension filtrates after oxidation experiments was measured to assess changes in the sorption equilibrium compared to experiments conducted under reducing conditions.

2.4   Results and Discussion

Adsorption of humic acids at native redox state. Adsorption isotherms for the three humic acids in their native redox state to the polar (aluminum oxide; Al_2O_3) and non-polar (hydrophobic resin DAX-8) were determined at pH 7 and are presented in **Fig. 6**. While the adsorption isotherm for Al_2O_3 generally were highly non-linear and of saturation type, the isotherms for DAX-8 exhibited neither pronounced non-linearity nor an apparent saturation level. These different isotherm features indicate that different types of interactions between the humic acids and Al_2O_3 or DAX-8 dominated the adsorption process.

The steep isotherm slopes at low HA concentrations and the apparent saturation level at higher sorbate concentrations indicate that specific interactions between HA functional groups with a limited number of surface sites occurred.[25,41] These findings agree with results of previous studies,[65-66] and have been attributed primarily to surface complex formation (ligand exchange) between Al_2O_3-surface hydroxyl groups and HA-carboxylate- or hydroxyl functional groups [67-69] as well as to coulombic interactions (Al_2O_3 is positively charged while HA carries a net negative charge at pH 7).[70-73] Given the inherent diversity of the individual HA components, such type of interactions would give rise to preferential adsorption of certain subfractions of HA components. As a consequence, changes of the average properties of dissolved and adsorbed HA pools upon sorption is expected with a depletion of HA components rich in phenolic and carboxylic groups in the aqueous HA pool and a relative enrichment of such compounds in the sorbed pool of humic acids, such a seggregation has been demonstrated earlier and is termed sorptive "fractionation" of humic acids.[36,38-39,74-75]

Langmuir model (equation 1) was applied to parameterize the apparent affinity (K_{ads} value) and adsorption capacity (HA_{max}) of the three humic acids to Al_2O_3 at given conditions. The apparent maximum HA adsorption capacities (HA_{max}) can be used to estimate surface coverage and/or adlayer thickness of HAs at aluminum oxide.[73] Surface coverage data (**Fig. SI3**) indicate that the whole range of reactive sites on the surface was covered (from low to high surface coverage (% HA_{sorb} / HA_{max})) in this experiment. Assuming complete surface coverage of HA at the respective HA_{max} value (see caption of **Fig. 6**) and homogeneous adlayer density of 1.05 $g*cm^{-3}$,[71,73] the adlayer thickness can be calculated. Estimates of the HA-adlayer thicknesses are: 0.30 nm for ESHA, 0.17 nm for PPHA and 0.17 nm for SRHA (calculations are presented in the **Table SI1**). Conversely, when using apparent maximum adsorption capacities reported for Al_2O_3 particles,[65-66,76] and assuming complete and homogeneous surface coverage, HA-adlayer thicknesses from 0.28 to 0.76 nm are obtained (**Table SI1**). These calculations will help to rationalize the causes of changes in the electrochemical properties of adsorbed vs. dissolved organic matter (see below).
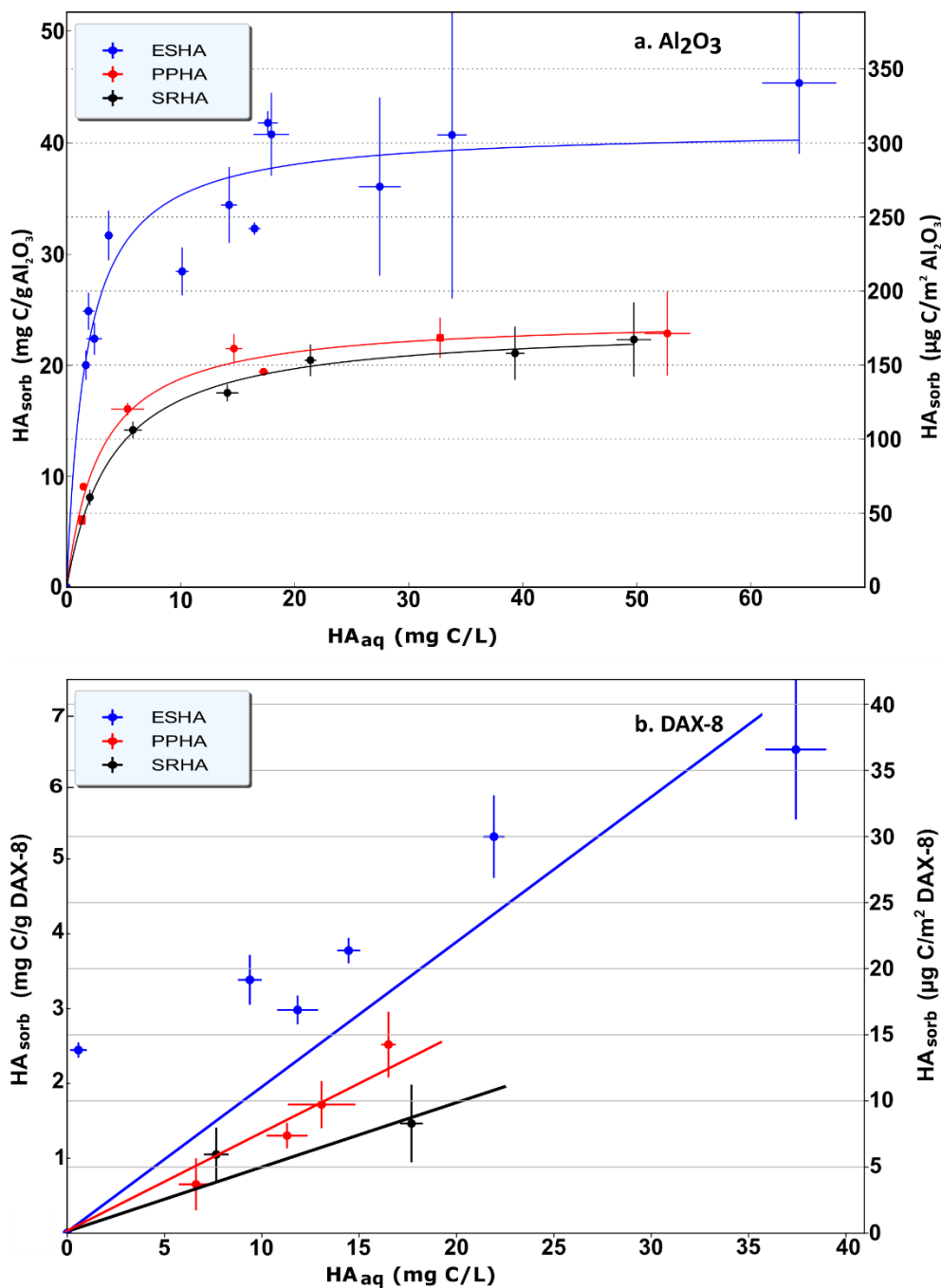
Figure 6. Sorption isotherms of humic acids in their native redox state (normalized to sorbent mass (left axis) and sorbent surface area (right axis)) at pH 7 and 0.1 M KCl for: **a)** aluminum oxide (Al_2O_3) and **b)** hydrophobic resin (DAX-8). The solid lines represent: in **Fig. 6a** isotherm fits (Langmuir), and in **Fig. 6b** linear regression parameters. Langmuir Isotherm parameter values for Al_2O_3 (**Fig. 6a**) are: Elliott Soil (ESHA): $K_{ads} = 0.59$ L/mg; $HA_{max} = 41.4$ mg C/g Al_2O_3; RMSE = 3.75 --- Pahokee Peat (PPHA): $K_{ads} = 0.34$ L/mg; $HA_{max} = 24.3$ mg C/g Al_2O_3; RMSE = 0.99 --- Suwannee River (SRHA): $K_{ads} = 0.25$ L/mg; $HA_{max} = 23.7$ mg C/g Al_2O_3; RMSE = 0.49. Linear regression parameters ($HA_{sorb.} = Kd * HA_{aq}$) for DAX-8 (**Fig. 6b**) are: Elliott Soil: $K_d(ESHA) = 0.208$ L/mg; $r^2 = 0.587$ --- Pahokee Peat: $K_d(PPHA) = 0.135$ L/mg; $r^2 = 0.948$ --- Suwannee River: $K_d(SRHA) = 0.091$ L/mg; $r^2 = 0.871$.

The hydrophobic resin DAX-8 (which has similar properties than its successor product XAD-8)[77] shows much lower adsorption affinity and thus weaker interactions to the three HAs than aluminium oxide (**Fig. 6b**). The low affinity together with the absence of significant non-linearity and the lack of reactive surface groups of the resin suggest that the strong intermolecular interactions of water (hydrophobic effect)[78] and weak non-specific Van der Waals interactions between HA-DAX-8 play major roles behind the adsorption to DAX-8. Since such non-specifc interaction forces scale with molecular size or surface area[79] rather than with specifc functional groups of humic substance components, sorptive fractionation by DAX-8 resin is generally expected to be less pronounced. Consequently, XAD-8 and DAX-8 resins are widely used to extract dissolved HA from water samples and during cleanup of natural organic matter.[79-81] Although sorptive fractionation at DAX-8 can not be avoided, it selects for apolarity and thus for size of HA components rather than for functional groups that can form surface complexes such as polypenolic and carboxylic groups.

Sorption of electrochemically reduced humic acids. To investigate how the sorption of humic acids is affected by their redox state, sorption isotherms for electrochemically reduced ESHA were measured. ESHA was selected because in its native (i.e. non-reduced) redox state it showed the highest affinity of the three model humic acids to Al_2O_3 and DAX-8. By choosing redox inert sorbents and conducting the experiments under anoxic conditions redox reactions of ESHA with other components of the systems and thus changes in the redox state of ESHA can be excluded. This experimental setup allowed us to conduct the sorption experiments at a well-defined and reduced redox state of ESHA. Similar to the sorption of native ESHA ([nat]ESHA), the sorption isotherm of reduced ESHA ([red]ESHA) at Al_2O_3 was highly non-linear and of saturation type, while the isotherm at DAX-8 exhibited neither pronounced non-linearity nor an apparent saturation level (see **Fig. 7**). Also the extent of [red]ESHA sorption was comparable to [nat]ESHA sorption as indicated by very similar isotherm parameters.

Note that electrochemical reduction of ESHA primarily causes a conversion of quinone moieties in ESHA to hydroquinones. As at pH 7 the majority of the hydroquinone moieties in humic acids are present in non-dissociated (neutral) form,[82-83] the change in redox state of ESHA should leave its overall charge largely unchanged. Furthermore, the abundance of redox active moieties (e.g., quinone, phenolic) in HAs is low compared to other functional groups involved in the sorption (e. g. carboxylic acids).[84] Hence, the properties of HA influencing sorption process (electric charge, polarity, binding sites) are not expected to be significantly altered by changes in redox state of HA moieties. The similar sorption behavior and extent of reduced and native ESHA both at Al_2O_3 and at DAX-8 resin is consistent with the mechanistic interpretation of the interactions of ESHA with these sorbents. It further points to a predominant role of carboxylic groups in surface complex formation with Al_2O_3 as compared to phenolic groups.
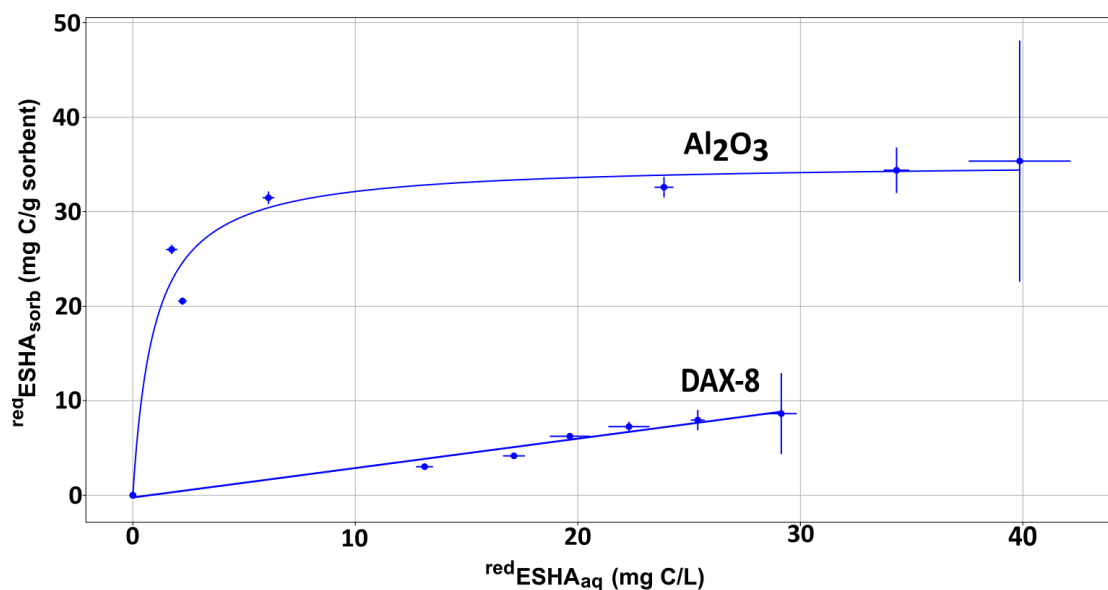
Figure 7. Sorption Isotherms of electrochemically reduced Elliott Soil humic acid (^{red}ESHA) on aluminum oxide (Al$_2$O$_3$) and hydrophobic resin (DAX-8) at pH 7 and 0.1 M KCl. The solid lines represent isotherm fits (Langmuir and linear). Langmuir Isotherm parameters values for Al$_2$O$_3$ are: Elliott Soil (ESHA): K_{ads} = 0.34 L / mg; ^{red}ESHA$_{max}$ = 35.7 g C/g Al$_2$O$_3$; RMSE = 2.27. Linear regression parameters (^{red}ESHA$_{sorb}$ = Kd * ^{red}ESHA$_{aq}$) for DAX-8 are: Elliott Soil: K$_d$(ESHA) = 0.299 L/mg; r^2 = 0.959.

Redox Properties of sorbed HA - Effects of extent of sorption and surface coverage. Experiments were designed to cover different degrees of HA adsorption (percentages of sorbed HA vs. total HA). For each type of HA the electrochemical properties were measured for i) the HA stock solution, HA$_{stock}$ (= reference); ii) the aqueous HA at sorption equilibrium, HA$_{aq}$ (= filtrate of the suspension containing sorbent and HA); iii) the whole suspension containing the sorbent and HA, HA$_{aq+sorb}$ (= HA sorbed + aqueous). Note that samples of i) and iii) should have identical EEC, EAC and EDC values if sorption of HAs had no effect on their redox properties as in both samples the entire amount of HA in the systems, HA$_{tot}$, is measured. In contrast to HA$_{stock}$ (i) and HA$_{aq+sorb}$ (iii), samples of HA$_{aq}$ (ii) represent only the sub-fraction of HA$_{tot}$ left behind in solution after adsorption of HA to the sorbent. Control experiments confirmed that aluminum oxide and DAX-8 particles were not electroactive in the absence of HA, i.e., suspensions of these sorbents had no detectable current responses in MER and MEO (**Fig. SI4**). Note that the measured EAC of the three HA standard isolates were in good agreement with reported values, while higher EDC values were obtained.[20] However, several independent determinations were done to assure the reproducibility of the electrochemical measurements conducted in this analysis. The typical time frame for mediated electrochemical reduction and oxidation of mediators and HA samples was somewhat longer than previously reported.[20,42]

49

Figure 8 illustrates how EEC, EDC and EEC of the three types of HAs changed upon sorption to Al_2O_3 or DAX-8. For Al_2O_3, all HAs displayed a similar trend with regard to changes in redox properties as a function of sorption level (**Fig. 8d**, **8e** and **8f**). The EDC of whole suspension samples ($HA_{aq+sorb}$) were significantly higher (up to 200 %) compared to HA_{stock} whereas the EAC remained unchanged. This effect was more pronounced with increasing amounts of sorbed HA. Given the absence of electron transfer between the HA and the redox inert aluminum oxide, these results can be associated to:

i) Conformational re-arrangements of HA moieties might take place on the Al_2O_3 surface; an opening of the HA supramolecular folding may render the electron donor groups (e.g., phenols, hydroquinones) accessible to electron exchange with the electron mediator ABTS, which were not accessible in solution, and thus the apparent EDC of adsorbed HA might be enhanced. This finding is in line with a study[21] that reported for a Humic Acid Like Poly-condensate (HALP) coated on SiO_2 nanoparticles a massive increase (300 %) of Interfacial Hydrogen Atom Transfer (HAT) compared to HALP in solution. This hypothesis account for the well-known potential for conformational re-arrangements of HA supramolecular structures that depend on the system features (HA concentration, pH, ionic strength, etc.).[85-87] In my experiments, pH 7, 0.1 M background electrolyte and low HA concentration (< 500 mgC*L^{-1}), HAs is expected to behave as a permeable polyelectrolyte[85] either in aqueous phase or in sorbed state. Nevertheless, HA_{sorb} fraction consistently presented (for SRHA and PPHA) higher EDC (calculated as follows: calc. EDC (HA_{sorb}) = meas. EDC ($HA_{aq+sorb}$) - meas. EDC (HA_{aq})) compared to HA_{stock} (**Fig. SI5**), making the sorbed redox active groups (e.g., phenols) reactive to redox mediators, which were not reactive in solution.

ii) Catalyzed polymerization of polyphenolic compounds in HA by the aluminum oxide under oxidizing conditions. This hypothesis was evaluated by measuring the EDC of a model polyphenol (CHL = chlorogenic acid) and of an electrochemically reduced hydroquinone (LAWred = lawsone), both adsorbed to Al_2O_3. Considering that polyphenol and hydroquinone moieties are the major electron donor groups within HA, determination of their EDC upon sorption to Al_2O_3 would be crucial to understand the increases in EDC described above for HA. Furthermore, previous studies have shown that polyphenolic compounds, including CHL, exhibit prominent radical scavenging activities,[88-89] and that the oxidized forms of polyphenols can undergo dimerization (or higher polymerization) to regenerate the oxidizable -OH moieties, resulting in larger number of transferred electron compared to the number of –OH (e.g., n = 2 for CHL) in the molecule.[90-92] Batch sorption experiments (**Table SI2**) were conducted with CHL and LAWred onto Al_2O_3 and showed higher apparent sorption of CHL than of LAWred (**Fig. SI6**). The EDC of CHL sorbed to Al_2O_3 was up to 50 % enhanced in suspension when CHL was almost completely adsorbed (~ 100 %), whereas no change in the EDC of sorbed LAWred was detected compared to dissolved LAWred (**Fig. SI7**). These findings suggest that polymerization of polyphenolic components of HA might be enhanced in the adsorbed

state at the conditions applied here (low HA surface coverage of Al_2O_3 and nearly 100% of HA adsorbed).

Furthermore, for Al_2O_3, HA_{aq} fractions tend to have smaller EEC compared to HA_{stock} regardless of the extent of adsorption. At nearly 100 % sorbed HA, the EEC of HA_{aq} was negligible for all three HAs studied. Thus, the HA components left in solution were very poor in redox active functional groups (e.g., quinone/hydroquinone, phenols).
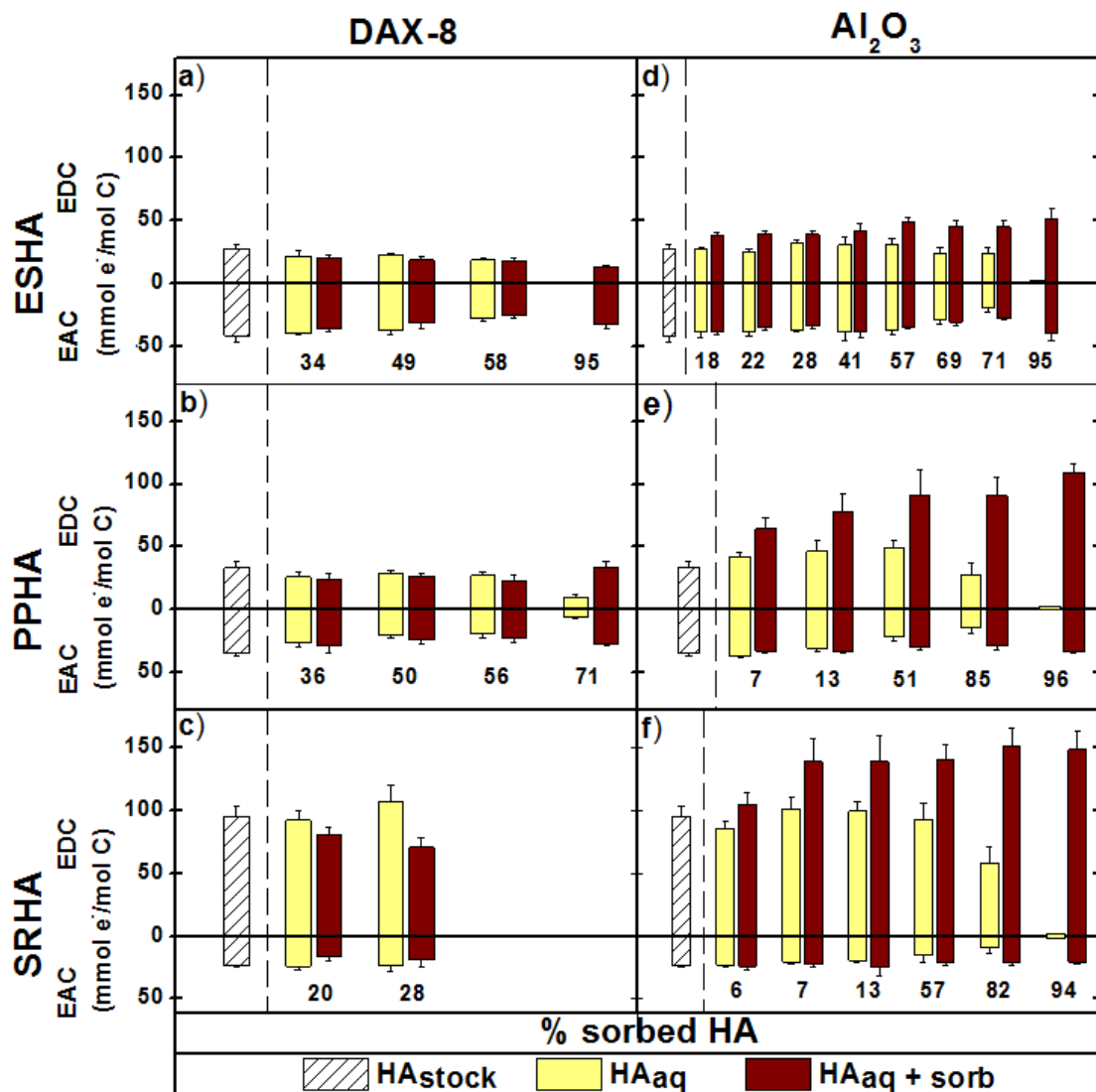
Figure 8. Electron Donating Capacities (EDC, E_H(pH 7) = 0.61 V vs. SHE.) and Electron Accepting Capacities (EAC, E_H(pH 7) = - 0.49 V vs. SHE.) as a function of percentage of sorbed Humic Acid of: **a)** Elliott Soil (ESHA), **b)** Pahokee Peat (PPHA) and **c)** Suwannee River (SRHA) humic acid upon sorption to hydrophobic resin (DAX-8) and, of: **d)** ESHA, **e)** PPHA and **f)** SRHA fractions upon sorption to aluminum oxide (Al_2O_3). HA stock solutions (HA_{stock}, white crossed-lined bars), 0.45 µm filtered fractions containing non-sorbed HA (HA_{aq}, light yellow bars) and whole suspensions containing sorbents + sorbed HA + non-sorbed HA ($HA_{aq+sorb}$, dark red bars). Data is arranged in ascending HA sorption level.

Conversely, for DAX-8 particles (panels a, b and c in **Fig. 8),** HA$_{aq+sorb}$ samples showed an inverse effect: lower EDC with increasing percentage of sorbed HA. This might also be due to conformational re-arrangements of HA moieties upon sorption to DAX-8, but based on different physico-chemical interactions than at Al$_2$O$_3$ and can be rationalized as follows: The absence of specific interactions such as ligand exchange between the DAX-8 and HA functional groups may allow for a hydrophobicity driven conformation of adsorbed HA components. Higher cohesion of HA at the non-polar DAX-8 surface may lead to more rigid HA structural entities by local accumulation of non-polar HA-domains at their surface and redox active polar groups within such entities resulting in a lower accessibility of redox active functional groups in HA at DAX-8. Similarly to Al$_2$O$_3$, the EEC of HAaq fractions in DAX-8 systems also decreased at high degrees of HA depletion from solution, which can be attributed to HA fractionation.

Effect of Sorption Mechanism on the Redox Properties of sorbed HA. **Figure 9** further highlights the different effects that sorption to either Al$_2$O$_3$ or DAX-8 has on the redox properties of HS by comparing EDC and EAC values for the two sorbents at comparable degrees of HA adsorption and for different sorption levels (low vs. medium vs. almost complete sorption). At aluminum oxide, whole suspensions containing sorbed HA showed substantially higher EDC values (up to 200 %) compared to HA stock solution. The EEC of filtered supernatants (after sorption to Al$_2$O$_3$) was comparable to HA stock solutions at low percentage of sorbed HA ($<$ 50 % sorbed PPHA). At almost 100 % sorbed HA, the EEC of non-sorbed HA fractions was negligible, being attributed to: i) most redox active molecules were depleted from solution by sorption to Al$_2$O$_3$ and ii) the transferred charge in MER-MEO was below quantification limit for those samples with very low carbon content. The quantification limit in this experimental set-up was about DOC ~ 5 mg C/L (sample volume $\leq$ 200 µL). At non-polar DAX-8, however, whole samples (containing sorbed HA) showed lower EDC (up to 50 percent for ESHA compared to ESHA stock solution), although for PPHA suspensions changes in EDC were negligible. For filtered supernatant fractions (HAaq after sorption to DAX-8), no change in the EDC was detected at low levels of sorbed HA (lower concentration of HA per mass of DAX-8), but for medium to high level of sorbed HA, strong depletion of the remaining HAaq with regard to redox active components occurred. This implies that under conditions where sorbed humic acid accounts for the major fraction of the total HS in the system, the remaining HS in solution are highly depleted in redox active components regardless of the type of sorptive interactions. Apparently, preferential sorption of larger HS components due to non-specific interactions at non-polar sorbents and specific adsorption of complexing components at polar minerals led to a similar result in terms of redox properties of the dissolved HS components at very high degrees of adsorption. Dissolved organic matter when present only as a minute fraction compared to sorbed organic matter, might exhibit very different redox properties as might be expected from analyses of total HS after harsh extractions. Conversely, at such conditions redox active components of HS are highly enriched at environmental relevant surfaces with so far unknown consequences for electron transfer across the mineral-water interface.

Furthermore, HAs adsorbed at polar and non-polar surfaces have a different redox capacity and a different redox state even in the absence of electron transfer with the supporting sorbent.
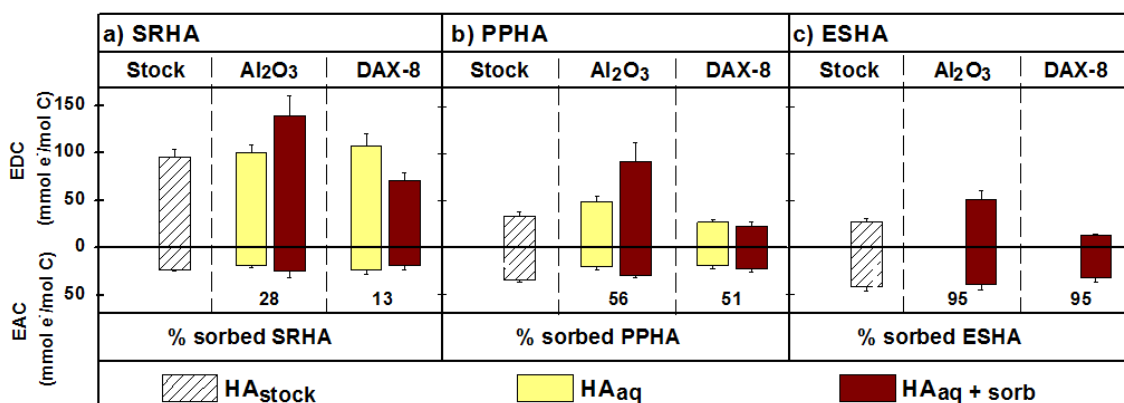
Figure 9. Electron Donating Capacities (EDC, E_H(pH 7) = 0.61 V vs. SHE.) and Electron Accepting Capacities (EAC, E_H(pH 7) = - 0.49 V vs. SHE.) of humic acids upon sorption to Al_2O_3 and DAX-8 at different sorption levels: **a)** Suwannee River (SRHA; 28 % (Al_2O_3) - 28 % (DAX-8) sorbed), **b)** center, Pahokee Peat (PPHA; 56 % (Al_2O_3) - 51 % (DAX-8) sorbed)) and **c)** Elliott Soil (ESHA; ~ 95 % sorbed for both sorbents). White crossed-line bars represent HA stock solutions (HA_{stock}), light yellow bars correspond to 0.45 µm filtered HA (HA_{aq}) and dark red bars correspond to the whole suspensions containing sorbents (Al_2O_3 or DAX-8) + sorbed HA + non-sorbed HA ($HA_{aq+sorb}$). Data was re-plotted from **Fig. 8.**

Effect of HA redox state on the Redox Properties of sorbed HA. By applying bulk direct electrochemical reduction, the redox state of ESHA was altered to obtain a preparation of ESHA at lower reduction potential ($^{red}ESHA_{stock}$). **Figure 10** compares, exemplified by ESHA, the effect of initial redox state of HAs on sorption-induced changes of their electrochemical properties. At Al_2O_3 and contrary to native ESHA, sorption of reduced ESHA ($^{red}ESHA_{aq+sorb}$) typically led to slightly lower EEC values of whole suspension samples compared to reduced ESHA stock solution ($^{red}ESHA_{stock}$) without apparent effects of the extent of sorption. This behavior might indicate that for reduced ESHA the diversity of redox active functional groups in the HA structure is dominated by reduced groups, and therefore, the weight of HA conformational re-arrangements onto the polar Al_2O_3 surface turns out to produce only minor variations on the EEC of HA.

The aqueous fractions ($^{red}ESHA_{aq}$), however, had a substantially lower EEC at all sorption levels compared to $^{red}ESHA_{stock}$, with negligibly low EEC values at very high sorption levels > 90 percent. The large changes in EEC of the latter $^{red}ESHA_{aq}$ fractions might be explained by strong depletion of aromatic components[61] due to sorptive fractionation as indicated by a decrease in $SUVA_{254}$ of up to ~ 75 % compared to $^{red}ESHA_{stock}$ **(Fig. 10c).** Note that bulk reduction of HAs does not significantly modify their UV−Vis absorbance spectra.[83] A low content of aromatic functional groups

including quinones and phenols correlates with low electron exchange capacities of HA.[15, 18, 20]

Sorption of $^{red}ESHA_{sorbed}$ to DAX-8 (**Fig. 10b**) resulted in significantly lower EDC and EAC values for both, whole suspensions and aqueous samples compared to $^{red}ESHA_{stock}$ at intermediate sorption levels (ca. 30-70% sorbed). Thus, at DAX-8 sorption induced effects for reduced ESHA were very similar to those of native ESHA. The SUVA$_{254}$ data for $^{red}ESHA_{aq}$ (panel **d** of **Fig. 10**) indicate that sorption to non-polar DAX-8 did not trigger strong fractionation and thus preferential sorption of reduced aromatic moieties at DAX-8 surface at intermediate sorption levels.
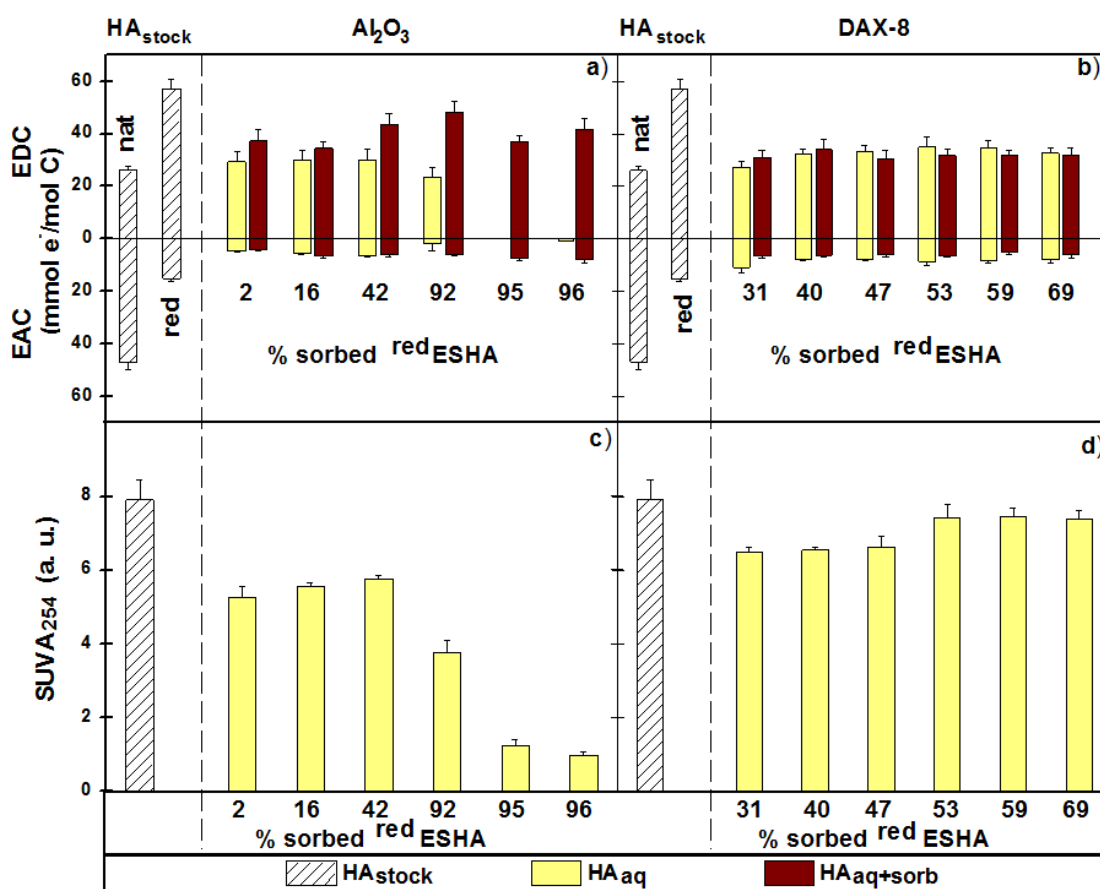
Figure 10. Upper panels (**a** and **b**): Effects of sorption at Al$_2$O$_3$ and DAX-8 of electrochemically reduced ($^{red}ESHA$) Elliott Soil Humic Acid (E$_H$ (pH 7) = - 0.59 V vs. SHE) on its Electron Donating Capacities (EDC, E$_H$(pH 7) = 0.61 V vs. SHE.) and Electron Accepting Capacities (EAC, E°$_H$(pH 7) = - 0.49 V vs. SHE.). Lower panels (**c** and **d**): Specific Ultraviolet Absorbance at 254 nm (SUVA$_{254}$) of reduced Elliott Soil Humic Acid (ESHA) samples corresponding to: native ($^{nat}ESHA_{stock}$) and reduced ($^{red}ESHA_{stock}$) ESHA stock solutions (white crossed-line bars), 0.45 µm filtrates ($^{red}ESHA_{aq}$; light yellow bars), and whole suspensions containing sorbents+ sorbed HA + non-sorbed HA ($^{red}ESHA_{aq+sorb}$; dark red bars).

54

Oxidation of aqueous and sorbed ESHA. From a biogeochemical perspective, one intriguing question is if sorption of humic acids affects the reversibility of their oxidation/reduction behavior. In electrochemically reduced dissolved humic acids, a small fraction of redox active groups is not readily oxidized by dissolved molecular oxygen (O_2). Repeated reduction-oxidation cycles, however, do not further change the electrochemical properties of HAs, neither their EEC nor their redox state after oxidation.[42] Thus, preliminary experiments were conducted to assess the effect of sorption on the oxidation of electrochemically reduced ESHA by O_2 (**Fig. 11**). Oxidation of ESHA in the stock solution did give neither the same redox state nor the same EEC as the native (untreated) ESHA. As expected, the treatment of ESHA by direct electrochemical reduction at - 590 mV (vs. SHE.) at pH 7 and subsequent oxidation by O_2 caused some irreversible changes in its redox properties in good agreement with a study on Leonardite Humic Acid.[42] As a validation step in our experiments, partially reduced ESHA (aliquot taken approximately at a half stage of the direct electrochemical reduction) and reduced ESHA had similar redox states after re-oxidation (**Fig. SI5**), it is suggested that the applied O_2 treatment oxidized ESHA to the highest possible extent under the applied conditions regardless of the degree of electrochemical reduction. Note that oxidation was performed separately for the filtrate and for the whole suspensions.

EDC/EEC	0.36	0.79	0.46	0.80	0.47	0.84	0.53	0.82	0.43	0.88	0.61
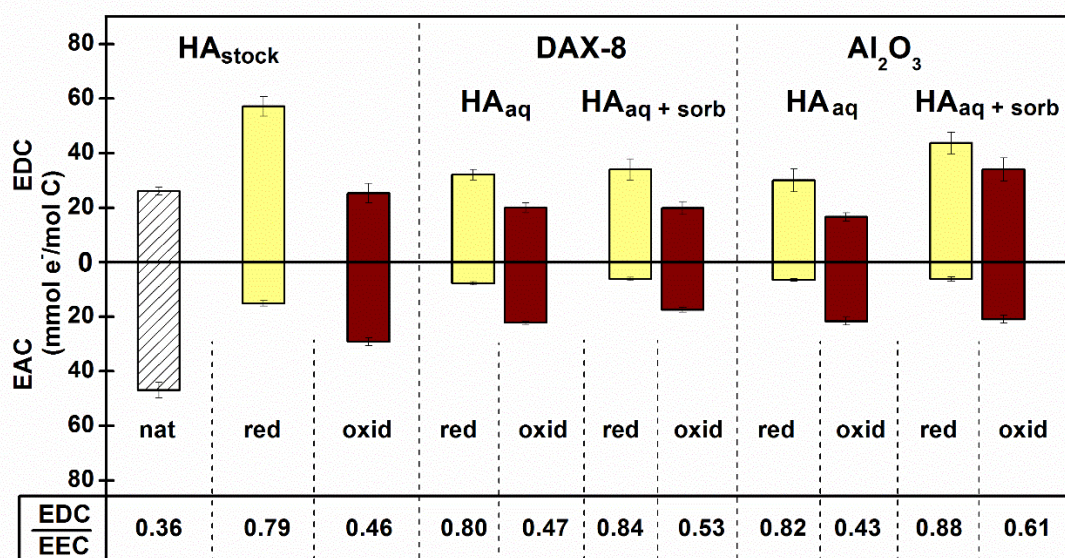
Figure 11. Effects of oxidation by O_2 of electrochemically reduced Elliott Soil Humic Acid in the presence and absence of Al_2O_3 and DAX-8 sorbents on its Electron Donating Capacities (EDC, E_H (pH 7) = 0.61 V vs. SHE.) and Electron Accepting Capacities (EAC, E_H(pH 7) = - 0.49 V vs. SHE.). Bar colors define the HA specific redox state: native HA (nat, crossed-line), reduced HA (red, Light yellow) and oxidized HA (oxid, red wine). For relative comparison, initial % of sorbed [red]ESHA was: 40 % on DAX-8 and 42 % on Al_2O_3. HA_{stock} corresponds to HA stock solutions at defined redox states, HA_{aq} to 0.45 µm filtrates, and $HA_{aq+sorb}$ represents whole suspensions containing sorbents+ sorbed HA + non-sorbed HA.

The redox state (i.e., EDC/EEC) of after oxidation of the filtrates and the ^{red}ESHA$_{stock}$ solutions were similar, regardless of the type of sorbent. While for DAX-8 also the whole suspensions were close to this common redox state, reoxidized ESHA in the presence of Al_2O_3 was up to 25 % less oxidized. Generally, the EEC of all oxidized ESHA fractions decreased notably. The decrease in EEC after oxidation, however, was smaller for the whole suspension samples in the presence of Al_2O_3 compared to the aqueous ESHA fractions. This finding might indicate that ESHA sorbed at Al_2O_3 is less reactive towards O_2 than dissolved ESHA. As oxidation of adsorbed reduced ESHA leads to an increase of the sorbed fraction at Al_2O_3 (**Fig. SI6**, **SI7**) and taking into account that adsorption of native ESHA increased its EEC (**Fig. 8**), a sound interpretation of the observed EEC changes in the whole suspension samples of Al_2O_3 and an assessment of their implications for the reactivity of adsorbed humic acids require further experimental studies.

2.5   Environmental Implications.

These results demonstrate that even in the absence of electron transfer to the sorbent, adsorption considerably affects the redox properties of humic substances. Since a large fraction of natural organic matter in soil, sediment, and groundwater is present in sorbed state, awareness of this phenomenon is important for assessing direct and mediated electron transfer processes involving NOM. Likewise, these findings might be crucial to better comprehend mineral stabilization and carbon sequestration process in the environment. This work sets the basis for a mechanistic understanding of processes in future studies dealing with more complex systems which might address redox active minerals (i.e., iron-bearing clay minerals and iron (oxyhydr-)oxides) and HA samples that are more representative for natural NOM. Furthermore, complementary characterization techniques of NOM could provide alternative lines of evidence for unraveling the molecular causes of the changes in the redox chemistry of HA upon sorption to minerals. For instance, high resolution mass spectrometry might help to quantify preferential sorption of certain HA subfractions (e. g., tannins) and thus potentially explain the changes in HA redox chemistry discussed here by composition changes.

2.6   References

1.   Suffet, I. H.; MacCarthy, P. Aquatic Humic Substances and Their Influence on the Fate and Treatment of Pollutants. In *Aquatic Humic Substances.* Advances in Chemistry, Vol. 219. American Chemical Society: Washington, DC, **1988**.
2.   Ghabbour, E. A.; Davies, G. *Understanding Humic Substances: Advanced Methods, Properties and Applications*. The Royal Society of Chemistry: Cambridge, UK, **1999**.
3.   D'Andrilli, J.; Foreman, C. M.; Marshall, A. G.; McKnight, D. M. Characterization of IHSS Pony Lake fulvic acid dissolved organic matter by electrospray ionization Fourier transform ion cyclotron resonance mass spectrometry and fluorescence spectroscopy. *Org. Geochem.*, **2013**, 65, 19-28.

4.   Qualls, R.G.; Haines, B.L.; Swank, W.T. Fluxes of dissolved organic nutrients and humic substances in a deciduous forest. *Ecology*, **1991**, 72, 254-266.

5.   McDonald, S.; Bishop, A. G.; Prenzler, P. D.; Robards, K. Analytical chemistry of freshwater humic substances. *Anal. Chim. Acta*, **2004**, 527 (2), 105-124.

6.   Schumacher, M.; Christl, I.; Vogt, R. D.; Barmettler, K.; Jacobsen, C.; Kretzschmar, R. Chemical composition of aquatic dissolved organic matter in five boreal forest catchments sampled in spring and fall seasons. *Biogeochemistry*, **2006**, 80 (3), 263-275.

7.   Lovley, D. R.; Coates, J. D.; Blunt-Harris, E. L.; Phillips, E. J. P.; Woodward, J. C. Humic substances as electron acceptors for microbial respiration. *Nature*, **1996**, 382 (6590), 445-448

8.   Jiang, J.; Kappler, A. Kinetics of microbial and chemical reduction of humic substances: Implications for electron shuttling. *Environ. Sci. Technol.*, **2008**, 42 (10), 3563-3569.

9.   Wolf, M.; Kappler, A.; Jiang, J.; Meckenstock, R. U. Effects of Humic Substances and Quinones at Low Concentrations on Ferrihydrite Reduction by Geobacter metallireducens. *Environ. Sci. Technol.*, **2009**, 43 (15), 5679-5685.

10.   Dunnivant, F. M.; Schwarzenbach, R. P.; Macalady, D. L. Reduction of substituted nitrobenzenes in aqueous solutions containing natural organic matter. *Environ. Sci. Technol.*, **1992**, 26 (11), 2133-2141.

11.   Curtis, G. P.; Reinhard, M. Reductive dehalogenation of hexachlorethane, carbon-tetrachloride and bromoform by anthrahydroquinone disulfonate and humic acid. *Environ. Sci. Technol.*, **1994**, 28 (13), 2393-2401.

12.   Aeschbacher, M.; Vergari, D.; Schwarzenbach, R. P.; Sander, M. Electrochemical Analysis of Proton and Electron Transfer Equilibria of the Reducible Moieties in Humic Acids. *Environ. Sci. Technol.*, **2011**, 45 (19), 8385-8394.

13.   Nurmi, J. T.; Tratnyek, P. G. Electrochemical properties of natural organic matter (NOM), fractions of NOM, and model biogeochemical electron shuttles. *Environ. Sci. Technol.*, **2002**, 36 (4), 617-624.

14.   Maximov, O. B; Glebko L. I. Quinoid groups in humic acids. *Geoderma*, **1974**, 11 (1), 17-28.

15.   Scott, D. T.; McKnight, D. M.; Blunt-Harris, E. L.; Kolesar, S. E.; Lovley, D. R. Quinone moieties act as electron acceptors in the reduction of humic substances by humics-reducing microorganisms. *Environ. Sci. Technol.*, **1998**, 32 (19), 2984-2989.

16.   Nurmi, J. T.; Tratnyek, P. G. Electrochemistry of Natural Organic Matter. In *Aquatic Redox Chemistry*; Tratnyek, P. G.; Grundl, T. J.; Haderlein, S. B., Eds.; Oxford University Press: Washington, **2011**, pp. 129-151.

17.   Macalady, D. L.; Walton Day, K. Redox Chemistry of Natural Organic Matter (NOM): Geochemist's Dream, Analytical Chemist's Nightmare. In *Aquatic Redox Chemistry*; Tratnyek, P. G.; Grundl, T. J.; Haderlein, S. B., Eds.; Oxford University Press: Washington, **2011**; pp 87-111.

18.   Struyk, Z.; Sposito, G. Redox properties of standard humic acids. *Geoderma*, **2001**, 102, 329-346.

19.   Helburn, R. S.; MacCarthy, P. Determination of some redox properties of humic acid by alkaline ferricyanide titration. *Anal. Chim. Acta*, **1994**, 295, 263-272.

20. Aeschbacher, M.; Graf, C.; Schwarzenbach, R. P.; Sander, M. Antioxidant properties of humic substances. *Environ. Sci. Technol.*, **2012**, 46 (9), 4916-4925.

21. Bletsa, E.; Stathi, P.; Dimos, K.; Louloudi, K.; Deligiannakis, Y. Interfacial Hydrogen Atom Transfer by nanohybrids based on Humic Acid Like Polycondensates. *J. Colloid Interface Sci.*, **2015**, 455 163-171.

22. Kaiser, K.; Guggenberger, G.; Zech, W. Sorption of DOM and DOM fractions to forest soils. *Geoderma*, **1996**, 74 (3-4), 281-303.

23. Avena, M. J.; Koopal, L. K. Desorption of humic acids from an iron oxide surface. *Environ. Sci. Technol.*, **1998**, 32 (17), 2572-2577.

24. Sander, S.; Mosley, L. M.; Hunter, K. A. Investigation of interparticle forces in natural waters: Effects of adsorbed humic acids on iron oxide and alumina surface properties. *Environ. Sci. Technol.*, **2004**, 38 (18), 4791-4796.

25. Murphy, E. M.; Zachara, J. M.; Smith, S. C. Influence of Mineral-Bound Humic Substances on the Sorption of Hydrophobic Organic Compounds. *Environ. Sci. Technol.*, **1990**, 24, 1507-1516.

26. Ochs, M.; Cosovic, B.; Stumm, W. Coordinative and hydrophobic interaction of humic hydrophobic mercury surfaces. *Geochim. Cosmochim. Acta*, **1994**, 58 (2), 639-650.

27. Gu, B.; Schmitt, J.; Chen, Z. H.; Liang, L. Y.; McCarthy, J. F. Adsorption and desorption of natural organic matter on iron oxide. Mechanisms and models. *Environ. Sci. Technol.*, **1994**, 28 (1), 38-46.

28. Kaiser, K.; Zech, W. Release of natural organic matter sorbed to oxides and a subsoil. *Soil Sci. Soc. Am. J.*, **1999**, 63 (5), 1157-1166.

29. Kang, S. H.; Xing, B. S. Humic acid fractionation upon sequential adsorption onto goethite. *Langmuir*, **2008**, 24 (6), 2525-2531.

30. Vermeer, A. W.; Koopal, L. K. Adsorption of Humic Acids to Mineral Particles. 2. Polydispersity Effects with Polyelectrolyte Adsorption. *Langmuir*, **1998**, 14, 4210-4216.

31. Guggenberger, G.; Kaiser, K. Dissolved organic matter in soil: challenging the paradigm of sorptive preservation. *Geoderma*, **2003**, 113, 293-310.

32. Kalbitz, K.; Schwesig, D.; Rethemeyer, J.; Matzner, E. Stabilization of dissolved organic matter by sorption to the mineral soil. *Soil Biol. Biochem.*, **2005**, 37, 1319-1331.

33. Kaiser, K.; Guggenberger, G. The role of DOM sorption to mineral surfaces in the preservation of organic matter in soil. *Org. Geochem.*, **2000**, 31, 711-725.

34. Hur, J.; Schlautman, M. A. Molecular weight fractionation of humic substances by adsorption onto minerals. *J. Colloid Interface Sci.*, **2003**, 264, 313-321.

35. Heidmann, I.; Christl, I.; Kretzschmar, R. Sorption of Cu and Pb to kaolinite–fulvic acid colloids: Assessment of sorbent interactions. *Geochim. Cosmochim. Acta*, **2005**, 69 (7), 1675-1686.

36. Meier, M.; Namjesnik-Dejanovic, K.; Maurice, P. A.; Chin, Y. P.; Aiken, G. R. Fractionation of aquatic natural organic matter upon sorption to goethite and kaolinite. *Chem. Geol.*, **1999**, 157, 275-284.

37. Claret, F.; Schaefer, T.; Brevet, J.; Reiller, P. E. Fractionation of Suwannee River Fulvic Acid and Aldrich Humic Acid on α-Al2O3: Spectroscopic Evidence. *Environ. Sci. Technol.*, **2008**, 42, 8809-8815.

38. Galindo, C.; Del Nero, M. Molecular Level Description of the Sorptive Fractionation of a Fulvic Acid on Aluminum Oxide Using Electrospray Ionization Fourier Transform Mass Spectrometry. *Environ. Sci. Technol.*, **2014**, 48, 7401-7408.

39. Galindo, C.; Del Nero, M. Chemical fractionation of a terrestrial humic acid upon sorption on alumina by high resolution mass spectrometry. *RSC Adv.*, **2015**, 5, 73058.

40. Tao, Z. Y.; Chu, T. W.; Du, J. Z.; Dai, X. X.; Gu, Y. J. Effect of fulvic acids on sorption of U(VI), Zn, Yb, I and Se(IV) onto oxides of aluminum, iron and silicon. *Applied Geochemistry*, **2000**, 15 (2), 133-139.

41. Yang, K.; Lin, D. H., Xing, B. S. Interactions of Humic Acid with Nanosized Inorganic Oxides. *Langmuir*, **2009**, 25 (6), 3571-3576.

42. Aeschbacher, M.; Sander, M.; Schwarzenbach, R. P. Novel electrochemical approach to assess the redox properties of humic substances. *Environ. Sci. Technol.*, **2010**, 44 (1), 87−93.

43. Aeschbacher, M.; Brunner, S. H.; Schwarzenbach, R. P.; Sander, M. Assessing the effect of humic acid redox state on organic pollutant sorption by combined electrochemical reduction and sorption experiments. *Environ. Sci. Technol.*, **2012**, 46 (7), 3882-3890.

44. Gorski, C. A.; Aeschbacher, M.; Soltermann, D.; Voegelin, A.; Baeyens, B.; Fernandes, M. M.; Hofstetter, T. B.; Sander, M. Redox properties of structural Fe in clay minerals. 1. Electrochemical quantification of electron-donating and -accepting capacities of smectites. *Environ. Sci. Technol.*, **2012**, 46 (17), 9360-9368.

45. Gorski, C. A.; Kluepfel, L.; Voegelin, A.; Sander, M.; Hofstetter, T. B. Redox properties of structural Fe in clay minerals. 2. Electrochemical and spectroscopic characterization of electron transfer irreversibility in ferruginous smectite, SWa-1. *Environ. Sci. Technol.*, **2012**, 46 (17), 9369-9377.

46. Gorski, C. A.; Kluepfel, L.; Voegelin, A.; Sander, M.; Hofstetter, T. B. Redox properties of structural Fe in clay minerals: 3. Relationships between smectite redox and structural properties. *Environ. Sci. Technol.*, **2013**, 47 (23), 13477-13485.

47. Kluepfel, L.; Piepenbrock, A.; Kappler, A.; Sander, M. Humic substances as fully regenerable electron acceptors in recurrently anoxic environments. *Nat. Geosci.*, **2014**, 7 (3), 195-200.

48. Kluepfel, L.; Keiluweit, M.; Kleber, M.; Sander, M. Redox properties of plant biomass-derived black carbon (biochar). *Environ. Sci. Technol.*, **2014**, 48 (10), 5601-5611.

49. Klein, A. R.; Silvester, E.; Hogan, C. F. Mediated electron transfer between Fe-II adsorbed onto hydrous ferric oxide and a working electrode. *Environ. Sci. Technol.*, **2014**, 48 (18), 10835-10842.

50. Orsetti, S.; Laskov, C.; Haderlein, S. B. Electron Transfer between Iron Minerals and Quinones: Estimating the Reduction Potential of the Fe(II)-Goethite Surface from AQDS Speciation. *Environ. Sci. Technol.*, **2013**, 47, 14161-14168.

51. Lau, M. P.; Sander, M.; Gelbrecht, J.; Hupfer, M. Solid phases as important electron acceptors in freshwater organic sediments. *Biogeochemistry*, **2015**, 123, 4961.

52. Sander, M.; Hofstetter, T. B.; Gorski, C. A. Electrochemical Analyses of Redox-Active Iron Minerals: A Review of Nonmediated and Mediated Approaches. *Environ. Sci. Technol.*, **2015**, 49, 5862-5878.

53. Hoving, A. L.; Sander, M.; Bruggeman, C.; Behrends, T. Redox properties of clay-rich sediments as assessed by mediated electrochemical analysis: Separating pyrite, siderite and structural Fe in clay minerals. *Chem. Geol.*, **2017**, 457, 149-161.

54. Hagemann, N.; Joseph, S.; Schmidt, H.P.; Kammann, C.I.; Harter, J.; Borch, T.; Young, R.B.; Varga, K.; Taherymoosavi, S.; Elliott, K.W.; McKenna, A.; Albu, M.; Mayrhofer, C.; Obst, M.; Conte, P.; Dieguez-Alonso, A.; Orsetti, S.; Subdiaga, E.; Behrens, S.; Kappler, A. Organic coating on biochar explains its nutrient retention and stimulation of soil fertility. *Nat. Commun.*, **2017**, 8, 1089.

55. Seaton, N. A.; Walton, J. P. R. B.; Quirke, N. A new analysis method for the determination of the pore size distribution of porous carbons from nitrogen adsorption measurements. *Carbon*, 1989, 27, 853-861.

56. Zsolnay, A. Dissolved organic matter: artefacts, definitions, and functions. *Geoderma*, **2003**, 113, 187-209.

57. Langmuir, I. The Adsorption of Gases on Plane Surfaces of Glass, Mica and Platinum. J. *Am. Chem. Soc.*, **1918**, 40, 9, 1361-1403.

58. Veith, J. A.; Sposito, G. On the Use of the Langmuir Equation in the Interpretation of "Adsorption" Phenomena. *Soil Sci. Soc. Am. J.*, **1977**, 41, 697-702.

59. Gu, B.; Mehlhorn, T. L.; Liang, L.; McCarthy, J. F. Competitive adsorption, displacement, and transport of organic matter on iron oxide: I. Competitive adsorption. *Geochim. Cosmochim. Acta*, **1996**, 60, 1943-1950.

60. Gu, B.; Schmitt J.; Chen Z.; Liang L.; McCarthy J. F. Adsorption and desorption of different organic matter fractions on iron oxide. *Geochim. Cosmochim. Acta*, **1995**, 59, 219-229.

61. Weishaar, J. L.; Aiken, G. R.; Bergamaschi, B. A.; Fram, M. S.; Fujii, R.; Mopper, R. Evaluation of Specific Ultraviolet Absorbance as an Indicator of the Chemical Composition and Reactivity of Dissolved Organic Carbon. *Environ. Sci. Technol.*, **2003**, 37, 20, 4702-4708.

62. Mobed, J. J.; Hemmingsen, S.L.; Autry, J. L.; McGown, L. B. Fluorescence characterization of IHSS humic substances: total luminescence spectra with absorbance correction. *Environ. Sci. Technol.*, **1996**, 30 (10), 3061-3065.

63. Coble, P. G. Characterization of marine and terrestrial DOM in seawater using excitation-emission matrix spectroscopy. *Mar. Chem.*, **1996**, 51, 325-346.

64. Chen, J.; LeBoeuf, E. J.; Dai, S.; Gu, B. Fluorescence spectroscopic studies of natural organic matter fractions. *Chemosphere*, **2003**, 50 (5), 639-647.

65. Shen, Y. Sorption of humic acid to soil: the role of soil mineral composition. *Chemosphere*, **1999**, 38, 11, 2489-2499.

66. Schlautman, M. A.; Morgan, J. J. Adsorption of aquatic humic substances on colloidal-size aluminum oxide particles: Influence of solution chemistry. *Geochim. Cosmochim. Acta*, **1994**, 58, 20, 4293-4303.

67. Davis, J. A. Adsorption of natural dissolved organic matter at the oxide/water interface. *Geochim. Cosmochim. Acta*, **1982**, 46 (11), 2381-2393.

68. Nordin, J.; Persson, P.; Laiti, E.; Sjoberg, S. Adsorption of o-Phthalate at the Water−Boehmite (γ-AlOOH) Interface: Evidence for Two Coordination Modes. *Langmuir*, **1997**, 13, 4085-4093.

69. Specht, C. H.; Frimmel, F. H. An in situ ATR-FTIR study on the adsorption of dicarboxylic acids onto kaolinite in aqueous suspensions. *Phys. Chem. Chem. Phys.*, **2001**, 3, 5444-5449.

70. Fein, J. B.; Boily, J. F.; Güçlü, K.; Kaulbach, E. Experimental study of humic acid adsorption onto bacteria and Al-oxide mineral surfaces. *Chem. Geol.*, **1999**, 162, 3345.

71. Eita, M. In situ study of the adsorption of humic acid on the surface of aluminium oxide by QCM-D reveals novel features. *Soft Matter*, **2011**, 7, 709-715.

72. Yan, M.; Liu, C.; Wang, D.; Ni, J.; Cheng, J. Characterization of adsorption of humic acid onto alumina using quartz crystal microbalance with dissipation. *Langmuir*, **2011**, 27, 9860-9865.

73. Armanious, A.; Aeppli, M.; Sander, M. Dissolved Organic Matter Adsorption to Model Surfaces: Adlayer Formation, Properties, and Dynamics at the Nanoscale. *Environ. Sci. Technol.*, **2014**, 48, 9420-9429.

74. Lv, J.; Zhang, S.; Wang, S.; Luo, L.; Cao, D.; Christie, P. Molecular-Scale Investigation with ESI-FT-ICR-MS on Fractionation of Dissolved Organic Matter Induced by Adsorption on Iron Oxyhydroxides. *Environ. Sci. Technol.*, **2016**, 50, 2328-2336.

75. Young, R. B.; Avneri-Katz, S.; McKenna, A. M.; Chen, H.; Bahureksa, W.; Polubesova, T.; Chefetz, B.; Borch, T. Composition-Dependent Sorptive Fractionation of Anthropogenic Dissolved Organic Matter by Fe(III)-Montmorillonite. *Soil. Syst.*, **2018**, 2 (1), 14.

76. Janot, N.; Reiller, P. E.; Zheng, X.; Croue, J. P.; Benedetti, M. F. Characterization of humic acid reactivity modifications due to adsorption onto α-Al2O3. *Water Res.*, **2012**, 46 (3), 731-740.

77. Peuravuori, J.; Ingman, P.; Pihlaja, K.; Koivikko, R. Comparisons of sorption of aquatic humic matter by DAX-8 and XAD-8 resins from solid-state ^{13}C NMR spectroscopy's point of view. *Talanta*, **2001**, 55 733-742.

78. Chandler, D. Interfaces and the driving force of hydrophobic assembly. *Nature*, **2005**, 437, 640-647

79. Aiken, G. R.; Thurman, E. M.; Malcolm, R. L.; Walton, H. F. Comparison of XAD macroporous resins for the concentration of fulvic acid from aqueous solution. *Anal. Chem.*, **1979**, 51, 1799-1803.

80. Mantoura, R. F. C.; Riley, J. P. The analytical concentration of humic substances from natural waters. *Anal. Chim. Acta*, **1975**, 76, 97-106.

81. Leenheer, J. A. Comprehensive approach to preparative isolation and fractionation of dissolved organic carbon from natural waters and wastewaters. *Environ. Sci. Technol.*, **1981**, 15 (5), 578-587.

82. Uchimiya, M.; Stone, A. T. Redox reactions between iron and quinones: Thermodynamic constraints. *Geochim. Cosmochim. Acta*, **2006**, 70, 1388-1401.

83. Maurer, F.; Christl, I.; Kretzschmar, R. Reduction and reoxidation of humic acid: Influence on spectroscopic properties and proton binding. *Environ. Sci. Technol.*, **2010**, 44, 5787-5792.

84. Thurman, E. M. *Organic Geochemistry of Natural Waters*; Martinus Nijhoff / Dr. W. Junk Publishers: Dordrecht, The Netherlands, **1985**, pp. 273-361.

85. Ghosh, K.; Schnitzer, M. Macromolecular structures of humic substances. *Soil Sci.*, **1980**, 129 (5), 266.

86. Vance, G. F.; Stevenson, F. J.; Sikora, F. J. Environmental Chemistry of Aluminum-Organic Complexes. In *The Environmental Chemistry of Aluminum*; Sposito, G., Eds.; Second Edition. CRC Press: Florida **1995**, pp. 169-220.

87. Duval, J. F. L.; Wilkinson, K. J.; Van Leeuwen, H. P.; Buffle, J. Humic Substances Are Soft and Permeable: Evidence from Their Electrophoretic Mobilities. *Environ. Sci. Technol.*, **2005**, 39, 6435-6445.

88. Villano, D.; Fernandez-Pachon, M. S.; Moya, M. L.; Troncoso, A. M.; Garcia-Parrilla, M.C. Radical scavenging ability of polyphenolic compounds towards DPPH free radical. *Talanta*, **2007**, 71, 230-235.

89. Born, M.; Carrupt, P.A.; Zini, R.; Bree, F.; Tillement, J. P.; Hostettmann, K.; Testa, B. Electrochemical behaviour and antioxidant activity of some natural polyphenols. *Helv. Chim. Acta*, **1996**, 79, 1147-1158.

90. Hotta, H.; Sakamoto, H.; Nagano, S.; Osakai, T.; Tsujino, Y. Unusually large numbers of electrons for the oxidation of polyphenolic antioxidants. *Biochim. Biophys. Acta*, **2001**, 1526, 159-167.

91. Hotta, H.; Nagano, S.; Ueda, M.; Tsujino, Y.; Koyama, J.; Osakai, T. Higher radical scavenging activities of polyphenolic antioxidants can be ascribed to chemical reactions following their oxidation. *Biochim. Biophys. Acta*, 2002, **1572**, 123-132.

92. Hotta, H.; Ueda, M.; Nagano, S.; Tsujino, Y.; Koyama, J.; Osakai, T. Mechanistic Study of the Oxidation of Caffeic Acid by Digital Simulation of Cyclic Voltammograms. Anal. Biochem., **2002**, 303**,** 66-72.

Chapter 3.

3. Preferential sorption of tannin-like compounds onto aluminum oxide trigger changes in the electron exchange capacities of natural organic matter

3.1   Abstract

Natural Organic Matter (NOM) is a major driver of biogeochemical redox processes in the environment including electron shuttling in microbial transformations, pollutant transformation and mineral stabilization. This work aimed to combine Fourier transform ion cyclotron resonance mass spectrometry (FT-ICRMS) data with emerging knowledge in the electron transfer activity of reducible/oxidizable moieties in humic acid isolates (HA) following adsorption to aluminum oxide (Al_2O_3) and hydrophobic resin (DAX-8). Mediated electrochemical analysis showed that filtered HA supernatants (after sorption to Al_2O_3) presented lower electron exchanges capacities than HA stock solution, being this trend more pronounced with increasing sorption level (up to be negligible at almost complete sorption). The FT-ICRMS data provided evidence for preferential sorption of mainly tannin-like compounds onto Al_2O_3 that contributed to explain electrochemical findings since selective sorption triggers depletion in aqueous phase of polyphenolic rich electron transfer compounds in NOM. Non-selective sorption of NOM to DAX-8 might explain the slight changes in electron exchanges capacities shown by filtered supernatants following sorption. These findings showed the meaningful suitability of combining molecular level and electrochemical approaches to comprehend systems of high complexity with biogeochemical relevance like mineral-organic associations.

3.2 Introduction

Natural Organic Matter (NOM) is an ubiquitous and tremendously complex mixture of up to millions of polyfunctional organic compounds in soils, sediments and aquifers.[1-5] Here, NOM composition and structure reflect ecosystem history, implying a certain uniqueness of each NOM sample.[6-9] NOM plays a major role in biogeochemical processes such as electron shuttling in microbial transformations,[10-13] electron transfer reactions,[14-15] mineral stabilization in the environment,[16-18] among others.

In soils, sediments and groundwater, a large fraction of NOM is commonly present in sorbed state as mineral coating or in particulate state. Therefore, it is expected that sorption on mineral surface often leads to selective fractionation of NOM constituents. Furthermore, the fate and extent of NOM sorptive fractionation is defined by the mineral surface and system characteristics (i.e., pH, ionic strength, porosity, polarity, etc.).[19-22] Prominence of selective as well as non-selective HA sorption was recently described in the context of iron containing clay surfaces.[23] Macroscopic approaches have shown the occurrence of sorptive fractionation of fulvic and humic acids (FA and HA) onto nano-particles of α-Al_2O_3 at pH 6-7 at high FA-HA sorption, highlighting preferred removal of aromatic rich as well as higher sized constituents from solution.[24-25] From the perspective of molecules in NOM, the fractionation of an aquatic FA and water soluble fraction of a terrestrial HA was described by using electrospray ionization Fourier transform mass spectrometry (ESI-FTMS) in negative ionization mode, revealing the great affinity of aromatic oxygen-functionalized compounds, polycyclic aromatics and aliphatic compounds with high O/C ratios to the Al_2O_3 surface and the major roles played by acidic and hydrophobic character on the size-fractionation of HA.[26-27] Despite of its undoubtedly ubiquity in the environment, the addition of salt (electrolyte solution) during the sorption experiments was avoided in these studies, since the salt presence negatively impacts the ESI-FTMS response.[26] Recently, solid phase extraction (SPE) methods have been intensively applied to produce trustworthy NOM isolation with appreciable recovery of NOM and remarkable discrimination against salts.[28-35] Considerable expenditure has been done to improve and to validate such isolation methods in different matrixes.[35-37] In particular, SPE methods using sorbents of functionalized styrene divinylbenzene polymer (PPL),[30] have been reported to recover up to 89 % dissolved organic carbon (DOC) from aquatic NOM samples and to provide advantageous characteristics for high-field Fourier transform ion cyclotron resonance mass spectrometry (FTICR-MS) and nuclear magnetic resonance spectroscopy (NMR) analysis.[33,38-39]

Up to now, investigations related to the effect of NOM fractionation on their redox properties following sorption to mineral surfaces are scarce despite their environmental significance in biogeochemical processes above mentioned. As shown in **Fig. 8**, changes in the Electron Exchange Capacities (EEC) of NOM upon sorption to redox inert sorbents are described. Thus, EEC provides direct quantification of the amount of redox active groups in a molecule and is the sum of the Electron -Donating and -Accepting Capacities (EDC and EAC, respectively) normalized to total mass of analyte. Due to the intrinsic

heterogeneity of NOM, a change in its EDC and/or EAC upon sorption is plausible due to NOM fractionation. In the present work, a systematic investigation of the NOM fractionation upon redox inert sorbents and the effects of polar (aluminum oxide; Al_2O_3) vs. non-polar (hydrophobic resin, DAX-8) sorption is reported. The molecular scale (FT-ICRMS) and mediated electrochemical analysis are combined to better understand the causes of alterations in redox properties of NOM following sorption. Sorption of three standard humic acids (i.e., Elliott Soil (ESHA), Pahokee Peat (PPHA) and Suwannee River (SRHA) to aluminum oxide (Al_2O_3) and a hydrophobic resin (DAX-8) was studied at pH 7 in batch sorption experiments. After pH equilibration time, samples were filtered and the EAC and EDC and specific UV-Vis absorbance at 254 nm ($SUVA_{254}$) were measured from stock HA solutions and filtered supernatants after sorption; high-field FT-ICR mass spectra were acquired following PPL-based solid phase extraction (SPE) to enable a molecular comprehension of the sorption-induced alterations in EEC of HA fractions.

3.3 Materials and methods

Materials used. Aluminum oxide (Al_2O_3 90% standardized; BET surface area = 133.6 ± 0.3 m^2*g^{-1} Merck) and Supelite DAX-8 resin (poly-methylmethacrylate; Supelco; BET surface area = 177 ± 1 m^2*g^{-1}; Sigma-Aldrich Co., USA) were used as sorbents. The Brunauer, Emmett and Teller (BET) method with N_2 adsorption was used to determine the total specific surface area (data not shown).[40] 1,10-Ethylene-2,20-bipyridiniumdibromide monohydrate (Diquat = DQ, Sigma-Aldrich Co., USA), 2,2′-azino-bis(3-ethylbenzothiazoline-6-sulfonic (ABTS, Sigma-Aldrich Co., USA), potassium chloride (KCl; 99+%; Across Organics; Germany), potassium dihydrogen phosphate (Merck; 99.5%; Germany) were used as purchased. All aqueous solutions were prepared in Millipore deionized water. Aluminum oxide was suspended in 0.1 M KCl. DAX-8 solid resin was washed several times with Millipore water up to its Dissolved Organic Carbon (DOC) content was approximately equal to the water blank (data not shown) before suspending 0.1 M KCl. Sorption and electrochemical experiments were conducted under anoxic atmosphere in a glovebox ($O_2 < 0.1$ ppm; N_2 atmosphere, M. Braun, Germany). Stock solutions (HAs, DAX-8, Al_2O_3) were made anoxic by purging with N_2 for 1 hour prior transfer into the glovebox.

Humic Substances (HS). Elliott Soil Humic Acid IV (ESHA; 4S102H), Pahokee Peat Humic Acid (PPHA; 1S103H) and Suwannee River Humic Acid (SRHA; 2S101H) standards were used as received from IHSS and were dissolved in 0.1 M KCl. pH was manually re-adjusted to experimental required conditions (pH = 7) using freshly made solutions (1, 0.1 or 0.01 M) of NaOH and HCl followed by filtration with pre-washed 0.45 µm membranes (Whatman[TM]; 0.45 µm; mixed cellulose ester ME25; Germany) to meet the DOC definition provided by Zsolnay.[41]

Sorption Experiments. Sorption of three humic acid standards to aluminum oxide (Al_2O_3) and hydrophobic resin, DAX-8, was assessed at pH 7 (0.1 M - KCl, no

buffer used) in duplicate batch experiments for several HA/sorbent mass ratios from low sorption up to nearly complete HA sorption according to **Table SI3**. For each HA studied, the UV-Vis spectra of a filtered (0.45µm) aliquot of sample (higher ratio HA/sorbent) was recorded at different time points and sorption equilibrium was assumed when no further changes in UV-Vis absorption spectra and pH were observed (data not shown). After pH stabilization was achieved, samples were filtered with 0.45 µm membranes (Sartorius; Minisart® syringe filter; 0.45µm; regenerate cellulose; Germany) and the filtered supernatants were kept in brown bottles for further analyses.

Characterization of HA. DOC was measured after acidification of filtered supernatants with HCl by using a Vario EL Cube elemental analyzer (Elementar; Hanau; Germany). UV-Vis spectra were acquired in 10 mm quartz cuvettes (Suprasil; Hellma Analytics; Germany) by and a photoLab 6600 UV−vis spectrophotometer (WTW; Germany), and the SUVA$_{254}$ (Specific UV-Vis Absorbance at wavelength (λ) = 254 nm), was computed as the absorbance at λ = 254 nm multiplied by 100 and divided by DOC concentration in mg C/L.[42] It has to be noted that structure-selective fractionation of DOM upon sorption will affect the DOC/SUVA$_{254}$ ratios.[24,43] Samples were diluted up to reaching target UV-Vis 0.3 absorbance at λ = 254 nm, to avoid inner-filtering effects.[44]

Electron Exchange Capacity (EEC) of HA. The redox properties of the HA fractions (stock solutions of HAs and 0.45 µm filtrates of HA after sorption), EAC and EDC, respectively were quantified following mediated electrochemical reduction (MER) and oxidation (MEO) procedures[45-46] by using an electrochemical analyzer (1000C Multi-potentiostat, CH Instruments, USA). Throughout the experiment, potentials were measured against a Ag/AgCl electrode but are reported here against Standard Hydrogen Electrode (E_H(pH 7) = - 0.49 V in MER and E_H(pH 7) = + 0.61 V in MEO). In short, MER and MEO were conducted at pH 7 in the presence of 0.1 M KCl and 0.1 M phosphate buffer using a glassy carbon cell (Sigradur G, HTW, Germany) as working electrode, a Pt wire (0.5 mm; 99.9 %) attached to Pt gauze (52 mesh, 99.9 %), both from Sigma-Aldrich Co., USA as auxiliary electrode and a Ag/AgCl as reference electrode (Bioanalytical systems Inc., USA). Diquat was used as electron transfer mediator for MER and ABTS for MEO. After mediators were spiked to the polarized reaction cell at either reductive or oxidative potentials, at least triplicates of each sample were measured by recording the temporal evolution of the current between the working electrode and the auxiliary electrode at constant potential. The total electron exchange capacity (EEC = EAC + EDC) was computed and presented here as DOC normalized properties. Transferred charge was estimated using the composite Simpson's rule as implemented in the SciPy library of Python after baseline correction of current peaks.

Fourier Transform Ion Cyclotron Resonance Mass Spectrometry (FT-ICRMS). Ultrahigh-resolution FT-ICR-MS analyses were acquired using a 12 Tesla Bruker Solarix mass spectrometer (Bruker Daltonics, Bremen, Germany) coupled to an Apollo II electrospray ionization source in negative mode [ESI(-)]. Samples were desalted using solid phase extraction by means of PPL, a styrene divinyl copolymer (PPL, Varian

Bond Elut).[33,47] The SPE samples were injected into the electrospray source using a micro-liter pump at a flow rate of 120 μL h^{-1} with a nebulizer gas pressure of 138 kPa and a drying gas pressure of 103 kPa. A source heater temperature of 200°C was maintained to ensure rapid desolvation in the ionized droplets. The spectra were acquired with a time domain of 4 MW, and 500 scans were accumulated for each mass spectrum. All spectra were internally calibrated using appropriate reference mass lists. It should be noted that the intensity depends on the ionization potential and different components may influence the ionization yield of each other.[4,47-49] Data processing was done using Compass Data Analysis 4.1 (Bruker, Bremen, Germany).

Molecular formula assignment. Once the exact masses of the detected ions had been determined, their molecular formulas were batch calculated by a software tool, written in-house (mass error ≤ 0.2 ppm). The generated formulas were validated by setting sensible chemical constraints (N rule, oxygen-to-carbon (O/C) ratio r1, hydrogen-to-carbon (H/C) ratio ≤ 2n+2, element counts: ≤ 80, H unlimited, ≤ 60 (where n refers to the number of carbon)) in conjunction with an automated theoretical isotope pattern comparison. The composition of elements was selected based on the generally observed elemental composition of such organic matter.[50] Final molecular formula assignments were branded into groups containing CHO, CHNO, and CHOS molecular compositions, which were used to reconstruct the group-selective mass spectra. Count and percentage of molecular formulas containing CHO, CHNO and CHOS molecular compositions as well as the computed average of H,C,N,O,S atoms and H/C, O/C, C/N, C/S and m/z (mass-to-charge) ratios were based upon intensity-weighted averages of mass peaks with assigned molecular formulas (**Table 2**).

3.4   Results and discussion

Optical and electrochemical analyses of non-sorbed HA. DOC measured by using a Vario Cube analyzer was compared to DOC quantified by UV-Vis spectroscopy at 254 nm. UV-vis-derived relationships between HA concentrations and absorbance showed excellent linearity and surprising concordance in absence of sorption (**Fig. SI11**). In case of sorption, the DOC content of filtered supernatants was underestimated when using NOM/SUVA$_{254}$ relationships obtained for non-sorbed HA, demonstrating a decrease of specific UV absorption (SUVA$_{254}$) with progressive sorption of HA for filtered supernatants and this effect turned out to be more important when the amount of sorbed HA came closer to 100 %, diminishing the accuracy of optical analysis in presence of large NOM fractionation (**Table SI4**), in agreement with previous studies.[31,43] It is remarkable that at high mass ratios PPHA/Al$_2$O$_3$ (>1/25), the DOC calculation by the absorbance at 254 nm shows an underestimation compared to the one measured with TOC analyzer. SUVA$_{254}$ did not indicate any clear enrichment of aromatic functional groups on filtered HA fractions (non-sorbed at alumina) at mass ratios of PPHA/Al$_2$O$_3$ lower than 1/12 while at higher ratios (almost complete sorption), SUVA$_{254}$ was at least 30 % lower for filtered fractions compared to HA stock, but in the case of 94% sorbed PPHA to Al$_2$O$_3$, SUVA$_{254}$ was negligible, as shown in **Fig. 12**. Hence, for EEC calculation, the DOC

measured by elemental analysis was used in all cases to avoid interference arising from structure-selective fractionation on the specific UV-Vis absorption of HA supernatants (HA$_{aq}$). Filtered PPHA supernatants showed lower EEC compared to PPHA stock solutions after sorption to aluminum oxide while the amount of sorbed PPHA increases (**Fig. 12**). At almost completely sorbed PPHA, EEC of filtered PPHA supernatants was negligible; and this trend was consistent for all three HA tested, independent of the sample origin (aquatic vs. terrestrial HA). This might indicate that the compounds left in the non-sorbed fraction were depleted in terms of redox active compounds (e.g. quinone moieties, phenols). Analogously, the EEC of the filtered PPHA supernatant following sorption to DAX-8 declined with decreasing amount of PPHA left in solution (**Fig. 12**), although to lower extent than PPHA non-sorbed fractions to Al$_2$O$_3$. Thus, in terms of redox properties, the two proposed sorption mechanisms (polar - Al$_2$O$_3$ vs. non-polar - DAX-8) trigger analogous alterations in EEC of non-sorbed HA, and establish fractionation as the main cause linked to the changes in redox properties observed on HA supernatants although the nature of fractionation mechanism is supposedly different. For further clarification, molecular changes of HA supernatants were investigated by negative electrospray ESI (-) FTICR mass spectrometry.
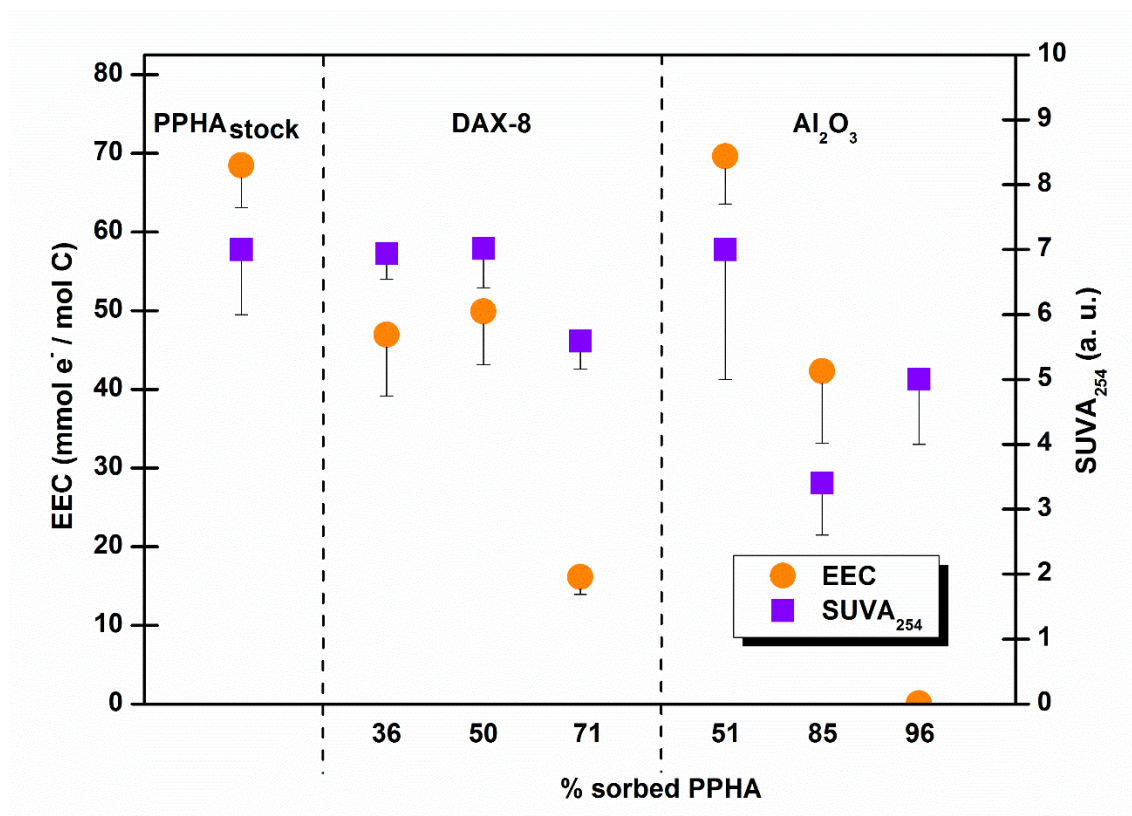
Figure 12. Electron Exchange Capacities (EEC) and Specific UV-Visible Absorption at 254 nm (SUVA$_{254}$) data for Pahokee Peat Humic Acid (PPHA) stock solution (PPHA$_{stock}$) and 0.45 μm filtered supernatants following sorption at aluminum oxide (Al$_2$O$_3$) and hydrophobic resin DAX-8. For filtered supernatants, data was arranged in ascending sorption level.

Molecular level analysis of HA stock solutions. HA stock solutions and filtered (0.45 µm) supernatants from sorption experiments (0.1 M KCl, 0.1 M phosphate buffer) were subjected to PPL-based SPE for desalination and subjected to negative electrospray ESI (-) FT-ICR mass spectrometry. **Table 2** summarizes the data for the mass spectra of HA stock solutions and filtered supernatants from each HA upon sorption to Al_2O_3 and DAX-8. In the case of aquatic SRHA stock solution, 3189 mass peaks were assigned, these formulas were composed of 73 % CHO, 9.9 % CHOS and 17 % CHNO, whereas lower counts of mass peaks were assigned for the terrestrial PPHA (1804 assigned formulas – 54.8 % CHO, 16.2 % CHOS and 29 % CHNO) and ESHA (1139 assigned formulas – 68.3 % CHO, 17.8 % CHOS and 13.9 % CHNO) stock solutions. This result can be explained by difference in solubility of the HA constituents following SPE under acidic conditions (pH = 2). Not surprisingly, the aquatic SRHA sample presents higher solubility while the terrestrial extracts (PPHA and ESHA) are less soluble at lower pH. In the case of filtered HA supernatants, only molecular compositions that were already observed in the HA stock solution were considered to be non-sorbed, as preferential ionization of DOM molecules might cause artifacts in the assessment of fractionation mechanism. However, reproducible results were found when the comparisons were made among the stock HA stock solutions as controls and filtered supernatants for all HAs. For improved understanding of NOM compositional diversity, van Krevelen diagrams, displaying O/C ratio and H/C ratios for the assigned molecular formulas have been used to classify categories of compounds in various NOM isolates.[51,52] **Fig. SI12** shows van Krevelen diagrams of the assigned masses for the stock solutions of SRHA, PPHA and ESHA disseminated by molecular series (e.g., CHO, CHNO and CHOS). In agreement with statement above, compounds containing only C, H and atoms (CHO) accounted for at least 54.8 % (PPHA) of the chemical composition in HA stock solutions (**Fig. SI12**), they were distributed along the aliphatics, carboxylic rich alicyclic molecules (CRAM) and polyphenols regions in the van Krevelen diagrams. Molecular masses with the elemental composition (i.e., C, H, N and O atoms) were located at O/C ratio > 0.35 and H/C ratios ranging from 0.5 to 1.3 for SRHA and PPHA stock solutions, whereas the content of compounds in this area of the van Krevelen diagram is significantly less pronounced for ESHA stock solution. Organosulfur compounds (CHOS) are mostly distributed in the area with O/C ratio < 0.4 and H/C ratio > 1 for all HA stock solutions although SRHA also contains CHOS molecules with O/C ratio ranging from 0.4 to 0.8 and H/C ratio ranging from 0.5 to 1.2 (**Fig. SI12**).

Table 2. Computed averages values of C, H, N, O, S, O/C, H/C, DBE, mass-to-charge (m/z) based upon intensity-weighted averages of mass peaks of Suwannee River (SRHA), Pahokee Peat (PPHA) and Elliott Soil (ESHA) humic acid stock solutions (HA[std]) and filtered supernatants after sorption to Al_2O_3 and DAX-8 as generated from negative electrospray 12T FT-ICMS. Percentages in first column indicate the % of non-sorbed HA (left in aqueous phase).

Member of molecular series	Compounds			Average (%)					Computed				Average DBE, intensity weighted	Average mass, intensity weighted
	CHO-	CHOS-	CHNO-	H	C	O	N	S	O/C ratio	H/C ratio	O/N ratio	O/S ratio		
SRHA[std]	2328 (73.0 %)	317 (9.9 %)	544 (17.1 %)	38.5	40.1	21.1	0.1	0.1	0.5	1.0	158.1	152.4	10	388
SRHA DAX-8 (89%)	1938 (76.0 %)	193 (7.6 %)	420 (16.5 %)	38.6	39.7	21.4	0.1	0.1	0.5	1.0	177.9	197.1	9	376
SRHA DAX-8 (83%)	1912 (76.4 %)	181 (7.2 %)	410 (16.4 %)	40.5	39.4	20.0	0.1	0.1	0.5	1.0	165.9	272.5	9	369
SRHA Al₂O₃ (43%)	1409 (80.0 %)	103 (5.8 %)	250 (14.2 %)	43.6	38.5	17.8	0.1	0.1	0.5	1.1	194.8	238.0	8	348
SRHA Al₂O₃ (6%)	1129 (83.1 %)	52 (3.8 %)	177 (13.0 %)	46.9	37.6	15.4	0.1	0.0	0.4	1.2	218.8	473.2	7	339
PPHA[std]	988 (54.8 %)	293 (16.2 %)	523 (29.0 %)	49.4	35.6	13.8	0.4	0.8	0.4	1.4	36.8	16.8	5	328
PPHA DAX-8 (62%)	695 (64.3 %)	76 (7.0 %)	310 (28.7 %)	44.6	37.4	17.4	0.4	0.2	0.5	1.2	39.2	75.6	7	310
PPHA DAX-8 (43.5%)	648 (62.0 %)	83 (7.9 %)	315 (30.1 %)	45.1	37.3	16.8	0.5	0.3	0.5	1.2	33.1	63.6	7	314
PPHA Al₂O₃ (49%)	722 (64.6 %)	94 (8.4 %)	301 (26.9 %)	45.72	37.5	15.96	0.53	0.29	0.43	1.22	30.21	55.8	6	301
PPHA Al₂O₃ (4%)	544 (63.6 %)	109 (12.7 %)	202 (23.6 %)	50.8	35.38	13.15	0.48	0.2	0.37	1.44	27.48	66.82	5	283
ESHA[std]	778 (68.3 %)	203 (17.8 %)	158 (13.9 %)	52.01	34.47	12.68	0.15	0.69	0.37	1.51	84.94	18.37	4	310
ESHA DAX-8 (50.5%)	623 (79.0 %)	92 (11.7 %)	74 (9.4 %)	47.71	36.65	15.1	0.12	0.41	0.41	1.3	124.21	36.49	6	311
ESHA DAX-8 (41.4%)	598 (79.9 %)	79 (10.6 %)	71 (9.5 %)	47.83	36.77	15.01	0.11	0.27	0.41	1.3	131.04	54.6	6	309
ESHA Al₂O₃ (72%)	528 (77.2 %)	113 (16.5 %)	43 (6.3 %)	53.50	34.43	11.25	0.08	0.74	0.33	1.55	134.20	15.27	4	301
ESHA Al₂O₃ (37.5%)	472 (78.8 %)	85 (14.2 %)	42 (7.0 %)	55.54	34.15	9.79	0.09	0.43	0.29	1.63	106.49	22.74	3	290

Selective sorption described by molecular analysis of HA filtered supernatants and HA stock solutions. The plot of double bond equivalents DBE as a function of number of carbon atoms (**Fig. 13**) and oxygen atoms (**Fig. SI13**) of HA stock solutions and supernatants provided comprehensive assessment of aromaticity-related unsaturation and O-functionalized NOM molecules. Two filtered HA supernatants samples for each sorbent following sorption to Al_2O_3 and DAX-8 were selected to exemplify two distinct sorption levels and simplify the analysis. The coarsely proportional relationships between DBE and count of oxygen atoms are causal with respect to aromatic and alicyclic carboxylic acids, but other NOM molecular features may cause additional superficial dependencies. Aluminum oxide presented significantly higher affinity to the components with higher amount of oxygen atoms (**Fig. SI13**), and higher affinity to compounds with higher degree of unsaturation (DBE), leading to prominent HA fractionation upon sorption, with a probable preferential sorption of aromatics and polyphenols, which are in line with recent studies on other oxide surfaces.[53] Such specific zones of large preferred compound removal were highlighted in **Fig. 13** and **Fig. SI13**. In contrast, hydrophobic resin DAX-8 showed less specific adsorption among the three HA with more limited fractionation (in agreement with data described above). Such behavior might be linked to less energetic interactions led by hydrophobic effect,[54] explaining the minor effects of HA selective sorption to DAX-8 on the electron exchange capacities of HA supernatants as well (**Fig. 12**).
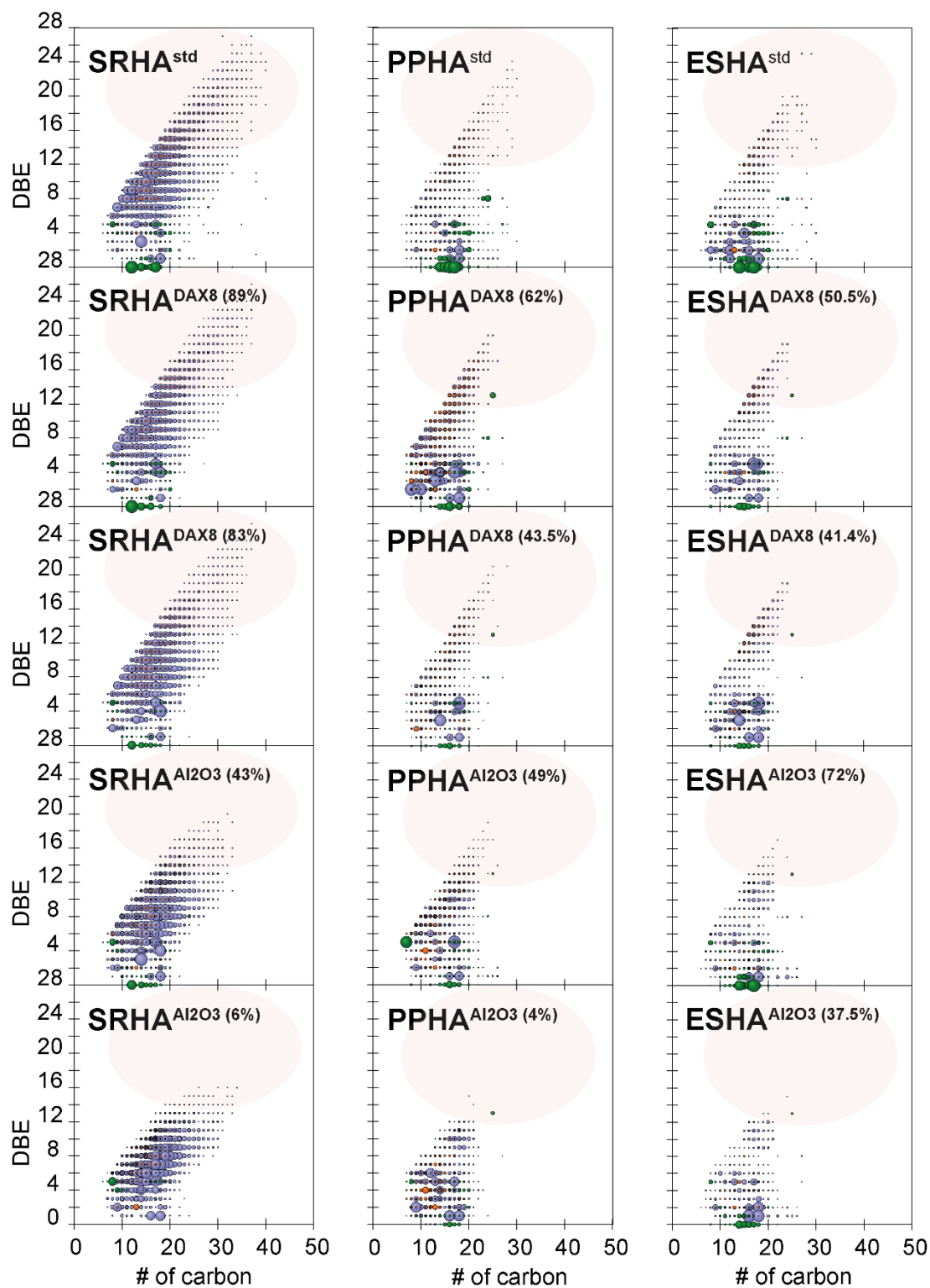
Figure 13. Double bond equivalents (DBE) versus number of carbon of Suwannee River (SRHA), Pahokee Peat (PPHA) and Elliott Soil Humic acid (ESHA) stock solutions (HA[std]) and filtered supernatants (containing non-sorbed molecular formulas) after sorption to DAX-8, Al_2O_3. Bubble Color for elemental compositions bearing combinations of C, H, O, N, and S atoms relates to: blue (CHO), orange (CHNO), green (CHOS). Bubble areas reflect the relative intensities of each mass peak in the sample. Percentages in brackets correspond to the amount (%) of non-sorbed HA (left in aqueous phase) after sorption.

Fig. 14 shows the van Krevelen diagrams of non-sorbed compounds (left in aqueous phase) to Al_2O_3 and DAX-8; featuring the common non-sorbed compounds to none of the sorbents and the unique non-sorbed compounds to each sorbent for two distinct sorption levels (in brackets). Non-sorbed HA compounds neither on Al_2O_3 nor DAX-8 were spread at O/C ratios 0.1 - 0.7 and H/C ratios 0.6 and 2, which do not provide indication of selective sorption. On the other hand, van Krevelen diagrams demonstrated removal of compounds with H/C ratio ranging from 0.5 to 1.5 and O/C ratio ranging from 0.4 to 0.8 after sorption to Al_2O_3 (**Fig. 14**), suggesting preferential sorption of aromatic compounds (low H/C with high O/C ratio). This is in line with the evolution of DBE vs. relative oxygenation (**Fig. SI13**) and DBE vs. carbon atom content (**Fig. 13**). It could be inferred that the preferential sorbed compounds on Al_2O_3 corresponded principally to tannin-like compounds upon comparison to useful reported patterns for NOM samples.[52] Thus, the proposed removal of tannin-like compounds by Al_2O_3, which are well-known as biological antioxidants,[55-57] can be ascribed to the observed decrease in the EEC of HA upon sorption (**Fig. 12**) and more detailed in **Fig. 8**. Conversely, van Krevelen diagrams for filtered supernatants after sorption to DAX-8 (**Fig. 14)** provided no substantial evidence of sorptive fractionation of specific HA compounds.

Molecular weight, carbon and oxygen fractionation (**Fig. SI14**) was demonstrated for all studied HA and showed stronger effects than on Al_2O_3 than on DAX-8. In general, HA molecular composition with higher molecular weight (MW), higher carbon and oxygen content were preferentially sorbed on Al_2O_3 surface, being the latter in line with a previous FT-ICRMS based studies which had described preferential sorption of HA compounds with multiple O-functionalized groups on alumina.[27] The counts of -CHNO and -CHOS molecular series as a function of number oxygen atoms in filtered supernatants (**Fig. SI15** and **Fig. SI16**, respectively) provided further evidence for preferential sorption of highly oxygenated SRHA molecules on Al_2O_3, a related but less distinct trend for sorption of PPHA molecules, and more unspecific trends for sorption of ESHA molecules on alumina. **Figure SI14** additionally shows that all filtered HA supernatants after sorption to Al_2O_3 were heavily deprived in constituents with higher carbon content after sorption regardless of the HA origin (aquatic vs. terrestrial) but with contrasting magnitude, reflecting the diversity in initial composition and structure (e.g. SRHA stock contained more numerous compounds with higher carbon counts than PPHA and ESHA). Likewise, the higher-molecular weight components (m/z > 400) were depleted from solution after being in contact with the aluminum oxide surface. In line with previous studies,[2,53,58] which have used size-exclusion chromatography for the assessment of the sorptive fractionation on iron oxy-hydroxide surfaces. Alternatively, in the case of hydrophobic resin DAX-8, evidence of preferential fractionation was observed on the lower-molecular weight HA fraction (m/z < 300) consistently among the different tested HA, but its incidence was more noticeable for histograms describing PPHA & ESHA (**Fig. SI14**).
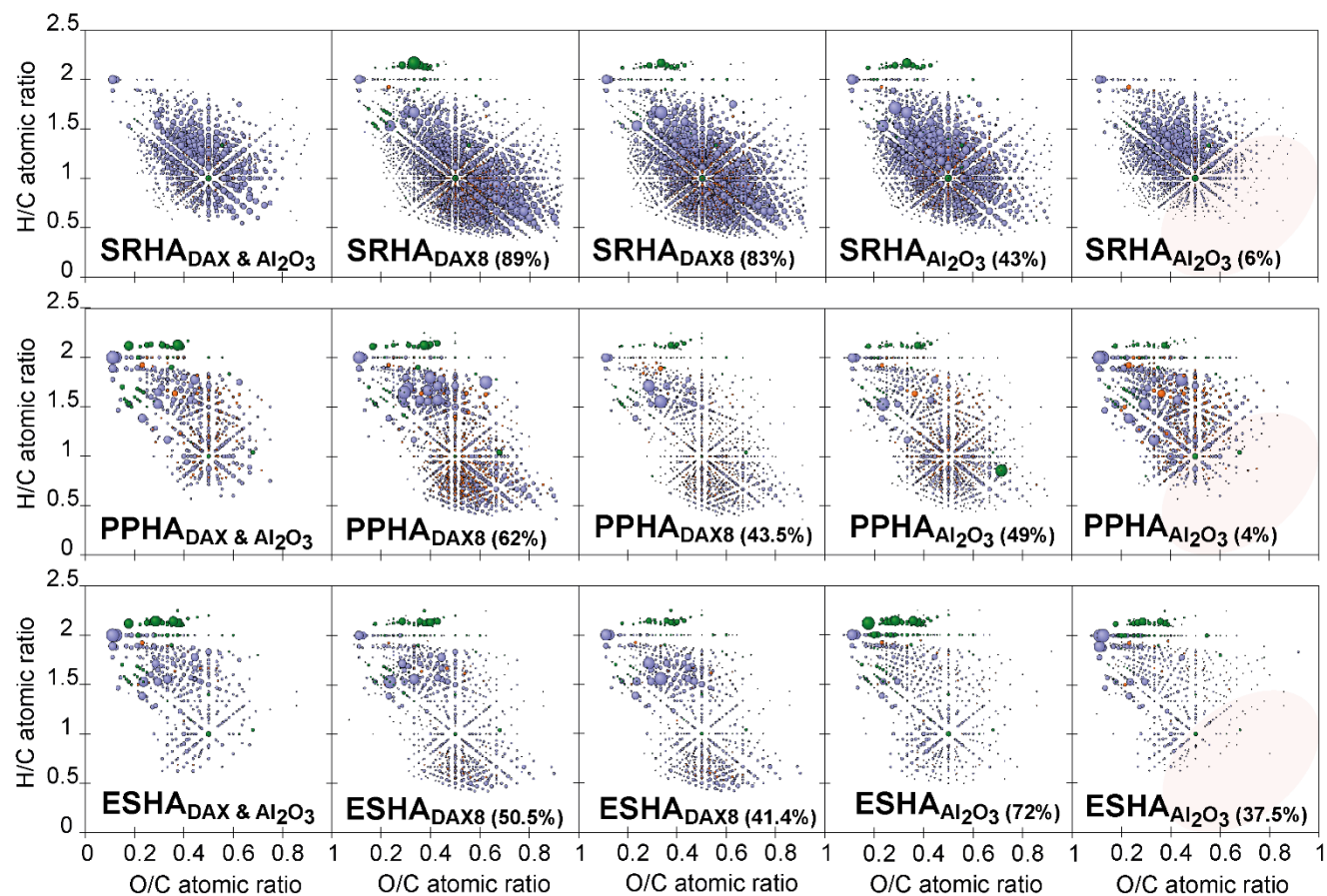
Figure 14. Calculated van Krevelen diagrams of non-sorbed molecular compositions (left in aqueous phase) for Suwannee River (SRHA), Pahokee Peat (PPHA) and Elliott Soil Humic acid (ESHA) to: neither DAX8 nor Al_2O_3 (first column), only to DAX-8 (second and third column) and only to Al_2O_3 (fourth and fifth column) for two different sorption levels in each sorbent, respectively. Bubble Color for elemental compositions bearing combinations of C, H, O, N, and S atoms relates to: blue (CHO), orange (CHNO), green (CHOS). Bubble areas reflect the relative intensities of each mass peak in the sample. Percentages in brackets correspond to the amount (%) of non-sorbed HA (left in aqueous phase) after sorption.

In order to statistically assess the chemical similarity among HA stock solutions and filtered supernatants, hierarchical clustering analysis (HCA) were used to classify the FT-ICR mass spectra using Pearson correlation coefficients (**Fig. SI17**). The HCA helped to unequivocally conclude that the SRHA and PPHA filtrates following sorption to DAX-8 had more similar chemical features to SRHA and PPHA stock solutions than the filtrates after sorption to Al_2O_3. In general, three groups can be distinguished according to decreasing degree in chemical composition similarity. For instance, in the case of PPHA samples, the group with the highest similarity includes the supernatants after sorption to DAX-8 (~ 0.6), the second group corresponds to the latter supernatants with PPHA stock solution (~ 0.4), and the third group with very low similarity is given by the PPHA supernatants after sorption to Al_2O_3 compared to PPHA stock solution and HA-DAX-8 supernatants (~ 0.1).

Selective sorption described by molecular analysis of sorbed HA to Al_2O_3 and DAX-8. By subtracting the assigned molecular masses in FT-ICRMS spectra of HA filtered supernatants from HA stock solutions, the assigned molecular masses in sorbed HA to Al_2O_3 and DAX-8 can be estimated. Van Krevelen diagrams were used in order to exhaustively assess the chemical features of the sorbed HA fractions (**Fig. 15**). Comprehensive analysis of mass spectra allowed further discrimination of sorbed HA molecules as follows: i) sorbed HA compounds with no distinct preferential sorption neither on Al_2O_3 nor DAX-8, ii) HA compounds preferentially sorbed only onto DAX-8 and iii) HA compounds preferentially sorbed only onto Al_2O_3 (**Fig. 15**). Two different levels of sorption are exemplified for each HA on each sorbent. Compounds sorbed at both Al_2O_3 and DAX-8 showed different pattern for the three HA, with relative compositional distinction decreasing in the following order SRHA ~ PPHA > ESHA. While a bimodal distribution of rather saturated [H/C ratio > 1.5 (SRHA) and > 1.3 (PPHA)] aliphatics-like molecules and supposed by aromatic (H/C ratio < 1) was observed for both SRHA and PPHA, less distinct compositional preference was observed for the adsorption of ESHA to both Al_2O_3 and DAX-8. However, the aliphatics and aromatics adsorbed compounds from SRHA and PPHA were largely dissimilar: PPHA-derived aliphatics-like compounds were much more numerous and showed much higher range of oxygen atoms than those derived from SRHA (O/C ratio from 0.1 – 0.4) and showed a much higher proportion of CHOS-organic compounds. Furthermore, the common sorbed aromatic compounds were distinct: SRHA showed more tightly clustered molecular compositions with high proportions of CHO-compounds whereas PPHA showed large proportions of CHNO-compounds of larger chemical diversity. Preferentially sorbed compounds onto DAX-8 were similar for PPHA and ESHA and encompassed primarily saturated S-organic compounds; a rather diffuse set of mainly CHO-compounds of higher unsaturation could be noticed, likely due to presence of non-selective rather than selective sorption processes taking place onto the DAX-8 surface. Sorbed SRHA compounds comprised mainly CRAM-like CHO-compounds with lower amount of oxygen atoms than those found in marine waters.[59]
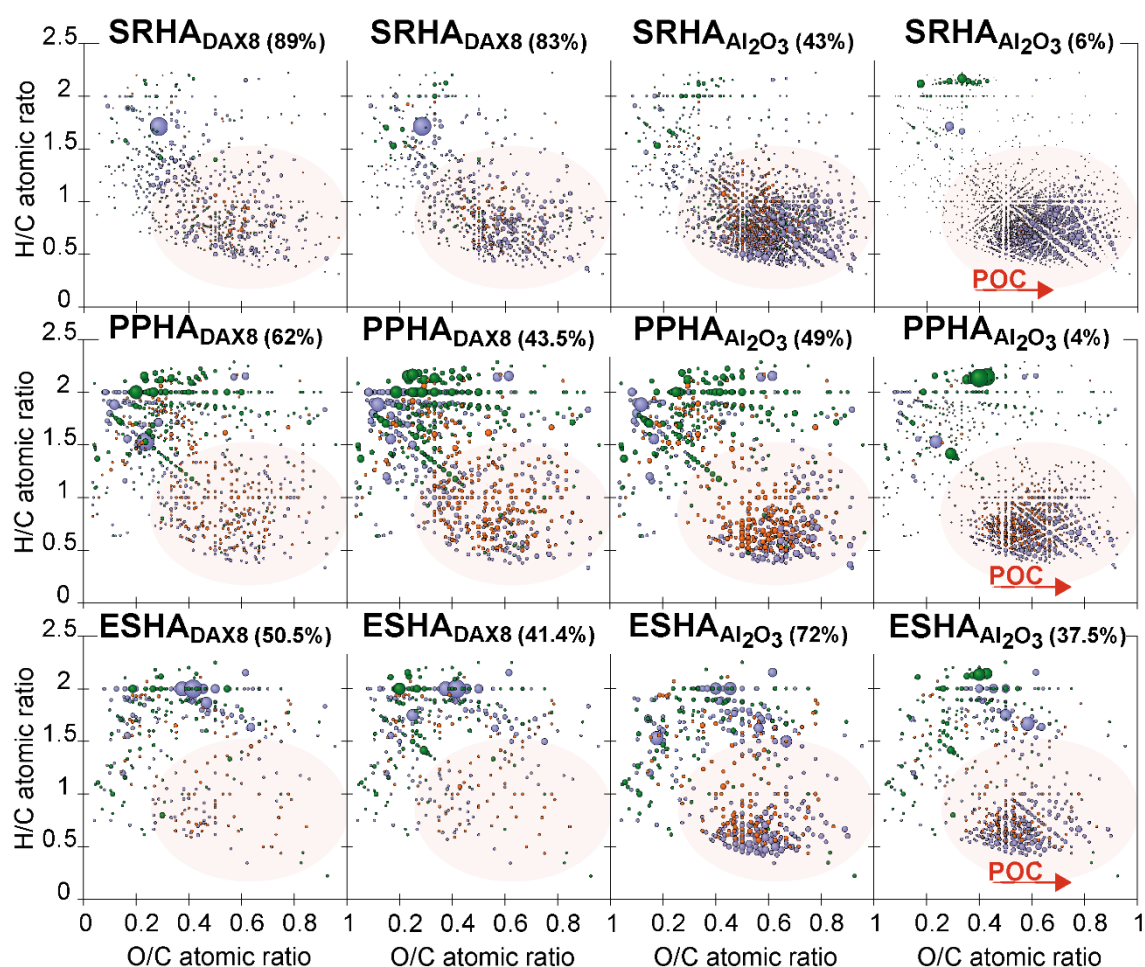
Figure 15. Calculated van Krevelen diagrams of sorbed molecular formulas for Suwannee River (SRHA), Pahokee Peat (PPHA) and Elliott Soil (ESHA) humic acid isolates sorbed only onto DAX-8 (columns 1 and 2), and sorbed Al_2O_3 materials. Bubble Color for elemental compositions bearing combinations of C, H, O, N, and S atoms relates to: blue (CHO), orange (CHNO), green (CHOS). Bubble areas reflect the relative intensities of each mass peak in the sample. Highlighted areas showed the molecular compositions mainly Polyphenolic Organic Compounds (POC) specifically sorbed to Al_2O_3 during experiments. Two distinct sorption levels for each humic acid on each sorbent are presented. Percentages in brackets correspond to the amount (%) of non-sorbed HA (left in aqueous phase) after sorption.

In contrast, HA molecules absorbed to Al_2O_3 occupied two distinct classes of polyphenolic organic compounds (POC) for SRHA, PPHA and ESHA (**Fig. 15**) for optimal data visualization, namely a class of CHOS-organic compounds of restricted chemodiversity in the order ESHA ~ PPHA < SRHA and a lignin - to tannin-like assortment of CHO-compounds with sizable shares of CHNO-compounds of yet unknown provenance. Hence, in contrast to sorption on Al_2O_3, substantial alterations in the EEC upon sorption to DAX-8 (**Fig. 12**) are less prone to happen for all studied HA since the likely richest fraction in terms of electron transfer (tannin-like compounds) remained in solution (**Fig. 15**). Van Krevelen diagrams also showed that sorption selectivity of HA on alumina was dependent on the sorption extent as well (**Fig. 15**). In general, sorption-induced molecular selectivity increased with increasing sorption level (less HA left in solution after sorption) or decreasing HA/Al_2O_3 mass ratio. While

depletion of tannin-like compounds in filtered supernatants is already evident (**Fig. 13**), computed difference spectra denote selectivity of sorbed HA molecules (**Fig. 15**) more clearly and demonstrated progressive increasing preferential sorption of tannin-like compounds at decreasing HA/Al_2O_3 mass ratios.

To further evaluate the aromatic driven sorption selectivity of HA molecules onto Al_2O_3 and DAX-8, the aromatic equivalent (X_c) was calculated for the preferentially sorbed assigned molecular masses and it was plotted as a function of the carbon number (**Fig. 16a** and Fig. **16b**, respectively). The aromatic equivalent is a recent approach that provides accurate identification and characterization of aromatic compounds from FT-ICRMS data of dissolved organic compounds.[60] **Fig. 16b** shows that condensed aromatic units ($2.7143 \leq X_c \leq 3$) and aromatics with benzene rich ($2.5 \leq X_c < 2.7143$) in SRHA and PPHA, clustered at higher number of carbons, were efficiently adsorbed onto Al_2O_3, while the compounds sorbed onto DAX-8 were more randomly distributed (**Fig. 16a**). The count of sorbed molecular formulas with non-fused-benzene rings ($X_c \leq 2.3333$), 1-fused benzene ring ($2.5 \leq X_c \leq 2.6667$), 2-fused benzene rings ($2.7143 \leq X_c \leq 2.7778$), 3-fused benzene rings ($2.8000 \leq X_c \leq 2.8333$) and 4-fused benzene rings ($X_c > 2.8462$) resulted in pronounced sorptive fractionation onto Al_2O_3 of compounds in HA containing 2-fused benzene rings or more condense aromatics (**Fig. 16c**), which was nicely connected to incidence of a significant number of compounds selectively sorbed to Al_2O_3 as a function of the number of atom oxygens in counted -CHO molecular series (**Fig. 16d**). Conversely, **Figure 16c** shows clear evidence of selective sorption of compounds containing non- or 1-fused-benzene rings to DAX-8 (specifically in PPHA and ESHA).

3.5   Environmental Implications.

These findings demonstrate that the combination of electrochemical and molecular level analysis is a powerful approach to evaluate alterations in the chemical/redox properties of NOM in presence of sorption processes. Considering that a large fraction of NOM in soil and groundwater is present in sorbed state, the presented results are fundamental for an improved understanding of biogeochemical processes in which electron transfer reactions involving NOM take place. To evaluate if and how the findings of this study are representative for environmental settings (e.g. matrixes richer in tannin-like compounds), experimental designs with focus in the sorbed fraction should be considered in future work. Furthermore, systems where electron transfer reactions in the mineral-organic interface take place should be considered as well.
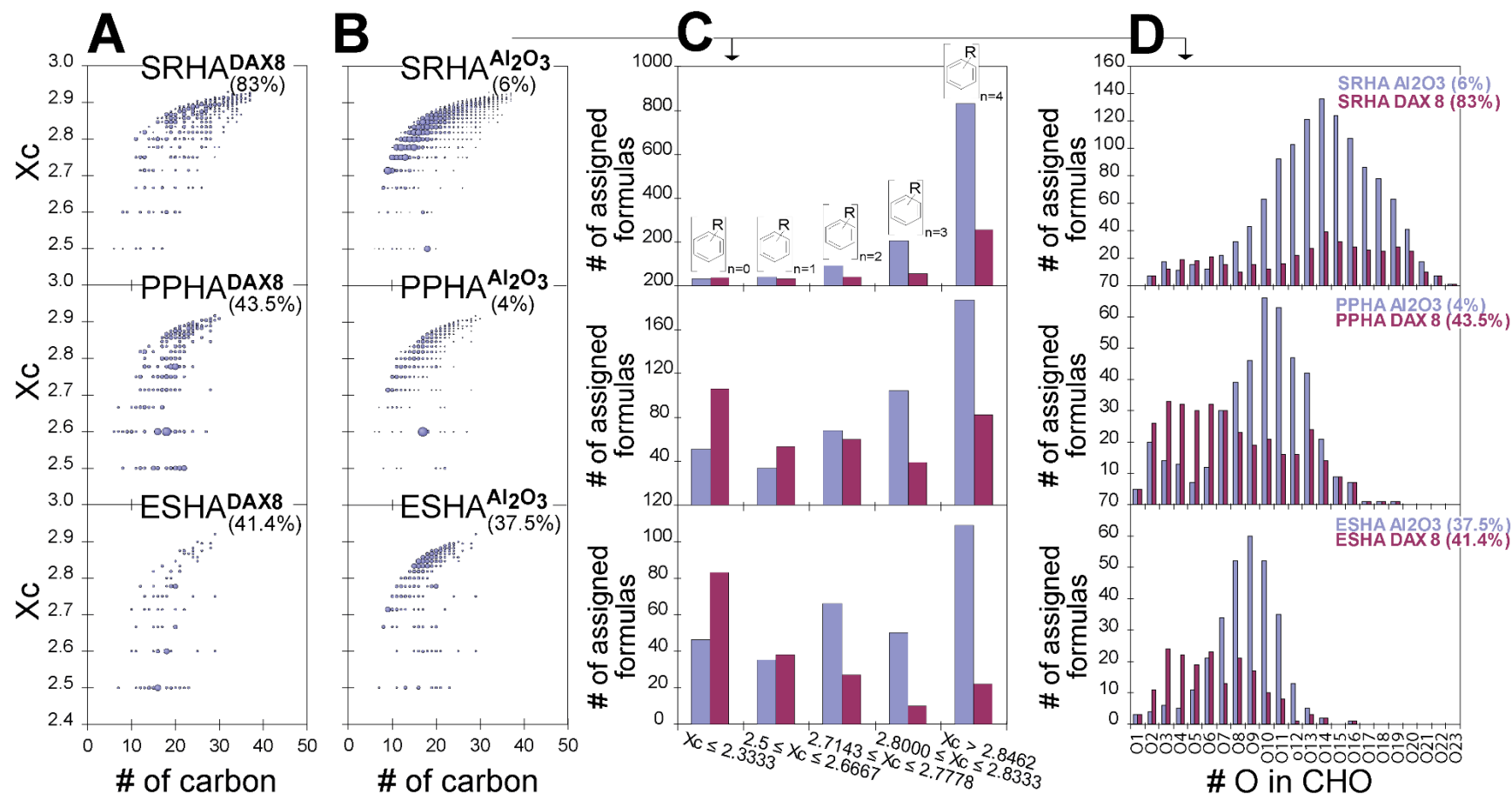
Figure 16. Comparison of sorbed CHO-molecules in Suwannee River (SRHA), Pahokee Peat (PPHA) and Elliott Soil (ESHA) humic acid isolates to a) DAX-8 and b) Al_2O_3 materials. Aromaticity equivalent (X_c) versus number of carbons for condensed aromatic units ($2.7143 \leq X_c \leq 3$) and aromatics with benzene ring ($2.5 \leq X_c < 2.7143$). c): Count of molecular formulas with non-benzene ring ($X_c \leq 2.3333$), 1-benzene ring ($2.5 \leq X_c \leq 2.6667$), 2-fused benzene rings ($2.7143 \leq X_c \leq 2.7778$), 3-fused benzene rings ($2.8000 \leq X_c \leq 2.8333$), and 4-fused benzene rings ($X_c > 2.8462$). (D): Counts of oxygen atoms involved in CHO-molecules in each case. Bubble areas indicate relative mass peak intensity. Aromatic equivalent can be calculated as follows: $X_c = [3 [DBE- (mO+nS)] - 2] / [DBE - (mO+nS)]$, where DBE is the double-bond equivalent, m and n are the fractions of oxygen and sulfur atoms involved in the π-bond structures of the molecule.[60]

78

3.6   References

1.   Suffet, I. H.; MacCarthy, P. Aquatic Humic Substances and Their Influence on the Fate and Treatment of Pollutants. In *Aquatic Humic Substances.* Advances in Chemistry, Vol. 219. American Chemical Society: Washington, DC, **1988**.

2.   Meier, M.; Namjesnik-Dejanovic, K.; Maurice, P. A.; Chin, Y. P.; Aiken, G. R. Fractionation of aquatic natural organic matter upon sorption to goethite and kaolinite. *Chem. Geol.*, **1999**, 157, 275-284.

3.   Koch, B. P.; Witt, M. R.; Engbrodt, R.; Dittmar, T.; Kattner, G. Molecular formulae of marine and terrigenous dissolved organic matter detected by electrospray ionization Fourier transform ion cyclotron resonance mass spectrometry. *Geochim. Cosmochim. Acta*, **2005**, 69, 3299-3308.

4.   Hertkorn, N.; Frommberger, M.; Witt, M.; Koch, B. P.; Schmitt-Kopplin, P.; Perdue, E. M. Natural organic matter and the event horizon of mass spectrometry. *Anal. Chem.*, **2008**, 80, 8908-8919.

5.   Macalady, D. L., & Walton Day, K. Redox Chemistry of Natural Organic Matter (NOM): Geochemist's Dream, Analytical Chemist's Nightmare. In *Aquatic Redox Chemistry*; Tratnyek, P. G., Grundl, T. J. & Haderlein, S. B., Eds.; Oxford University Press: Washington, **2011**; pp 87-111.

6.   Stevenson, F. J. *Humus Chemistry: Genesis, Composition, Reactions*, 2nd ed.; John Wiley & Sons: New York, **1994**.

7.   McDonald, S.; Bishop, A. G.; Prenzler, P. D.; Robards, K. Analytical chemistry of freshwater humic substances. *Anal. Chim. Acta*, **2004**, 527 (2), 105-124.

8.   Schumacher, M.; Christl, I.; Vogt, R. D.; Barmettler, K.; Jacobsen, C.; Kretzschmar, R. Chemical composition of aquatic dissolved organic matter in five boreal forest catchments sampled in spring and fall seasons. *Biogeochemistry*, **2006**, 80 (3), 263-275.

9.   Hayes, T. M.; Hayes, M. H. B.; Swift, R. S. Detailed investigation of organic matter components in extracts and drainage waters from a soil under long term cultivation. *Org. Geochem.*, **2012**, 52, 13-22.

10.   Lovley, D. R.; Coates, J. D.; Blunt-Harris, E. L.; Phillips, E. J. P.; Woodward, J. C. Humic substances as electron acceptors for microbial respiration. *Nature*, **1996**, 382, 445-448.

11.   Benz, M.; Schink, B.; Brune, A. Humic acid reduction by Propionibacterium freudenreichii and other fermenting bacteria. *Appl. Environ. Microbiol.*, **1998**, 64, 4507-4512.

12.   Kappler, A.; Benz, M.; Schink, B.; Brune, A. Electron shuttling via humic acids in microbial iron (III) reduction in a freshwater sediment. *FEMS Microbiol. Ecol.*, **2004**, 47, 85-92.

13.   Jiang, J.; Kappler, A. Kinetics of microbial and chemical reduction of humic substances: Implications for electron shuttling. *Environ. Sci. Technol.*, **2008**, 42 (10), 3563-3569.

14.   Dunnivant, F. M.; Schwarzenbach, R. P.;Macalady, D. L. Reduction of substituted nitrobenzenes in aqueous solutions containing natural organic matter. *Environ. Sci. Technol.*, **1992**, 26 (11), 2133-2141.

15.   Curtis, G. P.; Reinhard, M. Reductive dehalogenation of hexachlorethane, carbon-tetrachloride and bromoform by anthrahydroquinone disulfonate and humic acid. *Environ. Sci. Technol.*, **1994**, 28 (13), 2393-2401.

16. Kaiser, K.; Guggenberger, G. The role of DOM sorption to mineral surfaces in the preservation of organic matter in soil. *Org. Geochem.*, **2000**, 31, 711-725.
17. Guggenberger, G.; Kaiser, K. Dissolved organic matter in soil: challenging the paradigm of sorptive preservation. *Geoderma*, **2003**, 113, 293-310.
18. Kalbitz, K.; Schwesig, D.; Rethemeyer, J.; Matzner, E. Stabilization of dissolved organic matter by sorption to the mineral soil. *Soil Biol. Biochem.*, **2005**, 37, 1319-1331.
19. Heidmann, I.; Christl, I.; Kretzschmar, R. Sorption of Cu and Pb to kaolinite–fulvic acid colloids: Assessment of sorbent interactions. *Geochim. Cosmochim. Acta.*, **2005**, 69 (7), 1675-1686.
20. Kang, S. H.; Xing, B. S. Humic acid fractionation upon sequential adsorption onto goethite. *Langmuir*, **2008**, 24 (6), 2525-2531.
21. Sharma, P.; Ofner, J.; Kappler, A. Formation of Binary and Ternary Colloids and Dissolved Complexes of Organic Matter, Fe and As. *Environ. Sci. Technol.*, **2010**, 44 (12), 4479-4485.
22. Armanious, A.; Aeppli, M.; Sander, M. Dissolved Organic Matter Adsorption to Model Surfaces: Adlayer Formation, Properties, and Dynamics at the Nanoscale. *Environ. Sci. Technol.*, **2014**, 48, 9420-9429.
23. Young, R. B.; Avneri-Katz, S.; McKenna, A. M.; Chen, H.; Bahureksa, W.; Polubesova, T.; Chefetz, B.; Borch, T. Composition-Dependent Sorptive Fractionation of Anthropogenic Dissolved Organic Matter by Fe(III)-Montmorillonite. *Soil. Syst.*, **2018**, 2 (1), 14.
24. Claret, F.; Schaefer, T.; Brevet, J.; Reiller, P. E. Fractionation of Suwannee River Fulvic Acid and Aldrich Humic Acid on α-Al2O3: Spectroscopic Evidence. *Environ. Sci. Technol.*, **2008**, 42, 8809-8815.
25. Janot, N.; Reiller, P. E.; Zheng, X.; Croue, J. P.; Benedetti, M. F. Characterization of humic acid reactivity modifications due to adsorption onto α-Al2O3. *Water Res.*, **2012**, 46 (3), 731-740.
26. Galindo, C.; Del Nero, M. Molecular Level Description of the Sorptive Fractionation of a Fulvic Acid on Aluminum Oxide Using Electrospray Ionization Fourier Transform Mass Spectrometry. *Environ. Sci. Technol.*, **2014**, 48, 7401-7408.
27. Galindo, C.; Del Nero, M. Chemical fractionation of a terrestrial humic acid upon sorption on alumina by high resolution mass spectrometry. *RSC Adv.*, **2015**, 5, 73058-73067.
28. Benner, R.; Pakulski, D.; McCarthy, M.; Hedges, J. I.; Hatcher, P. G. Bulk Chemical Characteristics of Dissolved Organic Matter in the Ocean. *Science*, **1992**, 255, 1561-1564.
29. Mopper, K.; Stubbins, A.; Ritchie, J. D.; Bialk, H. M.; Hatcher, P. G. Advanced Instrumental Approaches for Characterization of Marine Dissolved Organic Matter: Extraction Techniques, Mass Spectrometry, and Nuclear Magnetic Resonance Spectroscopy. *Chem. Rev.*, **2007**, 107 (2), pp 419-442.
30. Dittmar, T.; Koch, B.; Hertkorn, N.; Kattner, G. A simple and efficient method for the solid-phase extraction of dissolved organic matter (SPE-DOM) from seawater. *Limnol. Oceanogr. Methods*, **2008**, 6, 230-235.
31. Kruger, B. R.; Dalzell, B. J.; Minor, E. C. Effect of organic matter source and salinity on dissolved organic matter isolation via ultrafiltration and solid phase extraction. *Aquat. Sci.*, **2011**, 73, 405-417.

32. Tfaily, M. M.; Hodgkins, S.; Podgorski, D. C.; Chanton, J. P.; Cooper, W. T. Comparison of dialysis and solid-phase extraction for isolation and concentration of dissolved organic matter prior to Fourier transform ion cyclotron resonance mass spectrometry. *Anal. Bioanal. Chem.*, **2012**, 404, 447-457.

33. Hertkorn, N.; Harir, M.; Koch, B. P.; Michalke, B.; Schmitt-Kopplin, P. High-field NMR spectroscopy and FTICR mass spectrometry: Powerful discovery tools for the molecular level characterization of marine dissolved organic matter. *Biogeosciences*, **2013**, 10, 1583-1624.

34. Zhang, F.; Harir, M.; Moritz, F.; Zhang, J.; Witting, M.; Wu, Y.; Schmitt-Kopplin, P.; Fekete, A.; Gaspar, A.; Hertkorn, N. Molecular and structural characterization of dissolved organic matter during and post cyanobacterial bloom in Taihu by combination of NMR spectroscopy and FTICR mass spectrometry. *Water Res.*, **2014**, 57, 280-294.

35. Minor, E. C.; Swenson, M. M.; Mattson, B. M.; Oyler, A. R. Structural characterization of dissolved organic matter: a review of current techniques for isolation and analysis. *Environ. Sci.: Processes Impacts*, **2014**, 16, 2064-2079.

36. Nebbioso, A.; Piccolo, A. Molecular characterization of dissolved organic matter (DOM): a critical review. *Anal. Bioanal. Chem.*, **2013**, 405 (1), 109-124.

37. Sandron, S.; Rojas, A.; Wilson, R.; Davies, N. W.; Haddad, P. R.; Shellie, R. A.; Nesterenko, P. N.; Kelleher, B. P.; Paull, B. Chromatographic methods for the isolation, separation and characterisation of dissolved organic matter. *Environ. Sci.: Processes Impacts*, **2015**, 17, 1531-1567.

38. Li, Y.; Harir, M.; Lucio, M.; Kanawati, B.; Smirnov, K. S.; Flerus, R.; Koch, B. P.; Schmitt-Kopplin, P.; Hertkorn, N. Proposed Guidelines for Solid Phase Extraction of Suwannee River Dissolved Organic Matter. *Anal. Chem.*, **2016**, 88, 6680-6688.

39. Li, Y.; Harir, M.; Uhl, J.; Kanawati, B.; Lucio, M.; Smirnov, K. S.; Koch, B. P.; Schmitt-Kopplin, P.; Hertkorn, N. How representative are dissolved organic matter (DOM) extracts? A comprehensive study of sorbent selectivity for DOM isolation. *Water Res.*, **2017**, 116, 316-323.

40. Seaton, N. A.; Walton, J. P. R. B.; Quirke, N. A new analysis method for the determination of the pore size distribution of porous carbons from nitrogen adsorption measurements. *Carbon*, **1989**, 27, 853-861.

41. Zsolnay, A. Dissolved organic matter: artefacts, definitions, and functions. *Geoderma*, **2003**, 113, 187-209.

42. Weishaar, J. L.; Aiken, G. R.; Bergamaschi, B. A.; Fram, M. S.; Fujii, R.; Mopper, R. Evaluation of Specific Ultraviolet Absorbance as an Indicator of the Chemical Composition and Reactivity of Dissolved Organic Carbon. *Environ. Sci. Technol.*, **2003**, 37 (20), 4702-4708.

43. Gu, B.; Mehlhorn, T. L.; Liang, L.; McCarthy, J. F. Competitive adsorption, displacement, and transport of organic matter on iron oxide: 1. Competitive adsorption. *Geochim. Cosmochim. Acta*, **1996**, 60, 1943-1950.

44. Mobed, J. J.; Hemmingsen, S. L.; Autry, J. L.; McGown, L. B. Fluorescence characterization of IHSS humic substances: total luminescence spectra with absorbance correction. *Environ. Sci. Technol.*, **1996**, 30 (10), 3061-3065.

45. Aeschbacher, M.; Sander, M.; Schwarzenbach, R. P. Novel electrochemical approach to assess the redox properties of humic substances. *Environ. Sci. Technol.*, **2010**, 44 (1), 87-93.

46.   Kluepfel, L.; Keiluweit, M.; Kleber, M.; Sander, M. Redox properties of plant biomass-derived black carbon (biochar). *Environ. Sci. Technol.*, **2014**, 48 (10), 5601-5611.

47.   Hertkorn, N.; Harir, M.; Cawley, K. M.; Schmitt-Kopplin, P.; Jaffe, R. Molecular characterization of dissolved organic matter from subtropical wetlands: a comparative study through the analysis of optical properties, NMR and FT-ICR/MS. *Biogeosciences*, **2016**, 13 (8), 2257-2277.

48.   Hertkorn, N. Environmental NMR: Solution-state methods. In Simpson, M. J.; Simpson, A. J. *NMR Spectroscopy: A Versatile Tool for Environmental Research*. Weinheim: Wiley, **2014**; pp. 3-30.

49.   Hertkorn, N.; Harir, M.; Schmitt-Kopplin, P. Nontarget analysis of Murchison soluble organic matter by high-field NMR spectroscopy and FTICR mass spectrometry. *Magn. Reson. Chem.*, **2015**, 53 (9), 754-768.

50.   Gaspar, A.; Harir, M.; Hertkorn, N.; Schmitt-Kopplin, P. Preparative free-flow electrophoretic offline ESI-Fourier transform ion cyclotron resonance/MS analysis of Suwannee River fulvic acid. *Electrophoresis*, **2010**, 31 (12), 2070-2079.

51.   Kim, S.; Kramer, R. W.; Hatcher, P. G. Graphical method for analysis of ultrahigh-resolution broadband mass spectra of natural organic matter, the Van Krevelen diagram. *Anal. Chem.*, **2003**, 75, 5336-5344.

52.   Guigue, J.; Harir, M.; Mathieu, O.; Lucio, M.; Ranjard, L.; Leveque, J.; Schmitt-Kopplin, P. Ultrahigh-resolution FT-ICR mass spectrometry for molecular characterisation of pressurised hot water-extractable organic matter in soils. *Biogeochemistry*, **2016**, 128, 307-326.

53.   Lv, J.; Zhang, S.; Wang, S.; Luo, L.; Cao, D.; Christie, P. Molecular-Scale Investigation with ESI-FT-ICR-MS on Fractionation of Dissolved Organic Matter Induced by Adsorption on Iron Oxyhydroxides. *Environ. Sci. Technol.*, **2016**, 50, 2328-2336.

54.   Chandler, D. Interfaces and the driving force of hydrophobic assembly. *Nature*, **2005**, 437, 640-647

55.   Hagerman, A. E.; Riedl, K. M.; Jones, G. A.; Sovik, K. N.; Ritchard, N. T.; Hartzfeld, P. W.; Riechel, T. L. High Molecular Weight Plant Polyphenolics (Tannins) as Biological Antioxidants. *J. Agric. Food Chem.*, **1998**, 46, 1887-1892.

56.   Barbehenn, R. V.; Jones, C. P.; Karonen, M.; Salminen, J. P. Tannin composition affects the oxidative activities of tree leaves. *J. Chem. Ecol.*, **2006**, 32, 2235-2251.

57.   Salminen, J.; Karonen, M. Chemical ecology of tannins and other phenolics: we need a change in approach. *Funct. Ecol.*, **2011**, 25, 325-338.

58.   Wang, L.; Chin, Y. P.; Traina, S. J. Adsorption of (poly)maleic acid and aquatic fulvic acids by goethite. *Geochim. Cosmochim. Acta*, **1997**, 61 (24), 5313-5324.

59.   Hertkorn, N.; Benner, R.; Frommberger, M.; Schmitt-Kopplin, P.; Witt, M.; Kaiser, K.; Kettrup, A.; Hedges, J. I. Characterization of a major refractory component of marine dissolved organic matter. *Geochim. Cosmochim. Acta*, **2006**, 70 (12), 2990-3010.

60.   Yassine, M. M.; Harir, M.; Dabek-Zlotorzynska, E.; Schmitt-Kopplin, P. Structural characterization of organic aerosol using Fourier transform ion cyclotron resonance mass spectrometry: Aromaticity equivalent approach.*Rapid Commun. Mass Spectrom.*, **2014**, 28, 2445-2454

Chapter 4.

5. Electron Exchange Capacities of Humic Acid Sorbed to Redox Active Clays.

4.1   Abstract

Iron (Fe) and Natural Organic Matter (NOM) are major drivers of biogeochemical redox processes in the environment. Electron transfer processes upon sorption of NOM to redox active minerals are likely to occur but have not been studied in detail so far. Despite of their structural complexity, Fe-bearing clays are suitable model systems to assess alterations in NOM redox properties upon sorption as they do not tend to release redox active Fe-species to the aqueous phase. While the redox properties of NOM or Fe within clay minerals have been studied individually using mediated electrochemical analysis, the effect of sorption to redox active clays on the redox properties of NOM has not been addressed yet. This chapter shows a preliminary assessment of whether changes in the Electron Accepting (EAC) and Donating (EDC) Capacities of NOM occur upon sorption to Fe-bearing clays as a consequence of NOM sorptive fractionation and electron transfer with structural Fe. Sorption of Pahokee Peat Humic Acid (PPHA) to Na-saturated montmorillonite (Na-SWy-2, Fe content 2.3 % wt) was studied at pH 7 in batch experiments for several PPHA/Na-SWy-2 ratios. EAC and EDC were quantified for PPHA stock solution, whole suspensions and filtered supernatants using mediated electrochemical analysis. The Total Electron Exchange Capacities (EEC = EDC + EAC) of PPHA in filtered supernatants was up to 60 % lower compared to PPHA stock solution, while its redox state was more oxidized after sorption (up to 70 % lower EDC). This can be explained by preferential sorption of electron donor groups in PPHA (e.g., hydroquinones/phenols). Suspensions containing PPHA + Na-SWy-2 showed up to 80 % lower EEC (normalized to total batch mass) compared to PPHA stock solution.

4.2   Introduction

Iron (Fe), by far the most abundant and redox active metal in the environment, and natural organic matter (NOM), are major drivers of biogeochemical redox processes in soils, sediments and aquifers. One prominent role of Fe-mineral surfaces in the environment is to be

responsible for reductive transformation of organic and inorganic pollutants in soils and groundwater.[1-2] Likewise, NOM readily acts as electron shuttle, enhancing reactions in microbial processes[3-4] and transformation of redox active pollutants.[5-6] Considering its intrinsic heterogeneity, the redox potential of given NOM samples is not a discrete value but comprises a range of potentials; for humic acids (HA), their redox potential (E°_H) has been reported to be from + 150 mV to – 300 mV vs. SHE.[7-8] The EEC is a direct measurement of the total amount of electrons that can be donated or accepted by the redox active groups in a molecule normalized to substance total mass. The electron accepting capacity within humic substances is provided by quinone moieties,[8-13] while polyphenols and hydroquinone are responsible for most of the electron donating capacity.[13-16]

The concomitant organic matter-mineral associations have been linked to stabilization of NOM in the environment.[17-18] NOM readily adsorbs from aqueous solution to mineral surface as a result of several processes with different energetic contributions including electrostatic interactions, ligand exchange and van der Waals interactions.[19-25] Thus, the potential for sorptive fractionation of NOM components is given by the type of mineral and other conditions (pH; ionic strength).[26-33] **Fig. 8** shows evidence of changes in the EEC of NOM (both sorbed and in solution) upon sorption to polar sorbents (e.g., aluminum oxide) even in the absence of electron transfer reactions, which were attributed to selective sorption of tannin compounds to the aluminum oxide surface as well as an enhancement in EDC of the sorbed fraction produced by: i) unfolding of the macromolecular conformation of HA, leaving redox active moieties more exposed to redox transfer mediators or ii) catalyzed polymerization of polyphenol compounds by Al_2O_3 surface under oxidizing conditions.[34-35] Although this previous work provided meaningful fundamental knowledge on the effect of redox inert sorption on the redox properties of organic matter, electron transfer processes upon sorption of NOM to redox active minerals are likely to occur but they have not been studied so far. Despite of their structural complexity, Fe-containing clays are suitable model systems to assess alterations in NOM redox properties upon sorption as they do not release a significant amount of redox active Fe-species to the aqueous phase. Besides the potential alterations in NOM redox properties triggered by fractionation and conformational changes taking place during NOM sorption, the electron transfer reaction between NOM and Fe-containing clays might also affect the redox properties of NOM (**Fig. 5**).

Recently established mediated electroanalytical techniques have been widely applied to quantify the EAC and EDC of humic substances[7, 15, 36] and Fe-containing clays,[37-39] but the redox properties of NOM and Fe-clays associations have not been described so far. The aim of this study was to evaluate the role of NOM sorption at an iron-bearing smectite on the redox properties of NOM (namely, EEC and redox state) in whole suspensions (containing NOM and Fe-containing clay) and aqueous phases following the sorption (containing non-sorbed NOM). To this end, batch sorption experiments with a standard humic acid isolate from the International Humic Substances Society (Pahokee Peat Humic Acid) and an iron-bearing smectite (Fe(III)-Montmorillonite) were conducted at pH 7 under anoxic conditions and the

redox properties of the system were determined by applying mediated electrochemical analysis.[36-37, 40]

4.3 Materials and Methods

Chemicals. Na-rich Montmorillonite (Wyoming; SWy-2; BET surface area: 25.7 ± 0.2 m²/g) was purchased from the Source Clay Mineral Society (Purdue University, West Lafayette, USA). The Brunauer, Emmett and Teller (BET) method with N_2 adsorption[41] was used to determine the total specific surface area with an ASAP 2000 system (Micromeritics, GA, USA) (data not shown). Its iron content has been reported at about 2.3 ± 0.2 wt %.[37] 1,10-Ethylene-2,20-bipyridiniumdibromide monohydrate (Diquat = DQ, Sigma-Aldrich Co., USA), 1,1′-trimethylene 2,2′-bipyridyl dibromide (Triquat; TQ; provided by M. Sander, ETH Zurich – Switzerland; synthesized following a reported procedure[37]), 2,2′-azino-bis(3-ethylbenzothiazoline-6-sulfonic (ABTS, Sigma-Aldrich Co., USA), 1 M NaOH and 1 M HCl solutions (Titripur; Reag. USP; Merck; Germany), $NaClO_4$ (99+ %; Across Organics; Germany) and MOPS (3-(N-morpholino)propanesulfonic acid); Merck; 99.5 %; Germany). All aqueous solutions were prepared in Millipore® deionized water. Stock suspensions of the sorbent SWy-2 were prepared in 0.1 M $NaClO_4$. Oxygen sensitive experiments were conducted in an anoxic glovebox ($O_2 < 0.1$ ppm; N_2 atmosphere, M. Braun, Germany). Stock suspensions of the sorbents were purged with N2 (purity grade > 99.999 %) for 1 hour prior transfer to the glovebox. Stock solutions (HA, SWy-2) were purged with N_2 for 1 hour prior transfer to glovebox.

Humic Substances (HS). Pahokee Peat Humic Acid (PPHA; 1S103H) standard material was used as received from IHSS. Stock solutions of PPHA were prepared in 0.1 M $NaClO_4$, manually titrated to pH 7 using fresh solutions (1, 0.1 or 0.01 M) of NaOH or HCl and filtered through pre-washed membranes (Whatman™; 0.45 µm; mixed cellulose ester ME25; Germany) to collect the operational DOC fraction (particle size < 0.45 µm). PPHA stock solution (500 mg PPHA / L) was stored in aluminum foiled Schott bottles and was purged with N_2 for 1 hour prior transfer to the glovebox.

Clay Purification and Stock Suspension Preparation. SWy-2 was saturated with Na^+ following previously described procedures.[36, 42] In brief, 1.6 g of SWy-2 was added to 200 mL of 1M $NaClO_4$ in a centrifuge bottle, the mixture was stirred for 3 hours and afterwards let settle. The supernatant was discarded, and fresh 1 M NaClO4 was added to the solid. This process was repeated three times. Following the last settling step, the centrifuge bottle was refilled with Millipore water, it was stirred for 3 hours and it was centrifuged for 15 minutes at 3000 g using a Hicen 21 centrifugation device (HeroLab, Germany). The supernatant was then discarded and the clay pellet was re-suspended in fresh Millipore water. This step was repeated four times until the supernatant remained clear after centrifugation. After the last washing step, the Na-saturated SWy-2 (Na-SWy-2) was dried at 60 °C for ~ 48 hours and stored in a desiccator until preparation of Na-SWy-2 suspension for suspension for batch sorption experiments (see below).

Sorption experiments. Sorption of PPHAs to Na-SWy-2 was studied in 50 mL serum brown glass bottles with butyl rubber stoppers at pH 7 in 0.1 M NaClO4 without addition of buffers in duplicate batch experiments at several ratios PPHA / SWy-2 (**Table 1**). Sorption was determined by suspending different amounts of Na-saturated SWy-2 of 0.1 M NaClO4 prior addition of a PPHA solution with a fixed total concentration. The pH of each sorption batch was manually adjusted to 7 before addition of PPHA solution and also afterwards for up to four consecutive days until apparent equilibration was achieved. Apparent sorption equilibrium was obtained after 2-4 days as indicated by constant UV-vis absorption spectra of filtered (0.45 µm) samples and constant pH values. These tests were performed at higher HA/sorbent ratios (data not shown). Aliquots of suspensions were taken and kept inside the glovebox for subsequent electrochemical analyses (see below). Afterwards, the remaining suspension was let undisturbed overnight, and the filtrate (Minisart® syringe filter; 0.45µm; regenerated cellulose, Sartorius, Germany) was collected for mediated electrochemical and optical analysis (see below).

Table 3. Experimental setups for sorption batch experiments.

Sample	PPHA / SWy-2 mass ratio	PPHA (mg / L)	Na-SWy-2 (mg / L)	Total volume (mL)
C1	1/5		250	
C2	1 / 10		500	
C3	1 / 20	~ 50	1000	
C4	1 / 50		2500	50
C5	1 / 100		5000	
C6	1 / 200		10000	
Na-SWy-2 control	0	0	2500	

Characterization of dissolved HA. Two independent methods to determine DOC were used: i) total carbon analyzer (TOC; Vario Cube; Elementar; Hanau; Germany) and ii) UV-Vis spectroscopy (10 mm quartz cuvettes (Suprasil; Hellma Analytics; Germany) and a photoLab 6600 UV−Vis spectrophotometer (WTW; Germany). Both methods were applied to HA stock solutions and HA filtrates following sorption (**Fig. SI18**). It has been reported that DOC analysis by UV-Vis in filtrates after sorption could be biased due to depletion of chromophoric DOC components upon sorption.[43] Therefore, DOC in filtrates from sorption experiments quantified by TOC was used for calculations in this study. The specific UV-Vis absorbance at 254 nm ($SUVA_{254} = L*(mgC*m)^{-1}$ = arbitrary units) of PPHA stock and filtrates was calculated as the measured absorbance using a 10 mm cuvette multiplied by 100 to transform length units to meters and normalization by DOC concentration ($mgC*L^{-1}$) ($SUVA_{254} = Abs_{254}*100*DOC^{-1}$).[44] Excitation-emission-matrix (EEM) fluorescence spectra of suspension filtrates were measured using a Fluoromax®4 (Horiba, Jobin-Yvon, Japan) spectrofluorometer. When necessary samples were diluted to UV-Vis absorbance values at 254 nm below 0.3 to avoid inner-filter effects.[45] EEM fluorescence spectra were recorded over a range of emission (350 −

600 nm) and excitation (250 - 500 nm) wavelength.[46-47] Carbon normalized fluorescence emission spectra were calculated at 470 nm excitation wavelength (**Fig. SI19**).

Electron Exchange Capacity (EEC) of HA. The redox properties of PPHA stock solution (PPHA$_{stock}$), SWy-2 stock suspension (SWy-2$_{stock}$), whole suspensions containing PPHA and SWy-2 (PPHA$_{aq+sorb}$) and filtrates (PPHA$_{aq}$) after sorption were determined by mediated electrochemical analysis.[36,40] The EAC and EDC were measured either by mediated reduction (MER) or oxidation (MEO) analysis. Briefly, MER and MEO were conducted at pH 7 in the presence of 0.1 M NaClO$_4$ and 0.01M MOPS (3-(N-morpholino)propanesulfonic acid) buffer using a glassy carbon crucibles (Sigradur G, HTW, Germany) as working electrode, Pt wire (0.5 mm; 99.9 %) attached to Pt gauze (52 mesh, 99.9 %), both from Sigma-Aldrich Co., USA as auxiliary electrode and a Ag/AgCl as reference electrode (Bioanalytical systems Inc., USA) connected to a potentiostat (1000C Multi-potentiostat, CH Instruments, USA). Electrochemical cells were polarized to either reductive (MER; E°_H(pH 7) = - 0.49 V vs. SHE for Diquat or E°_H(pH 7) = - 0.60 V vs. SHE) or oxidative (MEO; E°_H(pH 7) = + 0.61 V vs. SHE for Triquat) prior addition of redox transfer mediators (Diquat or Triquat in MER and ABTS in MEO). The adsorption behavior of Diquat, Triquat and ABTS to SWy-2 was assessed by UV-Vis spectroscopy (data shown in Supporting Information **Fig. SI20**). It was shown that Triquat adsorbed on the clay and this caused lost in reactivity of the electron transfer mediator during the course of the MER (data not shown). The current was recorded over time between the working electrode and the auxiliary electrode. The charge transferred from the sample via the mediator to the electrode was obtained by integrating the current signal after baseline correction using a composite rule as implemented in the SciPy library of Python. EAC, EDC and total Electron Exchange Capacities (EEC = EAC + EDC) were calculated by normalizing the transferred charged to: i) mass of organic carbon for HA in stock solution or HA in aqueous phase after sorption (PPHA$_{stock}$ or PPHA$_{aq}$) and ii) mass of PPHA, mass of SWy-2 or mass of PPHA + SWy-2 for whole suspensions (PPHA$_{stock}$, SWy-2$_{stock}$ or PPHA$_{aq+sorb}$, respectively).

4.5   Results and Discussion

Sorption of PPHA to SWy-2. Sorption results for PPHA in its native redox state to Na-saturated SWy-2 at pH 7 are presented in **Fig. 17.** The sorption isotherm is of saturation type and shows a plateau at a sorbed NOM concentration of approximately 6 mg C/g clay. No attempt to fit sorption models (e.g., Langmuir equation) to the data set was made due to the preliminary character of the experiments and the mismatch of the results with common isotherm shapes. The high standard deviations at high mass ratios of PPHA/Na-SWy-2 (1/5, 1/10) are linked to very low PPHA sorption (< 11 %). Additional experimental work is required to validate the results and extend the concentration range. The sorption batches were designed by setting a fixed initial PPHA concentration while changing the Na-SWy-2 particle concentrations, thus the effects of increasing Na-SWy-2 loadings on the redox properties of PPHA can be assessed.
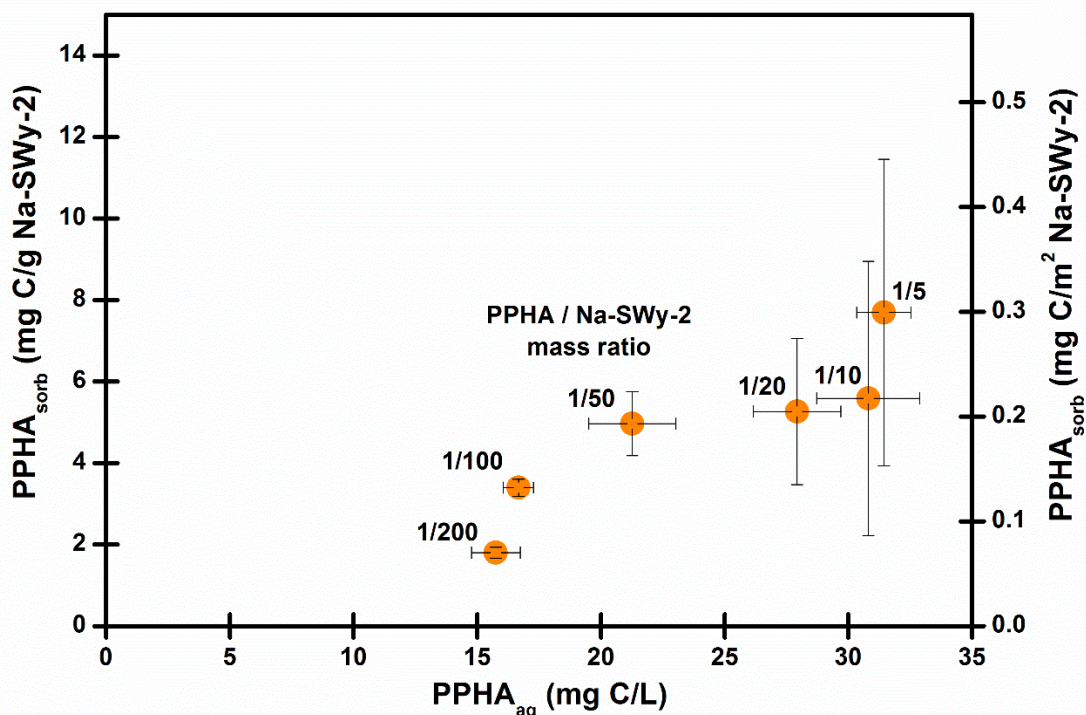
Figure 17. Sorption of Pahokee Peat Humic Acid (PPHA) normalized to total sorbent mass (left axis) and specific surface area (right axis) at pH 7 and 0.1 M $NaClO_4$ for Fe(III)-Montmorillonite (SWy-2). Data points fraction numbers represent PPHA/SWy-2 ratios in sorption batch experiments.

Redox Properties of PPHA after sorption to Na-SWy-2. The electrochemical properties (namely, EAC, EDC and EEC) were measured using mediated electrochemical reduction and oxidation for: i) native PPHA stock solution ($PPHA_{stock}$), ii) 0.45 µm filtrate of SWy-2 suspension ($SWy\text{-}2_{aq}$), iii) the aqueous PPHA fraction after sorption equilibrium ($PPHA_{aq}$; 0.45 µm filtrate of the suspension containing SWy-2 and PPHA), iv) SWy-2 stock suspension ($SWy\text{-}2_{stock}$), and v) whole suspensions containing SWy-2 and PPHA ($PPHA_{aq+sorb}$). **Fig. 18** illustrates the carbon normalized EAC, EDC and EEC of $PPHA_{stock}$, $SWy\text{-}2_{aq}$ and $PPHA_{aq}$ upon sorption to Na-SWy-2. As expected, the $SWy\text{-}2_{aq}$ sample did not present measurable EDC and negligible EAC, indicating that all iron remains on the Na-SWy-2 structure and potential clay dissolution does not generate current responses significantly different to the electrolyte blank.

The $PPHA_{aq}$ fractions consistently presented smaller EEC values than the $PPHA_{stock}$ solutions, regardless of the extent of sorption. This effect was more pronounced (up to 60 % decrease in EEC) at higher percentages of sorbed PPHA (~ 53 % sorbed PPHA). The decrease of EEC was dominated by the decrease in the EDC of $PPHA_{aq}$. Two processes might contribute to the lower EEC values of dissolved PPHA after sorption to Na-SWy-2: a) preferential sorption, in analogy to results obtained for PPHA sorption to Al_2O_3, the PPHA constituents left in aqueous phase were depleted in redox active functional groups (e.g. quinone/hydroquinone, phenols),[34] and/or b) the electron transfer between Fe(III) in Na-SWy-2 and PPHA (e. g. phenols) might shift the overall redox state of PPHA to more oxidized. The calculated ratio of

EDC/EEC changed from 0.47 for $PPHA_{stock}$ to 0.12 for $PPHA_{aq}$ after sorption at 53 % sorbed PPHA (**Fig. 18**).

Figure 18. Electron Donating Capacities (EDC, E_H(pH 7) = 0.61 V vs. SHE.) and Electron Accepting Capacities (EAC, E_H(pH 7) = - 0.49 V vs. SHE.) normalized to organic carbon content as a function of percentage of sorbed Pahokee Peat Humic Acid (PPHA) upon to Na- Montmorillonite (Na-SWy-2). PPHA stock solutions ($PPHA_{stock}$, white crossed-lined bars), 0.45 µm filtrate of SWy-2 suspension ($SWy-2_{aq}$, light yellow bars) and aqueous PPHA fraction after sorption equilibrium (0.45 µm filtrate of the suspension containing SWy-2 and PPHA, $PPHA_{aq}$, dark red bars). Total Electron Exchange Capacities (EEC) denotes the sum of Electron Accepting and Donating Capacities (EEC = EAC + EDC). Ratio of EDC/EEC (presented in bottom row) was calculated as an indicator of the redox state (oxidation degree) of samples.

Fig. 19 shows the EAC and EDC values of $PPHA_{stock}$ and $PPHA_{aq}$ samples normalized to their specific UV-Vis absorbance values at 254 nm ($SUVA_{254}$), a parameter frequently used to assess the aromatic content of dissolved NOM.[44] Up to 70 % decrease in $EDC/SUVA_{254}$ suggests that depletion of hydroquinone/phenol compounds from PPHA solution can explain the changes in EEC of $PPHA_{aq}$ after sorption to Na-SWy-2.
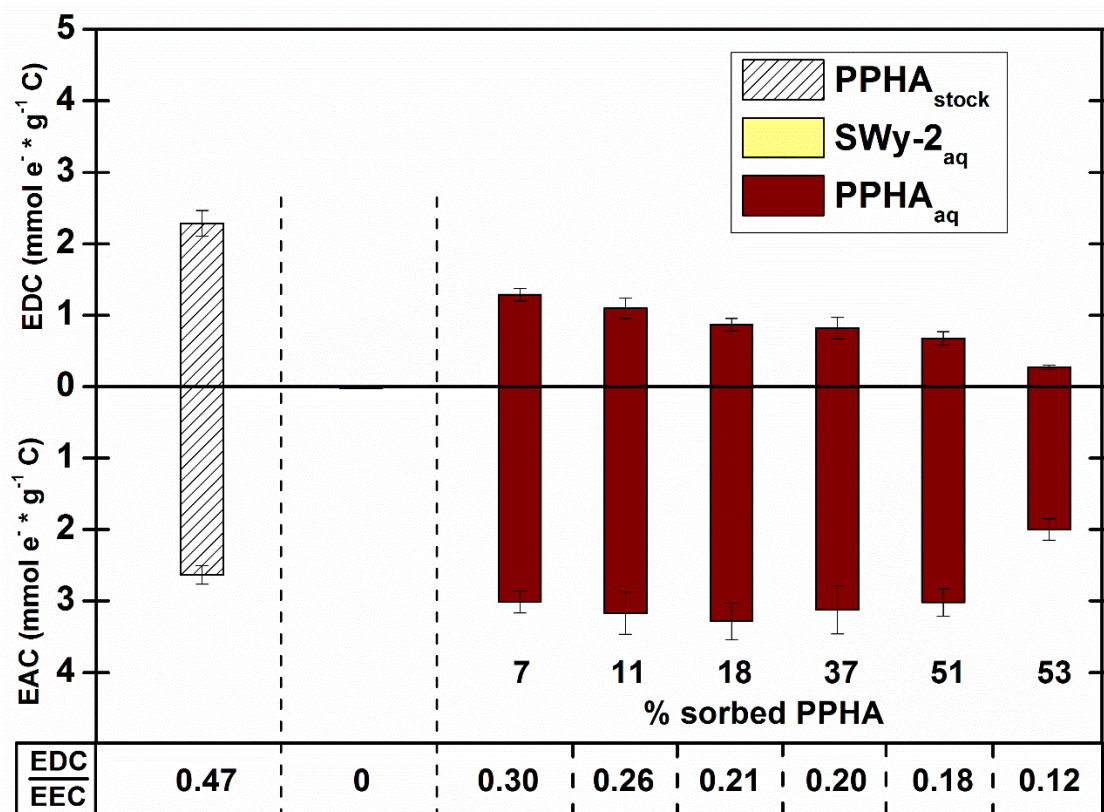
89

Figure 19. Electron Donating Capacities (EDC, E_H(pH 7) = 0.61 V vs. SHE.) and Electron Accepting Capacities (EAC, E_H(pH 7) = - 0.49 V vs. SHE.) normalized to specific UV-Vis absorbance values at 254 nm ($SUVA_{254}$) of Pahokee Peat humic acid stock solution ($PPHA_{stock}$) and PPHA in aqueous phase ($PPHA_{aq}$) upon sorption to Na-rich Montmorillonite (Na-SWy-2).

$PPHA_{stock}$ and $PPHA_{aq+sorb}$ should exhibit similar EAC, EDC and EEC values if there was no electron transfer between Na-SWy-2 and PPHA and sorption had no effect on the redox properties of PPHA. In order to confirm the lack of electron transfer between the clay and the humic acid, the EAC and EDC (mmol e-/mol C) of the suspension samples were normalized to the total organic carbon concentration (**Fig. SI21**). As expected from previous work,[37] SWy-2 containing 2.3 ± 0.2 wt % redox active Fe (III) shows a significant contribution to the total EAC of the suspension containing PPHA and Na-SWy-2, which increased with increasing amount of Na-SWy-2 in the suspension (note that the amount of PPHA in the system was kept constant). Given the intrinsic contribution of Na-SWy-2 to the EAC of suspensions, the EAC and EDC (**Fig. 20**) were normalized to the total mass of analyte (substance) to facilitate comparisons between $PPHA_{stock}$, $SWy-2_{stock}$ and $PPHA_{aq+sorb}$ samples, as follows: i) mmol e-/g PPHA for $PPHA_{stock}$, ii) mmol e-/g Na-SWy-2 for $NA-SWy-2_{stock}$, and iii) mmol e-/g Na-SWy-2+gPPHA) for PPHAaq+sorb samples. **Figure 20** shows how EAC, EDC, EEC and the redox state (EDC/EEC) of $PPHA_{aq+sorb}$ changed in the presence of increasing concentration of Na-SWy-2 in sorption batches (from high to low mass PPHA/Na-SWy-2 ratio). The normalized EEC of $PPHA_{stock}$ samples was at least 20 times higher than the normalized EEC of the $SWy-2_{stock}$. The EAC of $SWy-2_{stock}$ was (0.14 ± 0.01) mmol e-/g, whereas its EDC was below detection limit (EDC/EEC ~ 0) under the electrochemical conditions followed in this experiment. The data shown in **Fig. 20** also allowed evaluating the additivity of EEC in the suspensions containing

90

PPHA and Na-SWy-2. EEC of whole suspension samples (PPHA$_{aq+sorb}$) were up to 80 % lower than of PPHA$_{stock}$, thus the decrease in EEC was more pronounced at low PPHA/Na-SWy-2 ratios (1/200). This result can be explained by separately looking at the relative EAC and EDC of the PPHA$_{stock}$ and SWy-2$_{stock}$ in the system. Considering that SWy-2$_{stock}$ had much lower EEC than PPHA$_{stock}$ (above discussed), it would be expected to see a decrease in the EEC of the mixture, and the effect becomes even more prominent as the mass of Na-SWy-2 exceeds the mass of PPHA in the sorption batch (independent of the sorption extent). Likewise, the high amount of Na-SWy-2 in the sorption batch (compared to PPHA) pushed the redox state of the entire sample towards the redox state of Na-SWy-2$_{stock}$ (EDC/EEC ~ 0).

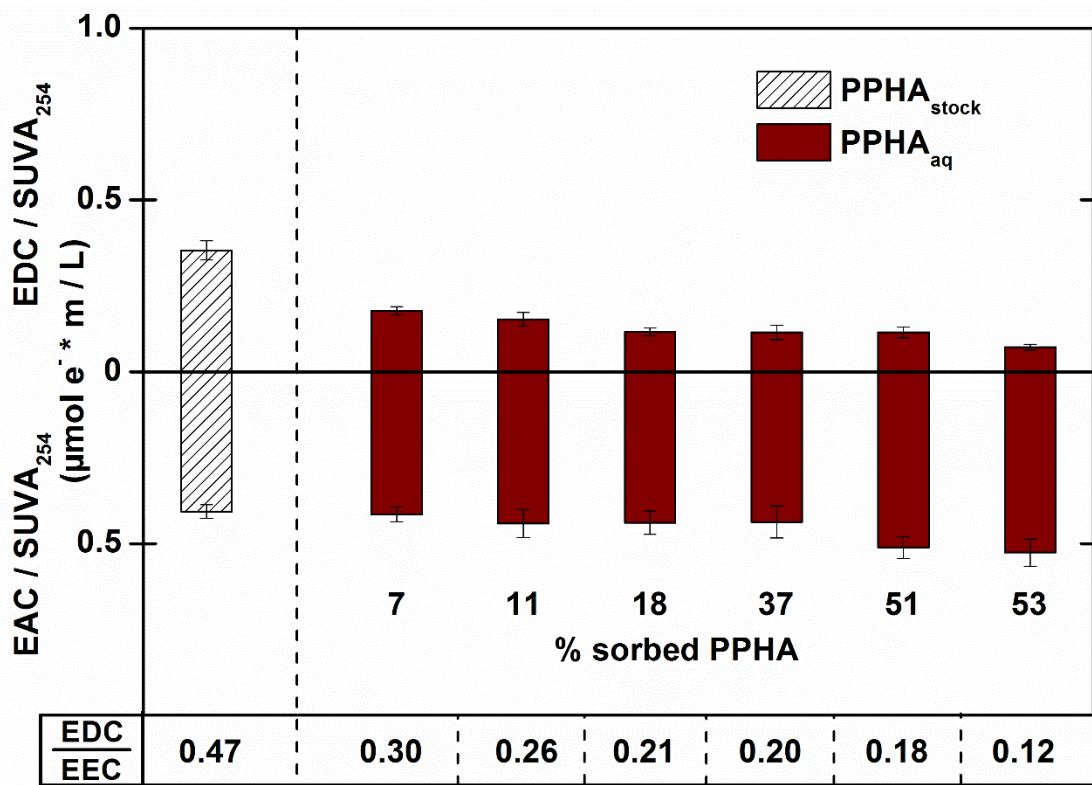**Figure 20.** Electron Donating Capacities (EDC, E_H(pH 7) = 0.61 V vs. SHE.) and Electron Accepting Capacities (EAC, E_H(pH 7) = - 0.49 V vs. SHE.) normalized to total mass of analyte (substance) in the sample (mass of PPHA for PPHA$_{stock}$, mass of Na-SWy-2 for SWy-2$_{stock}$ or mass of PPHA+Na-SWy-2 for PPHA$_{aq+sorb}$) as a function of percentage of sorbed Pahokee Peat Humic Acid (PPHA) to Na-Montmorillonite (Na-SWy-2) and the mass ratio PPHA/Na-SWy-2. PPHA stock solutions (PPHA$_{stock}$, white crossed-lined bars), Na-SWy-2 stock suspension (SWy-2$_{stock}$, green bars) and the whole suspensions containing Na-SWy-2 and PPHA (PPHA$_{aq+sorb}$, orange bars). Total Electron Exchange Capacities (EEC) denotes the sum of Electron Accepting and Donating Capacities (EEC = EAC + EDC). Ratio of EDC/EEC (presented in bottom row) was calculated as an estimation of the redox state (oxidation degree) of samples.

Further analysis on the EEC of PPHA in suspension with Na-SWy-2 was done by subtracting the expected electron transfer contribution of Na-SWy-2 from the total electron transfer of the whole suspension (PPHA$_{aq+sorb}$) and normalizing the electron transfer outcome to the total mass of PPHA in the suspension (**Fig. 21**). Thus, the EEC of only the PPHA in

aqueous and sorbed phase (PPHA$_{aq-sorb}$ – Na-Swy-2) can be calculated. The higher the sorption level, the higher the EAC of PPHA after the correction. Likewise, the comparison among the calculated (PPHA$_{aq+sorb}$ calculated; from specific electron transfer contributions of PPHA and SWy-2 according to the sorption batch composition without accounting for any electron transfer) and the measured (PPHA$_{aq+sorb}$ measured) EAC and EDC values of whole suspensions (**Fig. SI22**), resulted in up to 30 % higher measured EAC values independent of the sorption extent. This provides an indication of electron transfer between the electron donor moieties (hydroquinone/phenols) in PPHA and the iron (III) present in the structure of Na-SWy-2.

More experimental work will be required to confirm the additivity of changes in EEC of PPHA in the presence of redox active clays and the electron transfer reaction on the surface. By testing Fe-containing clays with higher iron content (e.g., nontronite), the potential additivity in EEC in the presence of redox active sorption processes could be demonstrated.
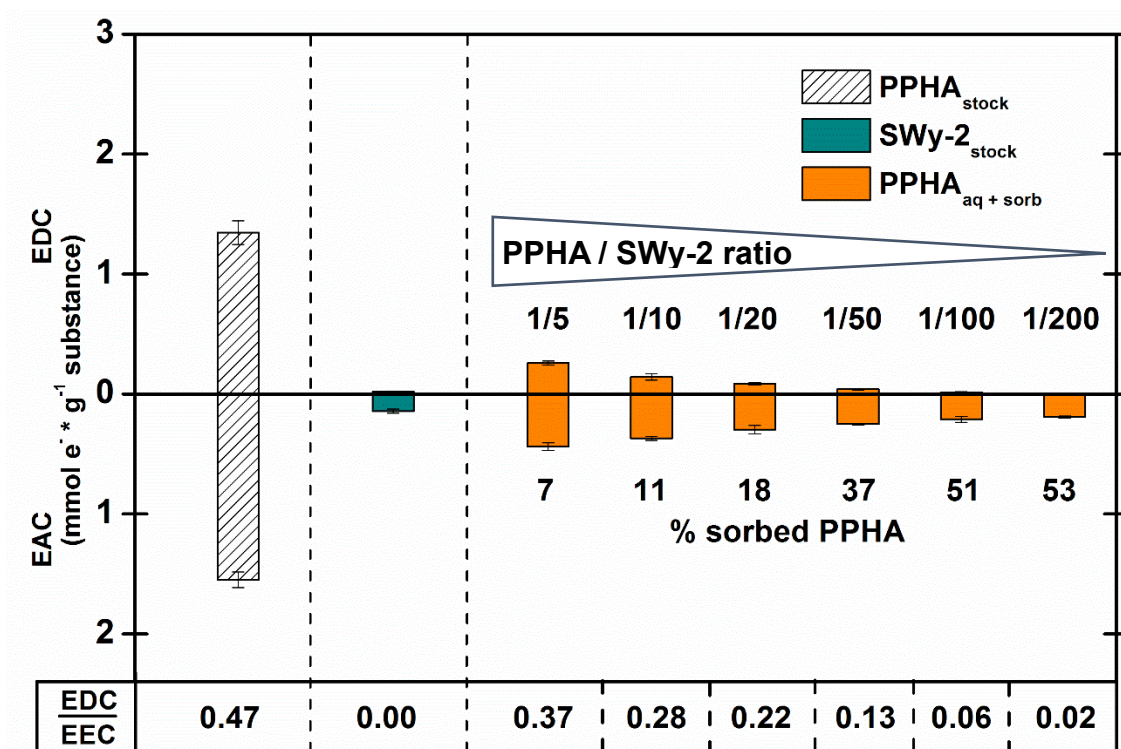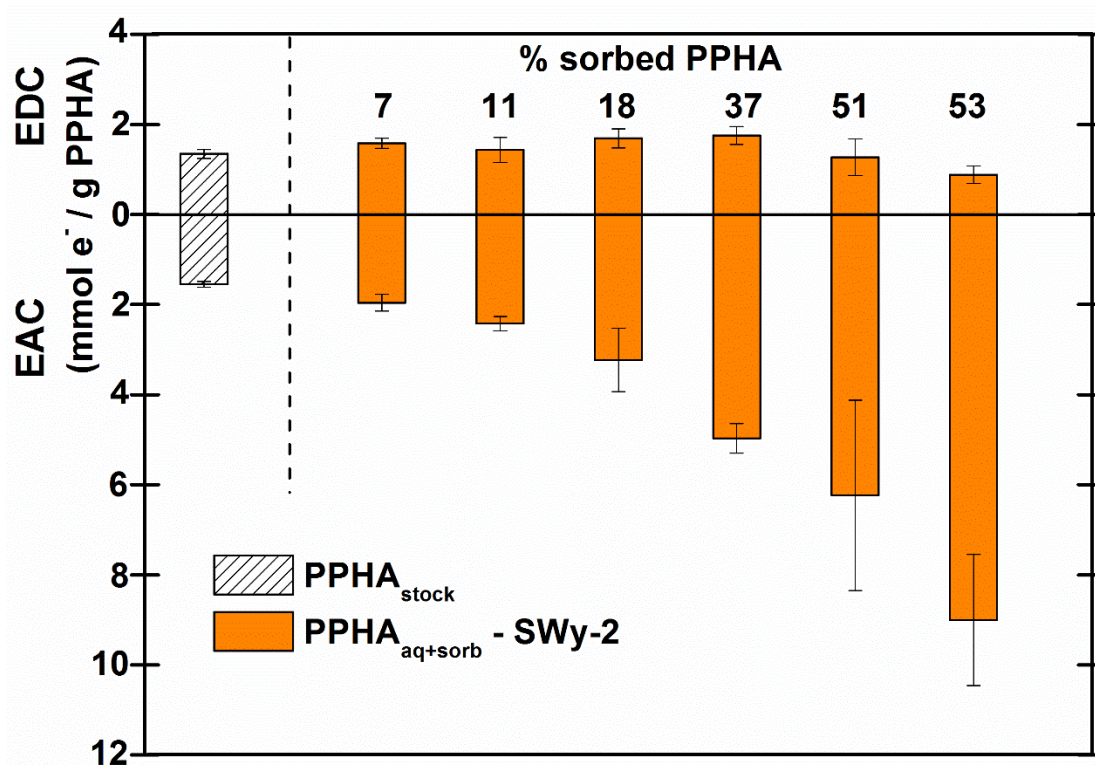

Figure 21. Electron Donating Capacities (EDC, E_H(pH 7) = 0.61 V vs. SHE.) and Electron Accepting Capacities (EAC, E_H(pH 7) = - 0.49 V vs. SHE.) normalized to mass of Pahokee Peat Humic Acid (PPHA) of: PPHA stock solution (PPHA$_{stock}$, white crossed-lined bars) and whole suspensions after electron transfer correction from SWy-2 (PPHA$_{aq+sorb}$ − SWy-2, orange bars). Data for whole suspensions was arranged in ascending PPHA sorption level.

4.6   Environmental Implications.

The preliminary results presented in this chapter demonstrate that the redox properties of NOM are significantly altered upon sorption to redox active clays. Both selective humic acid sorption processes and electron transfer reactions among humic acid and structural iron on the clay triggered up to 60 % decrease in the EEC or 70 % decrease in EDC/SUVA$_{254}$ of PPHA in aqueous phase compared to PPHA stock solution. In sorbed state, the presence of an exceeding amount of SWy-2 in the sorption batch caused a decrease in the EEC of PPHA as well as a shift in the redox state towards the redox state of Na-SWy-2 (EDC/EEC ~ 0). Additional experiment work is needed to confirm the additivity of changes in EEC of PPHA upon redox active sorption. Iron containing clays with higher redox active iron content (e.g., nontronite) should be tested since such additivity in EEC will not be driven by the exceeding amount of one redox active component (e.g., clay) but the actual transfer taking place in the system. This study provides meaningful findings to be used in future work dealing with more complex redox active systems (e.g., iron(oxyhydr-)oxides). These findings might help understanding biogeochemical processes where electron transfer reactions occur among the mineral phase and NOM.

4.7   References

1.   Elsner, M.; Schwarzenbach, R. P.; Haderlein, S. B., Reactivity of Fe(II)-Bearing Minerals toward Reductive Transformation of Organic Contaminants. *Environ. Sci. Technol.,* **2003**, 38, (3), 799-807.

2.   Amstaetter, K.; Borch, T.; Larese-Casanova, P.; Kappler, A., Redox Transformation of Arsenic by Fe(II)-Activated Goethite (α-FeOOH). *Environ. Sci. Technol.*, **2009**, 44, (1), 102-108.

3.   Jiang, J.; Kappler, A. Kinetics of microbial and chemical reduction of humic substances: Implications for electron shuttling. *Environ. Sci. Technol.*, **2008**, 42 (10), 3563-3569.

4.   Wolf, M.; Kappler, A., Jiang, J.; Meckenstock, R. U. Effects of Humic Substances and Quinones at Low Concentrations on Ferrihydrite Reduction by Geobacter metallireducens. *Environ. Sci. Technol.*, **2009**, 43 (15), 5679-5685.

5.   Dunnivant, F. M.; Schwarzenbach, R. P.; Macalady, D. L. Reduction of substituted nitrobenzenes in aqueous solutions containing natural organic matter. *Environ. Sci. Technol.*, **1992**, 26 (11), 2133-2141.

6.   Curtis, G. P.; Reinhard, M. Reductive dehalogenation of hexachlorethane, carbon-tetrachloride and bromoform by anthrahydroquinone disulfonate and humic acid. *Environ. Sci. Technol.*, **1994**, 28 (13), 2393-2401.

7.   Aeschbacher, M.; Vergari, D.; Schwarzenbach, R. P., & Sander, M. Electrochemical Analysis of Proton and Electron Transfer Equilibria of the Reducible Moieties in Humic Acids. *Environ. Sci. Technol.*, **2011**, 45 (19), 8385-8394.

8.   Nurmi, J. T.; Tratnyek, P. G. Electrochemical properties of natural organic matter (NOM), fractions of NOM, and model biogeochemical electron shuttles. *Environ. Sci. Technol.*, **2002**, 36 (4), 617-624.

9.   Maximov, O. B; Glebko L. I. Quinoid groups in humic acids. *Geoderma*, **1974**, 11 (1), 17-28.

10. Scott, D. T.; McKnight, D. M.; Blunt-Harris, E. L.; Kolesar, S. E.; Lovley, D. R. Quinone moieties act as electron acceptors in the reduction of humic substances by humics-reducing microorganisms. *Environ. Sci. Technol.*, **1998**, 32 (19), 2984-2989.

11. Macalady, D. L., & Walton Day, K. Redox Chemistry of Natural Organic Matter (NOM): Geochemist's Dream, Analytical Chemist's Nightmare. In *Aquatic Redox Chemistry*; Tratnyek, P. G., Grundl, T. J. & Haderlein, S. B., Eds.; Oxford University Press: Washington, **2011**; pp 87-111.

12. Struyk, Z.; Sposito, G. Redox properties of standard humic acids. *Geoderma*, **2001**, 102, 329-346.

13. Helburn, R. S.; MacCarthy, P. Determination of some redox properties of humic acid by alkaline ferricyanide titration. *Anal. Chim. Acta*, **1994**, 295, 263-272.

14. Aeschbacher, M.; Graf, C.; Schwarzenbach, R. P.; Sander, M. Antioxidant properties of humic substances. *Environ. Sci. Technol.*, **2012**, 46 (9), 4916-4925.

15. Bletsa, E.; Stathi, P.; Dimos, K.; Louloudi, K.; Deligiannakis, Y. Interfacial Hydrogen Atom Transfer by nanohybrids based on Humic Acid Like Polycondensates. *J. Colloid Interface Sci.*, **2015**, 455, 163-171.

16. Murphy, E. M.; Zachara, J. M.; Smith, S. C. Influence of Mineral-Bound Humic Substances on the Sorption of Hydrophobic Organic Compounds. *Environ. Sci. Technol.*, **1990**, 24, 1507-1516.

17. Ochs, M.; Cosovic, B.; Stumm, W. Coordinative and hydrophobic interaction of humic hydrophobic mercury surfaces. *Geochim. Cosmochim. Acta*, **1994**, 58 (2), 639-650.

18. Gu, B.; Schmitt, J.; Chen, Z. H.; Liang, L. Y.; McCarthy, J. F. Adsorption and desorption of natural organic matter on iron oxide. Mechanisms and models. *Environ. Sci. Technol.*, **1994**, 28 (1), 38-46.

19. Kaiser, K.; Zech, W. Release of natural organic matter sorbed to oxides and a subsoil. *Soil Sci. Soc. Am. J.*, **1999**, 63(5), 1157-1166.

20. Kang, S. H.; Xing, B. S. Humic acid fractionation upon sequential adsorption onto goethite. *Langmuir*, **2008**, 24 (6), 2525-2531.

21. Vermeer, A. W.; Koopal, L. K. Adsorption of Humic Acids to Mineral Particles. 2. Polydispersity Effects with Polyelectrolyte Adsorption. *Langmuir*, **1998**, 14, 4210-4216.

22. Armanious, A.; Aeppli, M.; Sander, M. Dissolved Organic Matter Adsorption to Model Surfaces: Adlayer Formation, Properties, and Dynamics at the Nanoscale. *Environ. Sci. Technol.*, **2014**, 48, 9420-9429.

23. Jones, D. L.; Edwards, A. C. Influence of sorption on the biological utilization of two simple carbon substrates. *Soil Biol. Biochem.*, **1998**, 30 (14), 1895-1902.

24. Kaiser, K.; Guggenberger, G. Sorptive stabilization of organic matter by microporous goethite: sorption into small pores vs. surface complexation. *Eur. J. Soil Sci.*, **2007**, 58 (1), 45-59.

25. Guggenberger, G.; Kaiser, K. Dissolved organic matter in soil: challenging the paradigm of sorptive preservation. *Geoderma*, **2003**, 113, 293-310.

26. Kalbitz, K.; Schwesig, D.; Rethemeyer, J.; Matzner, E. Stabilization of dissolved organic matter by sorption to the mineral soil. *Soil Biol. Biochem.*, **2005**, 37, 1319-1331.

27. Kaiser, K.; Guggenberger, G. The role of DOM sorption to mineral surfaces in the preservation of organic matter in soil. *Org. Geochem.*, **2000**, 31, 711-725.

28. Hur, J.; Schlautman, M. A. Molecular weight fractionation of humic substances by adsorption onto minerals. *J. Colloid Interface Sci.*, **2003**, 264, 313-321.

29. Heidmann, I.; Christl, I.; Kretzschmar, R. Sorption of Cu and Pb to kaolinite–fulvic acid colloids: Assessment of sorbent interactions. *Geochim. Cosmochim. Acta*, **2005**, 69 (7), 1675-1686.

30. Meier, M.; Namjesnik-Dejanovic, K.; Maurice, P. A.; Chin, Y. P.; Aiken, G. R. Fractionation of aquatic natural organic matter upon sorption to goethite and kaolinite. *Chem. Geol.*, **1999**, 157, 275-284.

31. Claret, F.; Schaefer, T.; Brevet, J.; Reiller, P. E. Fractionation of Suwannee River Fulvic Acid and Aldrich Humic Acid on α-Al2O3: Spectroscopic Evidence. *Environ. Sci. Technol.*, **2008**, 42, 8809-8815.

32. Galindo, C.; Del Nero, M. Molecular Level Description of the Sorptive Fractionation of a Fulvic Acid on Aluminum Oxide Using Electrospray Ionization Fourier Transform Mass Spectrometry. *Environ. Sci. Technol.*, **2014**, 48, 7401-7408.

33. Subdiaga, E.; Orsetti, S.; Haderlein, S. B. Effect of Sorption on Redox Properties of Natural Organic Matter. In preparation

34. Subdiaga, E.; Orsetti, S.; Harir, M.; Hertkorn, N.; Schmitt-Kopplin, P.; Haderlein, S. B. Preferential sorption of tannin-like compounds on aluminum oxide trigger changes in the electron exchange capacities of natural organic matter. In preparation.

35. Aeschbacher, M.; Sander, M.; Schwarzenbach, R. P. Novel electrochemical approach to assess the redox properties of humic substances. *Environ. Sci. Technol.*, **2010**, 44 (1), 87-93.

36. Gorski, C. A.; Aeschbacher, M.; Soltermann, D.; Voegelin, A.; Baeyens, B.; Fernandes, M. M.; Hofstetter, T. B.; Sander, M. Redox properties of structural Fe in clay minerals. 1. Electrochemical quantification of electron-donating and -accepting capacities of smectites. *Environ. Sci. Technol.*, **2012**, 46 (17), 9360-9368.

37. Gorski, C. A.; Kluepfel, L.; Voegelin, A.; Sander, M.; Hofstetter, T. B. Redox properties of structural Fe in clay minerals. 2. Electrochemical and spectroscopic characterization of electron transfer irreversibility in ferruginous smectite, SWa-1. *Environ. Sci. Technol.*, **2012**, 46 (17), 9369-9377.

38. Gorski, C. A.; Kluepfel, L.; Voegelin, A.; Sander, M.; Hofstetter, T. B. Redox properties of structural Fe in clay minerals: 3. Relationships between smectite redox and structural properties. *Environ. Sci. Technol.*, **2013**, 47 (23), 13477-13485.

39. Kluepfel, L.; Keiluweit, M.; Kleber, M.; Sander, M. Redox properties of plant biomass-derived black carbon (biochar). *Environ. Sci. Technol.*, **2014**, 48 (10), 5601-5611.

40. Seaton, N. A.; Walton, J. P. R. B.; Quirke, N. A new analysis method for the determination of the pore size distribution of porous carbons from nitrogen adsorption measurements. *Carbon*, **1989**, 27, 853-861.

41. Gnann, S. Redox Reactions Between Iron-bearing Clays (SWy-2) and Model Quinones (ADQS). *Bachelor Thesis, Eberhard Karls Universität Tübingen*, Germany, **2013**.

42. Claret, F.; Schaefer, T.; Brevet, J.; Reiller, P. E. Fractionation of Suwannee River Fulvic Acid and Aldrich Humic Acid on α-Al2O3: Spectroscopic Evidence. *Environ. Sci. Technol.*, **2008**, 42, 8809-8815.

43. Weishaar, J. L.; Aiken, G. R.; Bergamaschi, B. A.; Fram, M. S.; Fujii, R.; Mopper, R. Evaluation of Specific Ultraviolet Absorbance as an Indicator of the Chemical

Composition and Reactivity of Dissolved Organic Carbon. *Environ. Sci. Technol.*, **2003**, 37, 20, 4702-4708.

44. Mobed, J. J.; Hemmingsen, S.L.; Autry, J. L.; McGown, L. B. Fluorescence characterization of IHSS humic substances: total luminescence spectra with absorbance correction. *Environ. Sci. Technol.*, **1996**, 30 (10), 3061-3065.

45. Coble, P. G. Characterization of marine and terrestrial DOM in seawater using excitation-emission matrix spectroscopy. *Mar. Chem.*, **1996**, 51, 325-346.

46. Chen, J.; LeBoeuf, E. J.; Dai, S.; Gu, B. Fluorescence spectroscopic studies of natural organic matter fractions. *Chemosphere*, **2003**, 50 (5), 639-647.

Conclusions and Outlook

The main theme of this PhD thesis was to investigate the overall effects of NOM adsorption on its redox properties (i.e., electron exchange capacities and redox state). The framework of this dissertation comprised several well-controlled laboratory experiments, including batch sorption, mediated electrochemical and molecular scale characterization of NOM in different forms (dissolved, suspensions in the presence of mineral particles and filtrates after sorption).

Three humic acids (ESHA, PPHA and SRHA) isolated from different origins (terrestrial and aquatic) in their native redox state were adsorbed onto aluminum oxide (Al_2O_3) which exhibited saturation type adsorption isotherms. The source and composition of HAs had a minor effect on their general sorption behavior. HA-adlayer thickness ranged from ~ 0.30 nm for ESHA to ~ 0.17 nm for PPHA and SRHA. Furthermore, the sorption behaviors and extent of electrochemically reduced and native ESHA both at Al_2O_3 and at DAX-8 resin surfaces were comparable, which was confirmed by their isotherm parameters. The similar trends in sorption are supported by the relatively low abundance of redox active moieties in HA (e.g., quinone/hydroquinone, phenols) compared to other functional groups involved in the sorption (e.g., carboxylic acids).

Adsorption of native HA onto Al_2O_3 significantly decreased EEC of HA filtrates, while that of sorbed HA prominently increased. Sorptive fractionation of redox active components in HA was found responsible for the strong decrease in EEC of HA filtrates. Given the absence of electron transfer between HA and Al_2O_3, EDC of sorbed HA increased up to 200% which could be associated to: i) unfolding of HA supramolecular 3D conformation, rendering the electron donor groups (e.g., phenols, hydroquinones) more accessible to electron transfer and thus enhancing the EDC of sorbed HA, or/and ii) catalyzed polymerization of polyphenolic compounds under oxidizing (but anoxic) conditions by the alumina surface. The occurrence of surface catalyzed reactions was confirmed by measuring the EDC of two model compounds, i.e., chlorogenic acid (CHL) and electrochemical reduced lawsone (LAWred) sorbed to Al_2O_3. Interestingly, the EDC of the polyphenolic chlorogenic acid (CHL) was enhanced up to 50 % in the presence of aluminum oxide particles, but not for the hydroquinone (LAWred). This indicated that HA sorption might cause polymerization of polyphenolic compounds under oxidizing conditions more readily on the surface than in solution. Sorption of HA to the hydrophobic resin DAX-8, however, had little influence on the EEC of aqueous and adsorbed HA fractions due to the lack of specific interactions between HA components and the hydrophobic resin. Contrary to native HA, sorption of electrochemically reduced HA to Al_2O_3, exemplified by ESHA, led to slightly lower EEC of sorbed HA compared to reduced HA, which was linked to the lower diversity of redox active groups in reduced HA. Thus, the effects of

conformational changes of HA macrolecules are minimized within the structure of reduced HA. Strong depletion of aromatic components from solution (confirmed by $SUVA_{254}$) led to substantial decreases in EEC of aqueous HA fractions regardless the sorption level. At DAX-8, the effect of sorption on the redox properties of native HA were comparable for those of native HA. Moreover, the effect of sorption on the oxidation of electrochemically reduced HA by dissolved O_2 was assessed. While the redox states (EDC/EEC) after oxidation by O_2 of the HA filtrate and stock solution were similar, oxidation of sorbed HA decreased to an extent of 25% in the presence of Al_2O_3 after exposure to O_2. A mechanistic interpretation of the observed EEC changes in the whole suspension samples of Al_2O_3 and an assessment of their implications for the reactivity of sorbed NOM, however, requires further experimental studies. Sorption and oxidation-reduction cycles studies of pristine natural NOM as well as of adsorbed model compounds should be considered to better understand the reactivity of sorbed NOM. Sorbents having different characteristics (e.g. inert clays) should also be included in further studies.

High field Fourier transform ion cyclotron resonance mass spectrometry (FT-ICRMS) analysis provided molecular scale evidence of preferential sorption of tannin-like compounds onto Al_2O_3, being the effects more remarkable with the extent of sorption. Given that tannin-like compounds present in NOM are polyphenolic-rich substances and considering their frequent applications as antioxidants (i.e, wine production industry), it can be concluded that depletion of polyphenolic moieties upon sorption to Al_2O_3 led to a prominent decrease in the EDC of HA in aqueous phase in this study. The predominance of non-selective sorption at apolar surfaces (i.e., DAX-8 resin) explains the minor changes in EEC displayed by HA filtrates. These findings indicate that the sorption mechanisms at the NOM-sorbent interface lead to alterations in the redox properties of HA.

The effects of electron transfer upon sorption of PPHA to a Fe-bearing clay (Na-SWy-2 = Na-saturated montmorillonite) was preliminary studied at pH 7. While the EEC of PPHA left in aqueous phase after sorption decreased up to 60 % compared to PPHA stock solution, the adsorbed fraction became more oxidized (up to 70 % lower EDC). The changes in aqueous phase were associated to sorptive fractionation of redox active functional groups (e.g., quinone/hydroquinone, phenols) and/or electron transfer between Fe(III) in Na-SWy-2 and electron donor groups in PPHA. Given that the EEC of PPHA is at least 20 times higher than that of Na-SWy-2, the total EEC of whole suspensions was highly dependent on the mass ratio of PPHA to Na-SWy-2 in sorption batches. Thus in experiments with a low mass ratio of PPHA / Na-SWy-2, the EEC and redox state of the suspension was dominated by the properties of the Na-SWy-2 stock suspension (EDC/EEC ~ 0). In order to evaluate if changes in EEC of PPHA upon sorption to Fe-containing minerals are additive, different clay sorbents should be selected, e.g., nontronite which shows a higher content of redox active iron (~ 20 wt %). In such experimental setups the EEC of the whole suspension will not be driven by the exceeding amount of one redox active component over the other, but the actual electron transfer taking place in the system. Furthermore, I suggest applying molecular scale analysis (FT-ICRMS) to sorption studies involvingFe-bearing clays to elucidate the sorption mechanisms causing alterations in redox properties of NOM.

The results of this PhD work provide fundamental knowledge that can serve as a reference in future work dealing with more complex redox active systems, i.e., iron(oxyhydr-)oxides, where the electron transfer occurs at the surface as well as in solution. Likewise, these findings might improve understanding of biogeochemical processes where electron transfer reactions occur between the mineral phase and NOM.

Supporting Information

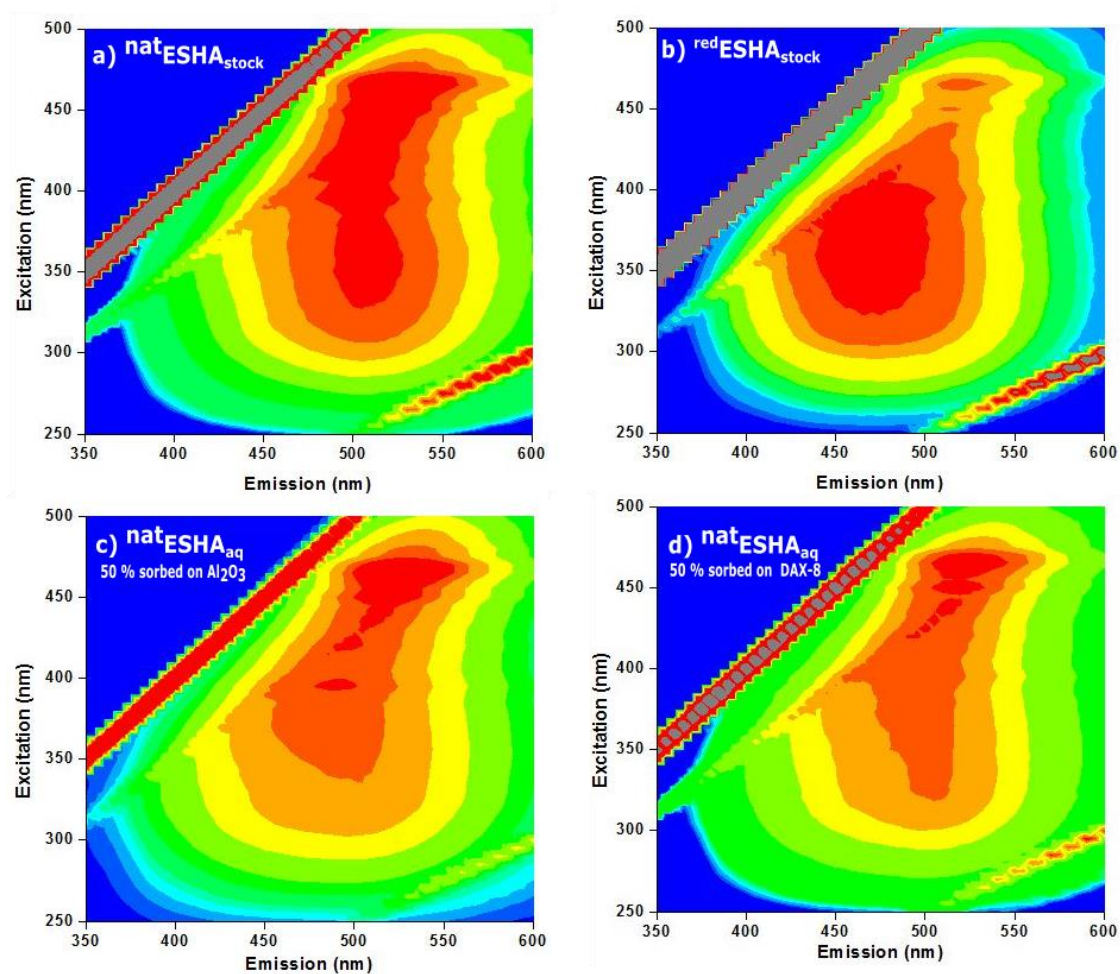## Chapter 2. Effect of Sorption on Redox Properties of Natural Organic Matter.

Figure SI1. Emission-Excitation Fluorescence Spectra (EEM) of Elliott Soil Humic Acid (ESHA) for: a) native ESHA stock solution (^{nat}ESHA$_{stock}$), b) reduced ESHA stock solution (^{red}ESHA$_{stock}$), c) native ESHA in aqueous phase (^{nat}ESHA$_{aq}$) after ~ 50% sorption at Al$_2$O$_3$ and d) native ESHA in aqueous phase (^{nat}ESHA$_{aq}$) after ~ 50% sorption at DAX-8.
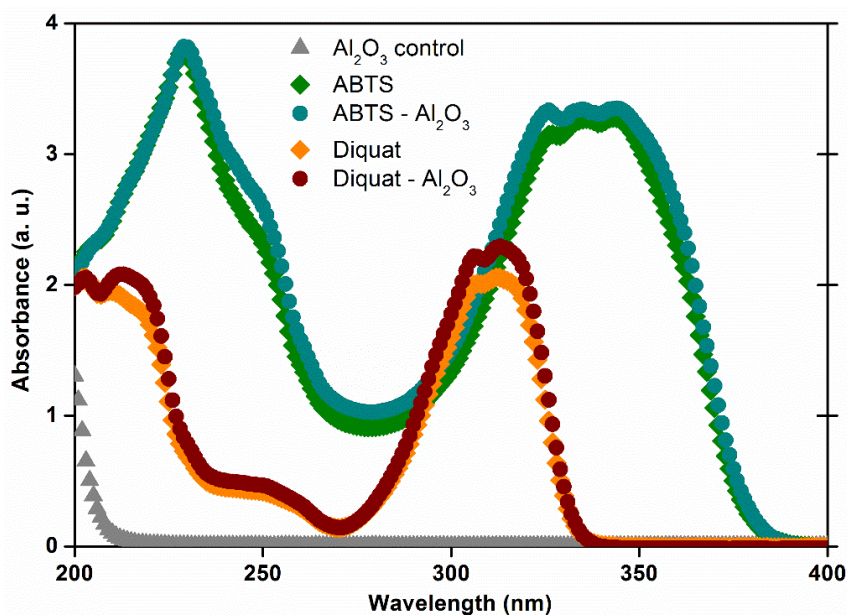
Figure SI2. UV-Vis absorption spectra of the electron transfer mediators used in the presence and absence of the sorbent Al_2O_3 to evaluate the degree of adsorption of the mediators using similar conditions as in MER-MEO techniques.[1]
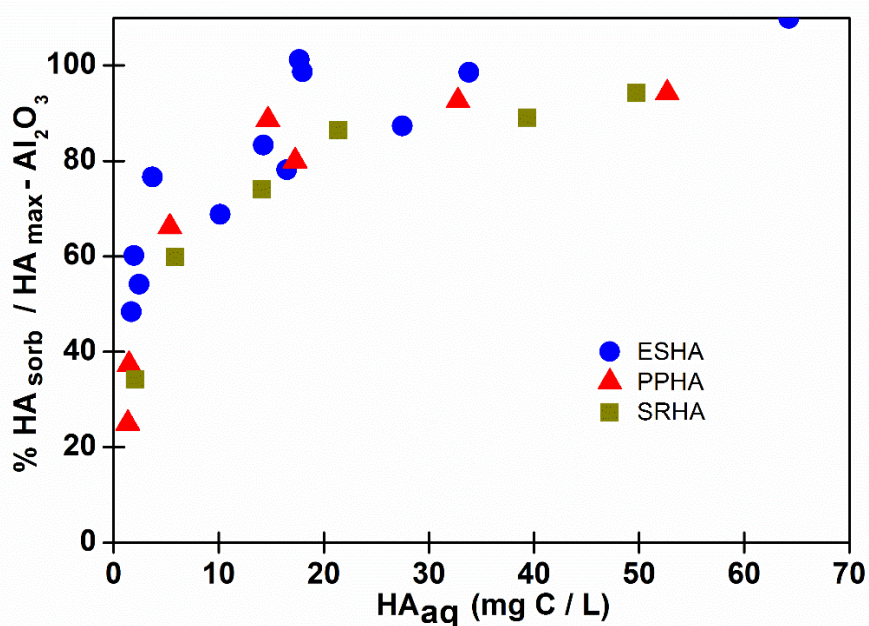

Figure SI3. Percentage of surface coverage (sorbed humic acid (HAsorb) / maximum sorbed capacity (HAmax)) of the humic acids investigated on aluminum oxides (Al_2O_3). HAmax was derived from Langmuir fits. Blue dots (●) = Elliott Soil humic acid (ESHA); red triangles (▲) = Pahokee Peat humic acid (PPHA); black squares (■) = Suwannee River humic acid correspond to non-sorbed re-oxidized ESHA fractions after 0.45µm filtration.

[1] Aeschbacher, M., Sander, M. & Schwarzenbach, R. P. Novel electrochemical approach to assess the redox properties of humic substances. Environ. Sci. Technol., **2010**, 44 (1), 87−93.

Table SI1. Adlayer thickness of HA sorbed at aluminum oxide (Al_2O_3) in this study and comparison with literature values.

Humic acid	This Study			Shen et al., 1999[2]	Schlautmann and Morgan, 1994[3]	Janot et al., 2012[4]
	ESHA	PPHA	SRHA	HA extracted from surface horizon of a peat soil-Taiwan	SRHA	Purified Aldrich HA
Al_2O_3 properties	90% standardized; Merck 70% between 0.063 - 200 mm			α-Al2O3 supplied, Degussa Corp., U.S.A	y-Al2O3 Degussa Corp., U.S.A	α-Al2O3, Interchim (pure 99.99%, size fraction 200-500 nm)
Specific Surface area (m^2/g)	133.6 ± 0.3			8.2	80	15
pH - batch experiments	7			6-7	7	7.2
HAmax (μg C/m^2)	309.9	181.9	177.4	290	484.6	~ 800
Adlayer density (g/ cm^3)				1.05[5]		
Adlayer thickness (nm)	0.30	0.17	0.17	0.28	0.46	0.76

2 Shen, Y. Sorption of humic acid to soil: the role of soil mineral composition. *Chemosphere*, **1999**, 38, 11, 2489-2499.

3 Schlautman, M. A.; Morgan, J. J. Adsorption of aquatic humic substances on colloidal-size aluminum oxide particles: Influence of solution chemistry. *Geochimica et Cosmochimica Acta.*, **1994**, 58, 20, 4293-4303.

4 Janot, N.; Reiller, P. E.; Zheng, X.; Croue, J. P.; Benedetti, M. F. Characterization of humic acid reactivity modifications due to adsorption onto α-Al2O3. *Water Res.*, **2012**, 46 (3), 731−740.

5 Armanious, A.; Aeppli, M.; Sander, M. Dissolved Organic Matter Adsorption to Model Surfaces: Adlayer Formation, Properties, and Dynamics at the Nanoscale. *Environ. Sci. Technol.*, **2014**, 48, 9420-9429.
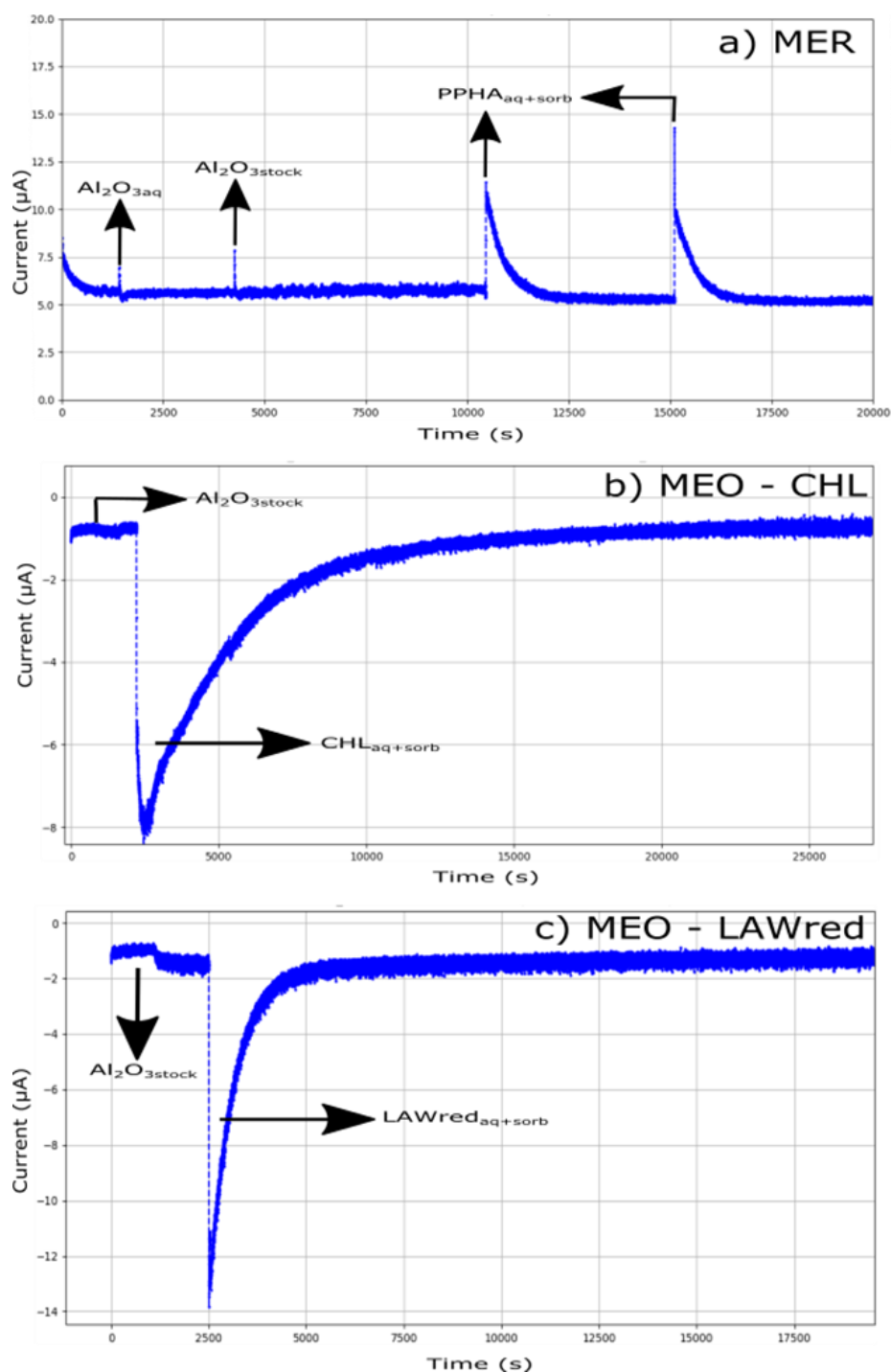
Figure SI4. Typical current traces in: a) mediated electrochemical reduction (MER) of filtered Al_2O_3 aluminum oxide (Al_2O_{3aq}), aluminum oxide stock suspension (Al_2O_{3stock}), and HA in suspension with Al_2O_3 ($HA_{aq+sorb}$), b) mediated electrochemical oxidation (MEO) of Al_2O_{3stock} and chlorogenic acid (CHL) in suspension with Al_2O_3 ($CHL_{aq+sorb}$), c) MEO of Al_2O_{3stock} and reduced form of lawsone (LAWred) in suspension with Al_2O_3 ($LAWred_{aq+sorb}$).
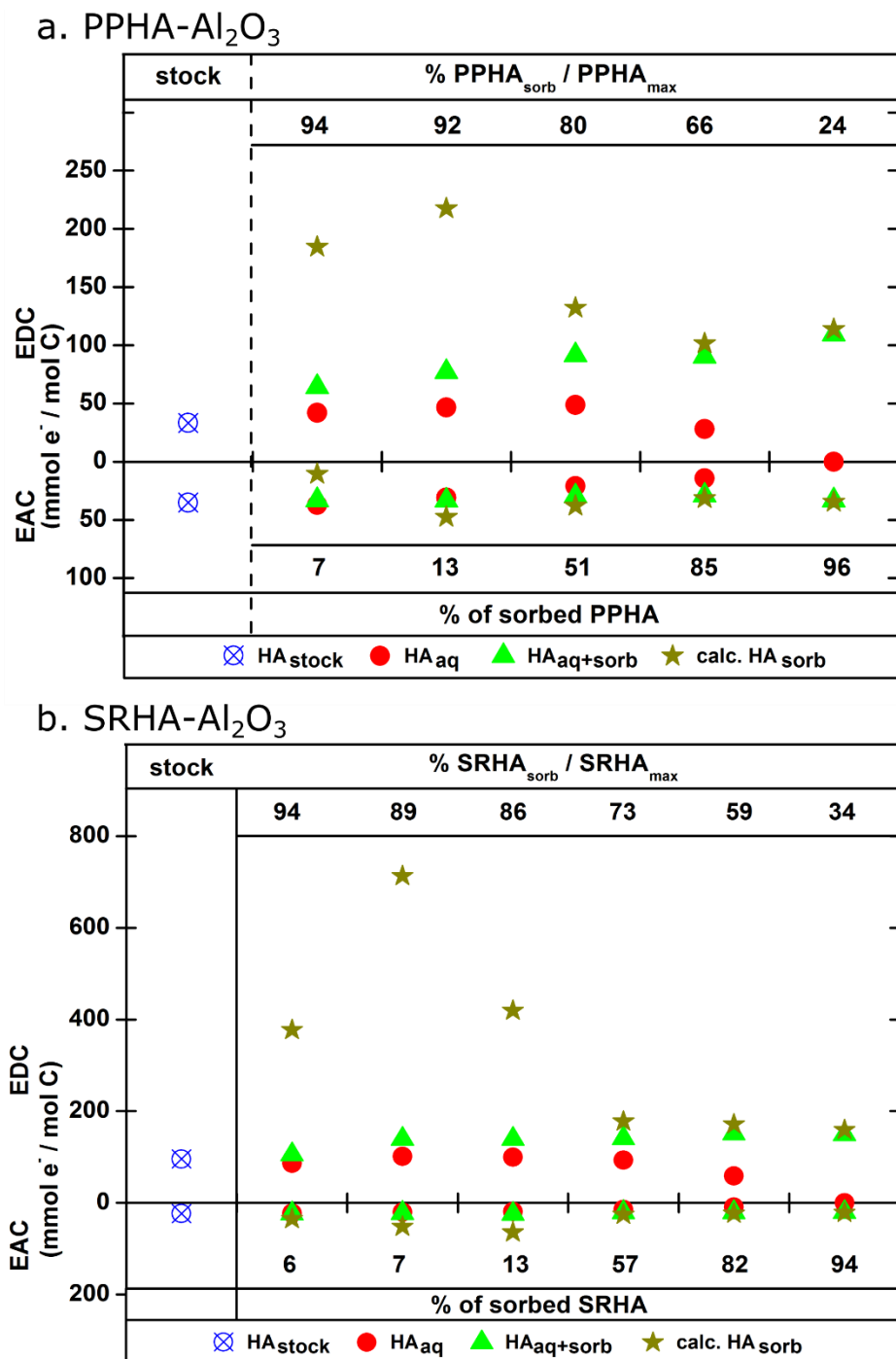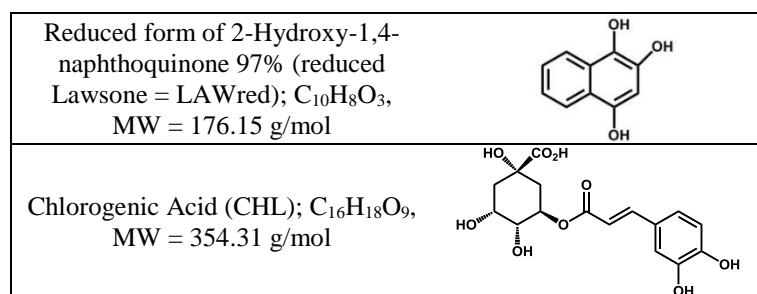
Figure SI5. Calculated Electron Donating Capacities (EDC, E_H(pH 7) = 0.61 V vs. SHE.) and Electron Accepting Capacities (EAC, E_H(pH 7) = - 0.49 V vs. SHE.) of sorbed fractions from measured EDC and EAC of whole suspensions and filtrates and after sorption. Panels correspond to: a) Pahokee Peat (PPHA) and b) Suwannee River (SRHA) humic acids at aluminum oxide (Al_2O_3). Markers correspond to: HA stock solutions (HAstock, white crossed-lined circles), 0.45 µm filtrates containing non-sorbed HA (HAaq, red circles), whole suspensions containing sorbents + sorbed HA + non-sorbed HA (HAaq+sorb, light green triangles) and calculated sorbed HA (HAsorb, brown stars). Data is arranged in ascending HA sorption level (% sorbed –PPHA and –SRHA) and descending level of surface coverage.

Table SI2. Experiment design of batch sorption experiments with reduced lawsone (LAWred) and chlorogenic acid (CHL) onto aluminum oxide (Al_2O_3) at pH 7 in conducted batch sorption experiments. The two rows at the bottom show the chemical structures of LAWred and CHL. LAWred was prepared by direct electrochemical reduction (see methods section in chapter 2) of lawsone. The full reduction of LAWred was confirmed by UV-Vis spectroscopy (data not shown).

Condition	Mass ratio model compound/Al_2O_3	Total Volumen (mL)	Mass Al_2O_3 (g)	Vol. LAWred (mL)	Vol. CHL (mL)	Vol. 0.1 M KCl (mL)
C$_1$ - LAWred	1/20			40 mL LAWred 2000 mg/L	-	-
C$_2$ - LAWred	1/40			20 mL LAWred 2000 mg/L	-	20
C$_3$ - LAWred	1/80			10 mL LAWred 2000 mg/L	-	30
C$_4$ - LAWred	1/160			20 mL LAWred 500 mg/L	-	20
C$_5$ - LAWred	1/320	100	1.6	10 mL LAWred 500 mg/L	-	20
C$_1$ - CHL	1/20			-	40 mL CHL 2000 mg/L	-
C$_2$ - CHL	1/40			-	20 mL CHL 20000 mg/L	20
C$_3$ - CHL	1/80			-	10 mL CHL 2000 mg/L	30
C$_4$ - CHL	1/160			-	20 mL CHL 500 mg/L	20
C$_5$ - CHL	1/320			-	10 mL CHL 500 mg/L	30

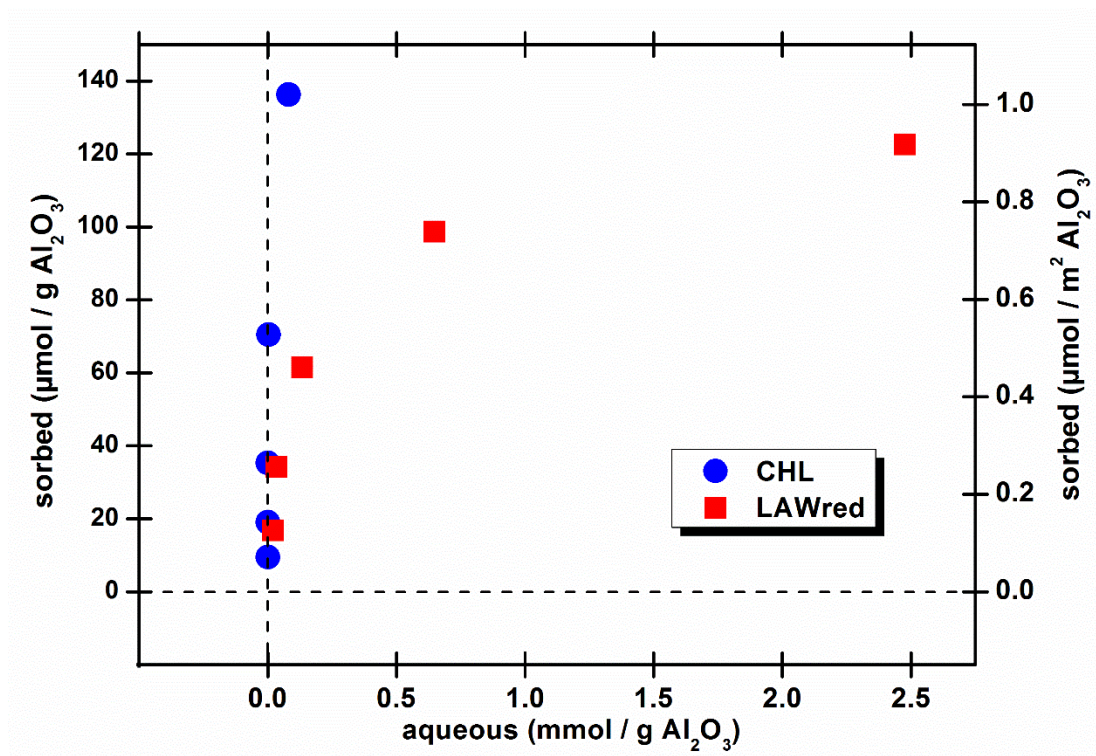|	
Reduced form of 2-Hydroxy-1,4-naphthoquinone 97% (reduced Lawsone = LAWred); $C_{10}H_8O_3$, MW = 176.15 g/mol	
Chlorogenic Acid (CHL); $C_{16}H_{18}O_9$, MW = 354.31 g/mol	

Figure SI6. Sorption of electrochemically reduced lawsone (LAWred) onto aluminum oxide (Al_2O_3) at pH 7 and 0.1 M KCl. The amount of model compound was normalized to Al_2O_3 mass (left axis, = µmol/g Al_2O_3) and Al_2O_3 specific surface area (right axis, = µmol/m^2 Al_2O_3).

a. EDC - LAWred
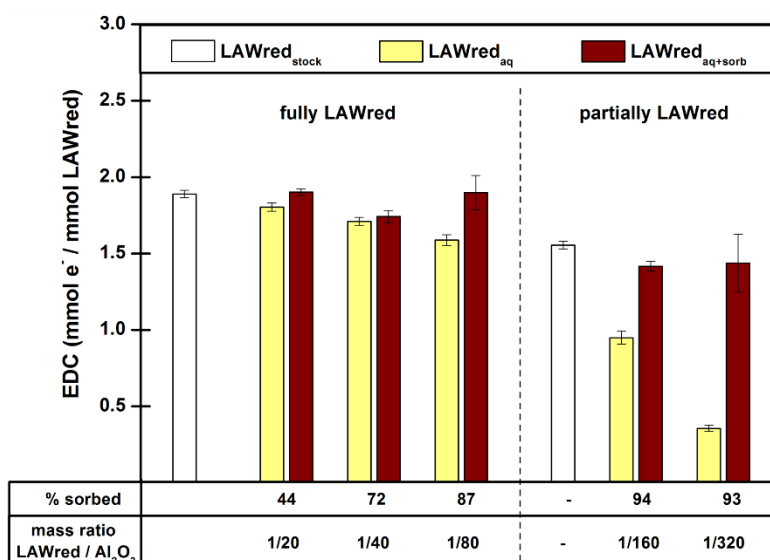
b. EDC - CHL

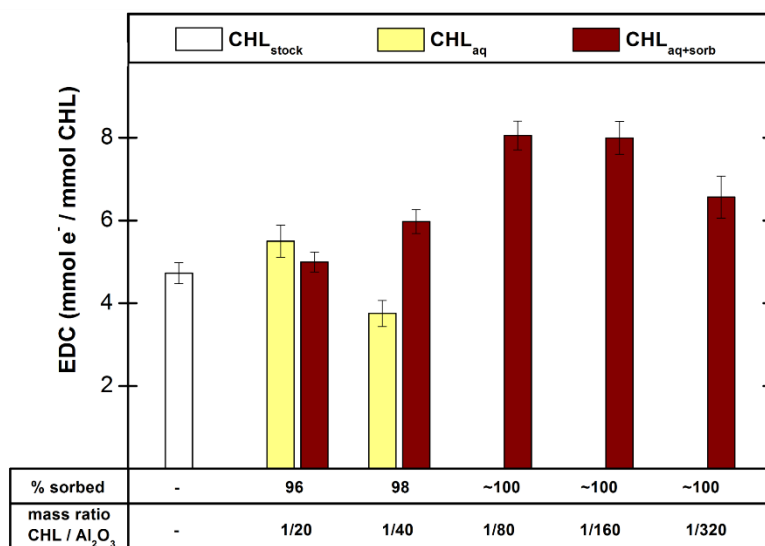**Figure SI7.** Electron Donating Capacities (EDC, E_H(pH 7) = 0.61 V vs. SHE.) as a function of percentage of sorbed model compound of: a) reduced form of lawsone (LAWred), b) chlorogenic acid (CHL) upon sorption to aluminum oxide (Al_2O_3). Model compounds stock solutions (compound$_{stock}$, white bars), 0.45 µm filtrates (compound$_{aq}$, light yellow bars) and whole suspensions (compound$_{aq+sorb}$, dark red bars). Note in **Fig. 7a** that in order to have some additional data points, the original stock solution of LAWred was used, however, this solution became slightly oxidized (lower EDC) during the time in-between the two experiments (~ 60 days).
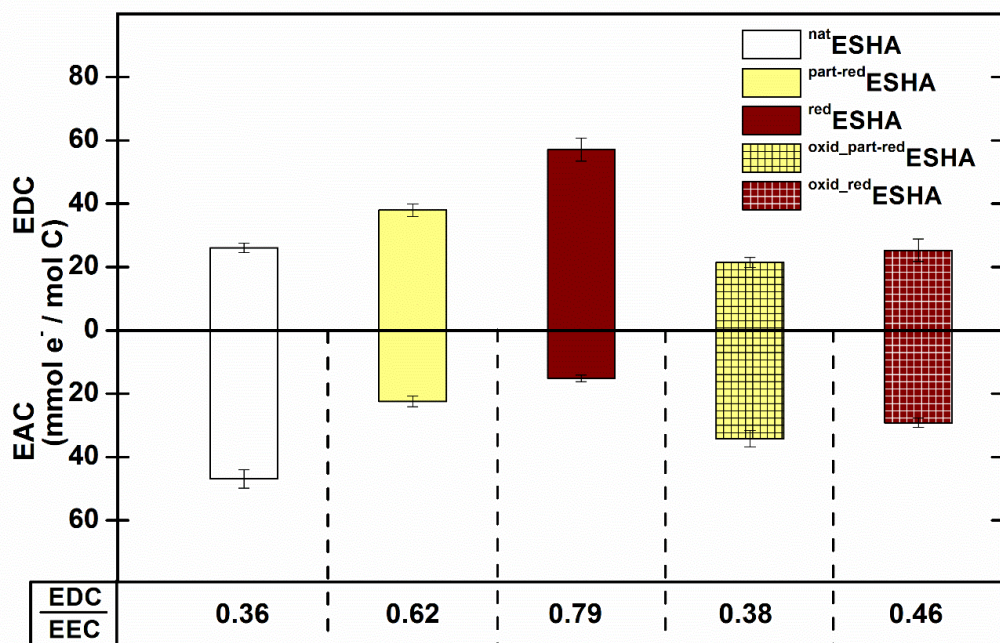
Figure SI8. Effect of oxidation by O_2 of electrochemically reduced Elliott Soil Humic Acid on its Electron Donating Capacities (EDC, E_H(pH 7) = 0.61 V vs. SHE.) and Electron Accepting Capacities (EAC, E_H(pH 7) = - 0.49 V vs. SHE.). Bar colors indicate the initial redox state of HAs: native HA (^{nat}ESHA), partially reduced HA ($^{part-red}$ESHA), reduced HA (^{red}ESHA): Hatched patterns indicate HAs samples after oxidation: electrochemical partially reduced HA ($^{oxid\_part-red}$ESHA) and oxidized electrochemical reduced HA ($^{oxid\_red}$ESHA).
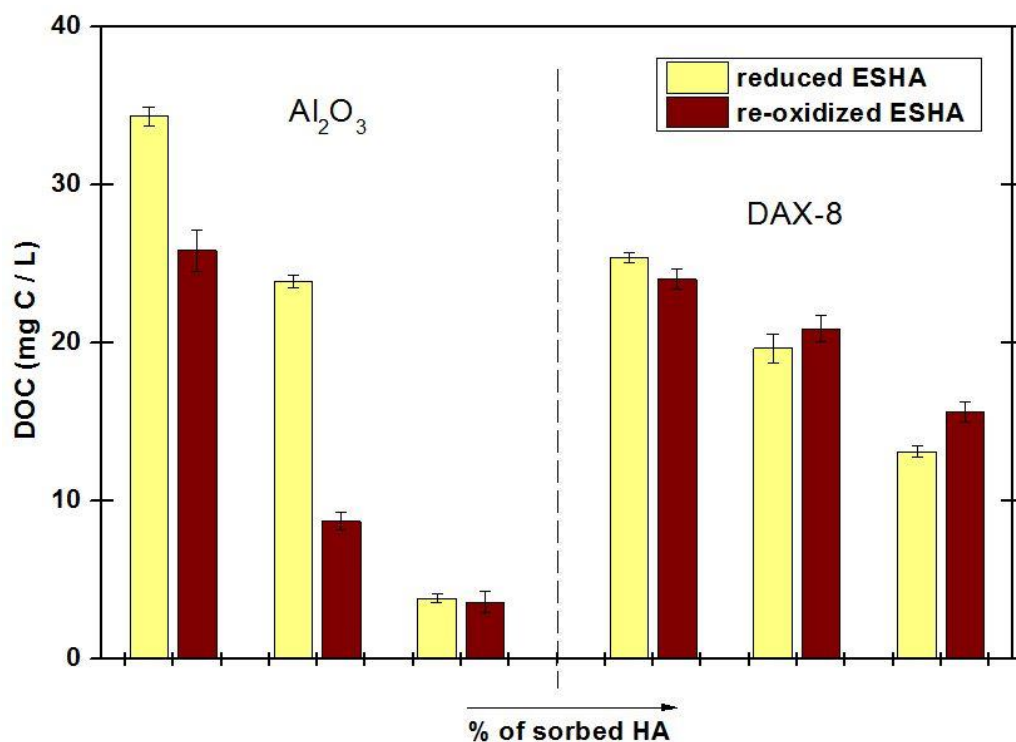

Figure SI9. Dissolved Organic Carbon (DOC) concentrations of ESHA filtrates in reoxidation experiments in the presence of aluminum oxide (Al_2O_3) and hydrophobic resin DAX-8.
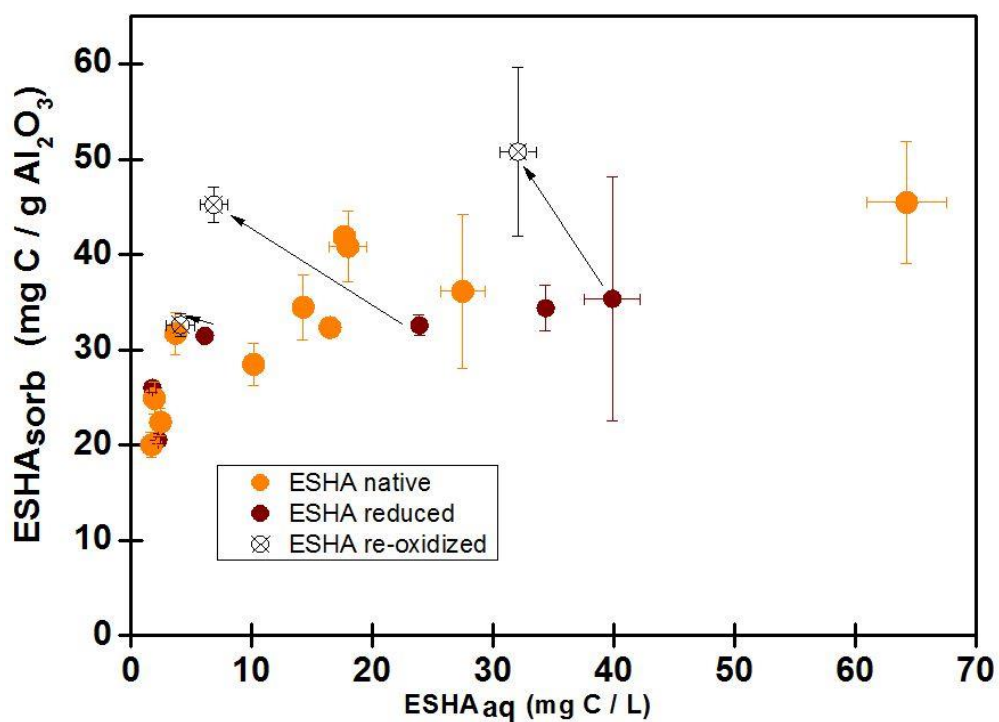
Figure SI10. Sorption isotherms of Elliott Soil Humic Acid (ESHA) at Al_2O_3 (pH=7). Dot colors represent: Orange (●) = native ESHA; dark red (●) = electrochemically reduced ESHA; white crossed line dots (X) = re-oxidized ESHA.

Chapter 3. Preferential sorption of tannin-like compounds onto aluminum oxide trigger changes in the electron exchange capacities of natural organic matter.

Table SI 3. Humic Acids to sorbent ratios in conducted batch sorption experiments conducted on hydrophobic resin (DAX-8) and at aluminum oxide (Al_2O_3) for Elliott Soil (ESHA), Pahokee Peat (PPHA) and Suwannee River (SRHA). Non-sorbed HA (mg $C*L^{-1}$) indicates the carbon concentration in supernatants following sorption (mean ± standard deviation, n at least 4). Sorbed HA corresponds to computed amounts of HA linked to normalized sorbent mass. % of sorbed HA indicates the proportion of HA that remained on the sorbent surface to the total HA amount added in suspension.

| Tested Condition	Ratio HA/sorbent	Non-sorbed HA [mg $C*L^{-1}$]	Sorbed HA [mg $C*g^{-1}$ sorbent]	% sorbed HA
SRHA Stock	-	15 ± 1	-	-
S1-SRHA-DAX-8	1/125	16 ± 1	0.7 ± 0.2	11 ± 3
S2-SRHA-DAX-8	1/250	17 ± 1	1.1 ± 0.3	17 ± 4
S1-SRHA-Al_2O_3	1/12	14 ± 1	6.1 ± 0.8	56 ± 8
S2-SRHA-Al_2O_3	1/25	6 ± 1	8.9 ± 0.7	82 ± 7
S3-SRHA-Al_2O_3	1/50	2.03 ± 0.03	10.1 ± 0.7	94 ± 7
PPHA Stock	-	20 ± 1	-	-
S1-PPHA-DAX-8	1/80	16.5 ± 0.4	2.5 ± 0.4	36 ± 6
S2-PPHA-DAX-8	1/120	13 ± 2	2.7 ± 0.5	38 ± 6
S3-PPHA-DAX-8	1/160	13 ± 1	1.7 ± 0.3	50 ± 7
S4-PPHA-DAX-8	1/240	11 ± 1	1.7 ± 0.2	56 ± 7
S1-PPHA-Al_2O_3	1/12.5	17.3 ± 0.4	11.3 ± 0.3	51 ± 3
S2-PPHA-Al_2O_3	1/25	5 ± 1	10.0 ± 0.6	85 ± 5
S3-PPHA-Al_2O_3	1/50	2.0 ± 0.1	6.1 ± 0.3	96 ± 4
ESHA Stock	-	20	-	-
S1-ESHA-DAX-8	1/80	14.5 ± 0.8	3.8 ± 0.2	50 ± 2
S2-ESHA-DAX-8	1/160	11.8 ± 0.9	3.0 ± 0.2	59 ± 3
S1-ESHA-Al_2O_3	1/3	41 ± 2	54 ± 6	28 ± 3
S2-ESHA-Al_2O_3	1/6	21 ± 1	38 ± 1	62 ± 1
S3-ESHA-Al_2O_3	1/9	18 ± 1	47 ± 2	68 ± 2
S4-ESHA-Al_2O_3	1/12	16 ± 1	32 ± 1	71 ± 1
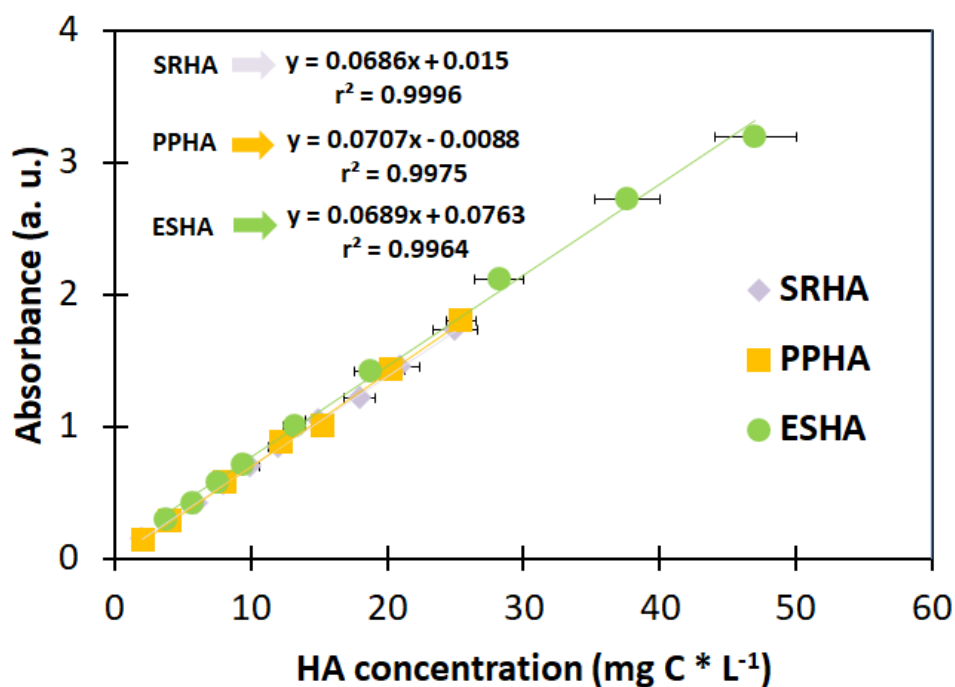
Figure SI11. Calibration curves for measurement of Total Organic Carbon (TOC) using UV-Vis spectroscopy at 254 nm of humic acid standards at pH 7: Suwanee River (SRHA, purple diamonds), Pahokee Peat (PPHA, yellow squares) and Elliott Soil (ESHA, green circles).

Table SI4. DOC results for HA stock solutions and 0.45 µm filtered HA fraction after sorption using pre-acidification elemental analysis method with TOC analyzer and UV-Vis spectroscopy at 254 nm. $SUVA_{254}$ was calculated from UV-Vis absorbance at 254 nm and DOC measured with TOC analyzer. Ratio HA/Al_2O_3 indicates the fraction of HA and Al_2O_3 in the suspension. % sorbed HA indicates the amount of HA that remained bound to aluminum oxide surface after 0.45 µm filtration.

Sample	Ratio HA/Al_2O_3	% sorbed HA	DOC TOC analyzer [mg C/L]	DOC UV-VIS 254 nm [mg C/L]	$SUVA_{254}$ [a. u.]
ESHA	-	-	3.8 ± 0.2	-	7.9 ± 0.5
S1-ESHA-Al₂O₃	1/3	20 ± 7	34 ± 1	33.9 ± 0.5	7.4 ± 0.3
S2-ESHA-Al₂O₃	1/5	35 ± 8	27 ± 2	29.7 ± 0.4	8.0 ± 0.6
S3-ESHA-Al₂O₃	1/10	66 ± 8	14.2 ± 0.7	16.1 ± 0.3	8.4 ± 0.4
S4-ESHA-Al₂O₃	1/15	91 ± 9	3.7 ± 0.4	2.8 ± 0.2	6.5 ± 0.7
S5-ESHA-Al₂O₃	1/20	95 ± 9	1.9 ± 0.5	2.0 ± 0.2	9 ± 2
S6-ESHA-Al₂O₃	1/25	96 ± 9	1.7 ± 0.3	BQL	0.4 ± 0.1
PPHA	-	-	4.1 ± 0.2	-	7 ± 1
S1-PPHA-Al₂O₃	1/12	57 ± 8	17.3 ± 0.4	17.2 ± 0.5	7 ± 2
S2-PPHA-Al₂O₃	1/25	82 ± 9	5 ± 1	4.1 ± 0.1	3.4 ± 0.8
S3-PPHA-Al₂O₃	1/50	94 ± 9	1.5 ± 0.1	0.4 ± 0.3	5 ± 2
SRHA	-	-	4.0 ± 0.3	-	7.4 ± 0.5
S1-SRHA-Al₂O₃	1/12	51 ± 3	14 ± 1	12.6 ± 0.1	7.2 ± 0.7
S2-SRHA-Al₂O₃	1/25	85 ± 5	6 ± 1	4.7 ± 0.1	7 ± 1
S3-SRHA-Al₂O₃	1/50	96 ± 4	2.03 ± 0.03	0.3 ± 0.1	13 ± 4

Table SI5. Computed averages values of C, H, N, O, S, O/C, H/C, DBE, mass-to-charge (m/z) based upon intensity-weighted averages of mass peaks of adsorbed molecules as generated from negative electrospray 12T FTICR mass spectra.

| Member of molecular series	Compounds			Average (%)					Computed				Average DBE, intensity weighted	Average mass, intensity weighted
	CHO-	CHOS-	CHNO-	H	C	O	N	S	O/C ratio	H/C ratio	O/N ratio	O/S ratio		
SRHA DAX-8 (89%)	390 (61.1%)	124 (19.4%)	124 (19.4%)	41.3	39.8	18.2	0.3	0.3	0.5	1.0	65.3	55.2	11	462
SRHA DAX-8 (83%)	418 (60.6%)	136 (19.8%)	134 (19.5%)	39.1	40.2	20.2	0.3	0.3	0.50	1.0	73.8	59.9	12	470
SRHA Al$_2$O$_3$ (43%)	919 (64.4%)	214 (15.0%)	294 (20.6%)	34.3	41.7	23.5	0.3	0.2	0.6	0.8	79.6	105.2	14	497
SRHA Al$_2$O$_3$ (6%)	1199 (65.5%)	265 (14.5%)	367 (20.0%)	34.1	41.3	24.2	0.2	0.3	0.6	0.8	129.3	95.5	12	430
PPHA DAX (62%)	293 (40.5%)	217 (30.0%)	213 (29.5%)	50.7	35.2	12.7	0.6	0.9	0.4	1.4	23.0	14.3	5	345
PPHA DAX-8 (43.5%)	340 (44.9%)	210 (27.7%)	208 (27.4%)	50.2	35.4	13.0	0.5	0.8	0.4	1.4	24.5	16.1	6	350
PPHA Al$_2$O$_3$ (49%)	266 (38.7%)	199 (29.0%)	222 (32.3%)	44.7	37.3	16.6	0.7	0.8	0.4	1.2	23.5	21.0	8	372
PPHA Al$_2$O$_3$ (4%)	444 (46.8%)	184 (19.4%)	321 (33.8%)	41.5	38.4	18.5	0.6	1.0	0.5	1.1	31.9	18.5	8	367
ESHA DAX-8 (50.5%)	155 (44.3%)	111 (31.7%)	84 (24.0%)	52.2	33.9	12.8	0.4	0.6	0.4	1.5	33.4	20.1	4	332
ESHA DAX-8 (41.4%)	180 (46.0%)	124 (31.7%)	87 (22.3%)	53.0	33.9	12.0	0.3	0.7	0.4	1.6	36.3	16.5	4	329
ESHA Al$_2$O$_3$ (72%)	250 (54.9%)	90 (19.8%)	115 (25.3%)	43.1	38.4	17.6	0.5	0.4	0.5	1.1	33.8	44.7	8	356
ESHA Al$_2$O$_3$ (37.5%)	306 (56.7%)	118 (21.9%)	116 (21.5%)	42.7	38.3	17.9	0.4	0.7	0.5	1.1	46.8	24.8	8	349
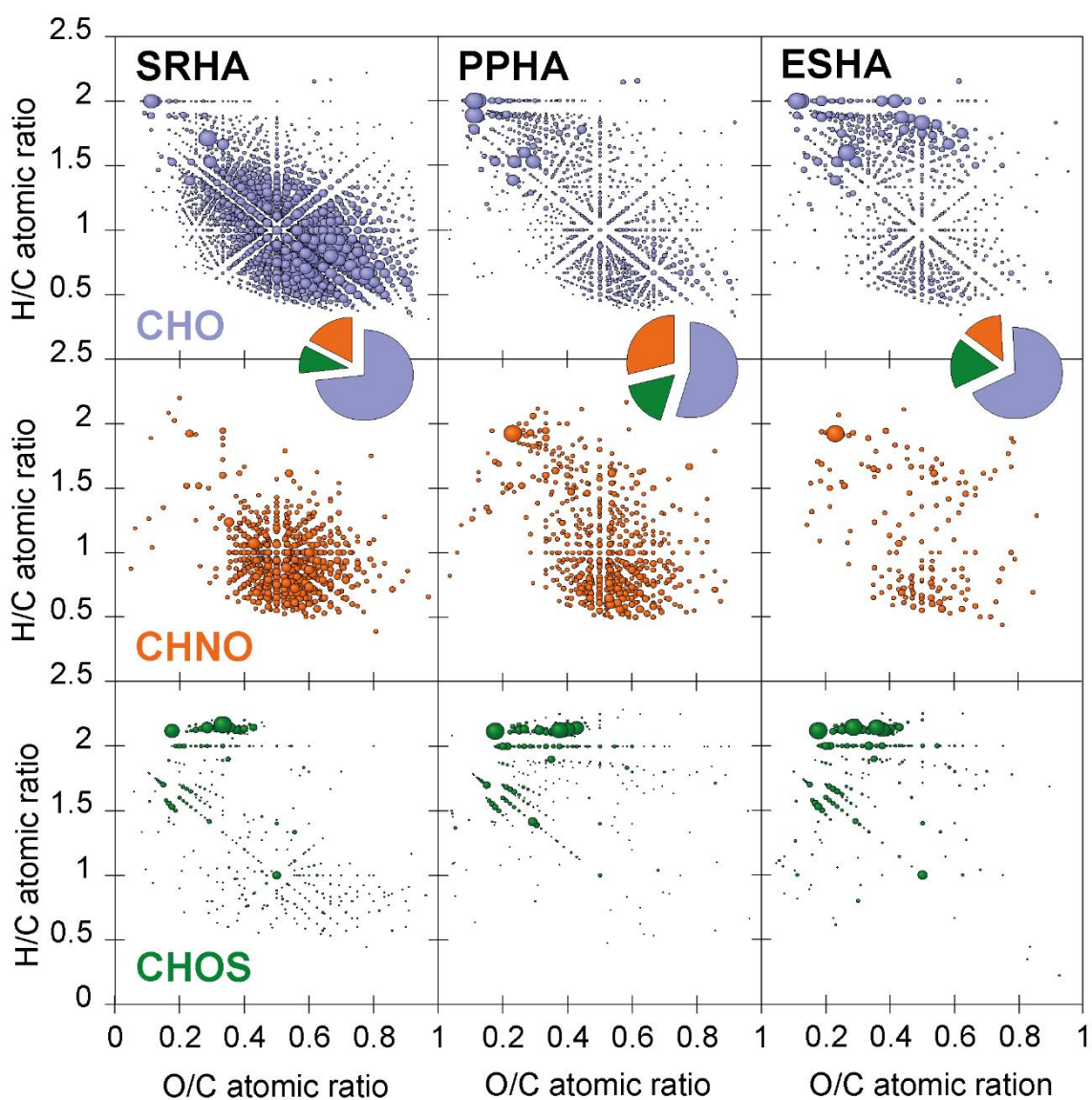
Figure SI12. Van Krevelen diagrams of the assigned molecular series (i.e., CHO, CHNO and CHOS) of Suwannee River Humic Acid (SRHA), Pahokee Peat Humic Acid (PPHA) and Elliott Soil Humic Acid (ESHA) standard samples. Bubble Color for elemental compositions bearing combinations of C, H, O, N, and S atoms relates to: blue (CHO), orange (CHON), green (CHOS). Bubble areas reflect the relative intensities of each mass peak in the sample.
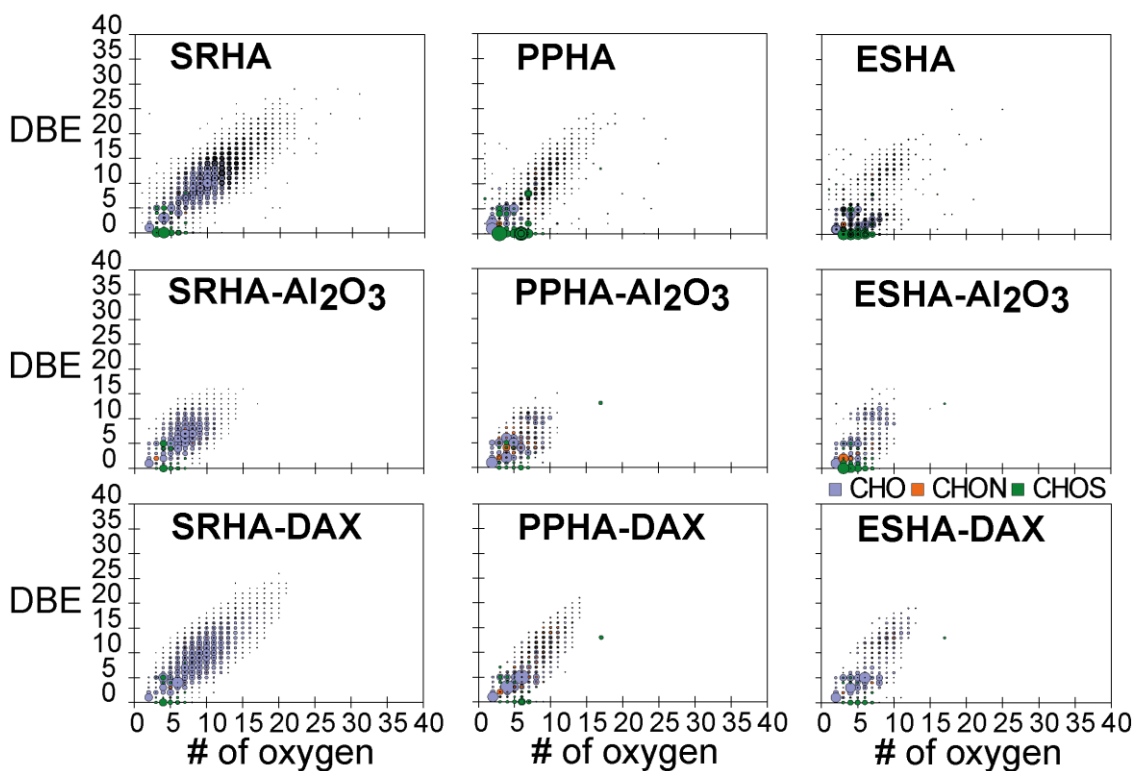
Figure SI13. Display of double bond equivalents (DBE) vs. number (#) of oxygen atoms in molecules of Elliott Soil (ESHA), Pahokee Peat (PPHA) and Suwannee River (SRHA) stock solutions (top row), 0.45 µm non-sorbed fraction after sorption at aluminum oxide (Al_2O_3, medium row) and hydrophobic resin (DAX-8, bottom row). Bubble Color for elemental compositions bearing combinations of C, H, O, N, and S atoms relates to: blue (CHO), orange (CHNO), green (CHOS). Bubble areas reflect the relative intensities of each mass peak in the sample.
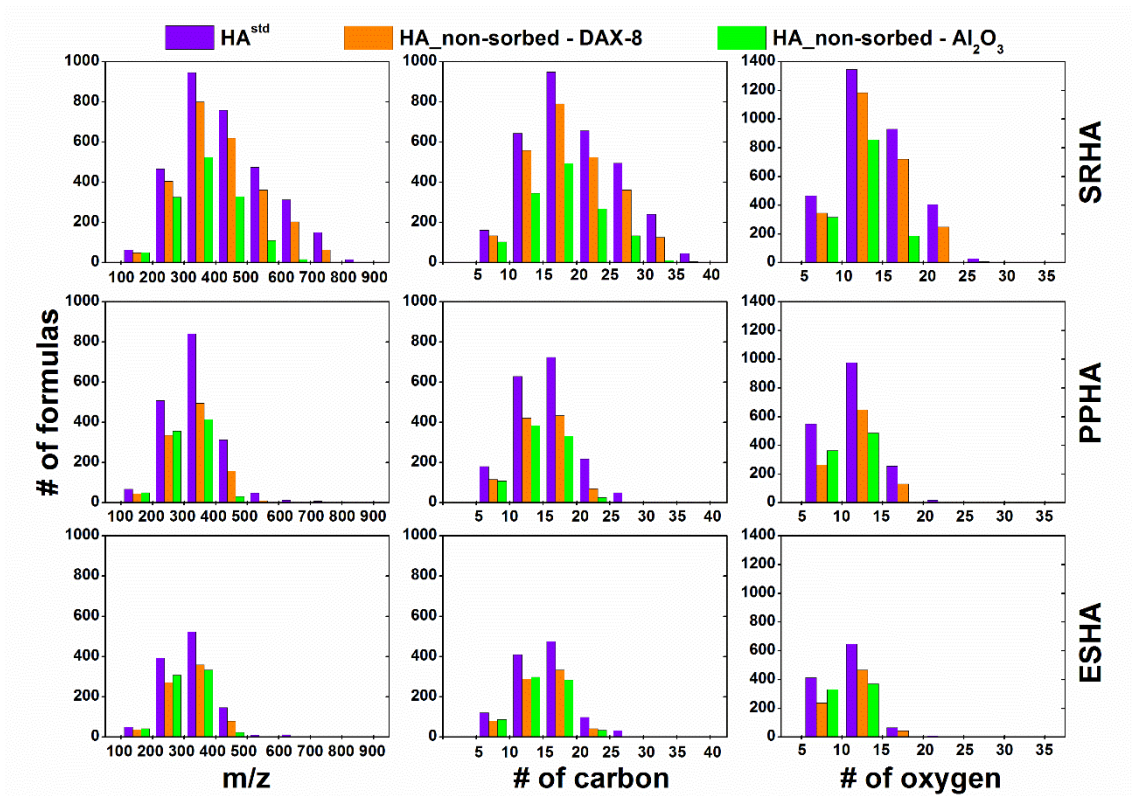
Figure SI14. Histogram with counts of: a) m/z, b) carbon and c) oxygen atoms for Elliott Soil (ESHA), Pahokee Peat (PPHA) and Suwannee River (SRHA) stock solutions (purple bars) and 0.45 µm filtered supernatant fractions following sorption at hydrophobic resin (DAX-8, orange bars) and at aluminum oxide (Al₂O₃, green bars).
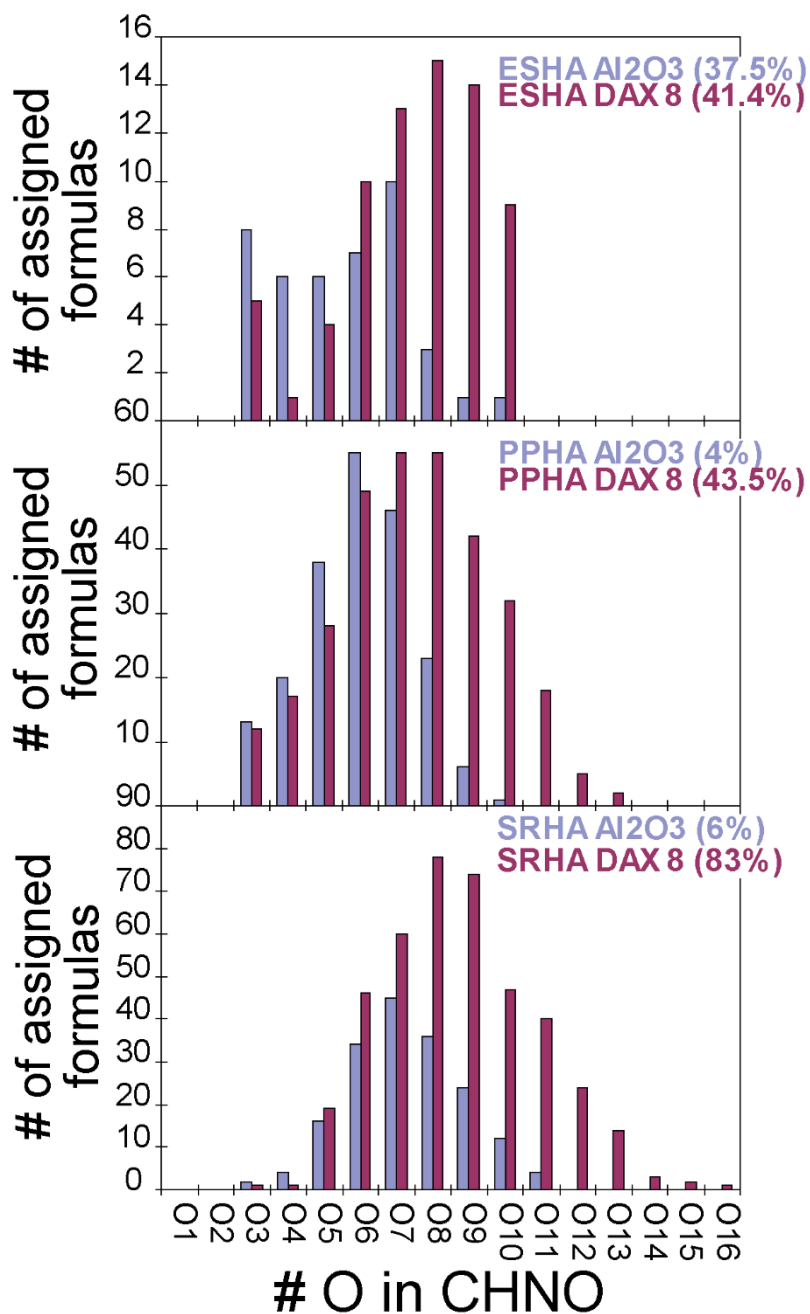
Figure SI15. Counts of oxygen atoms involved in non-sorbed CHNO-molecules when comparing pairs of samples separately.
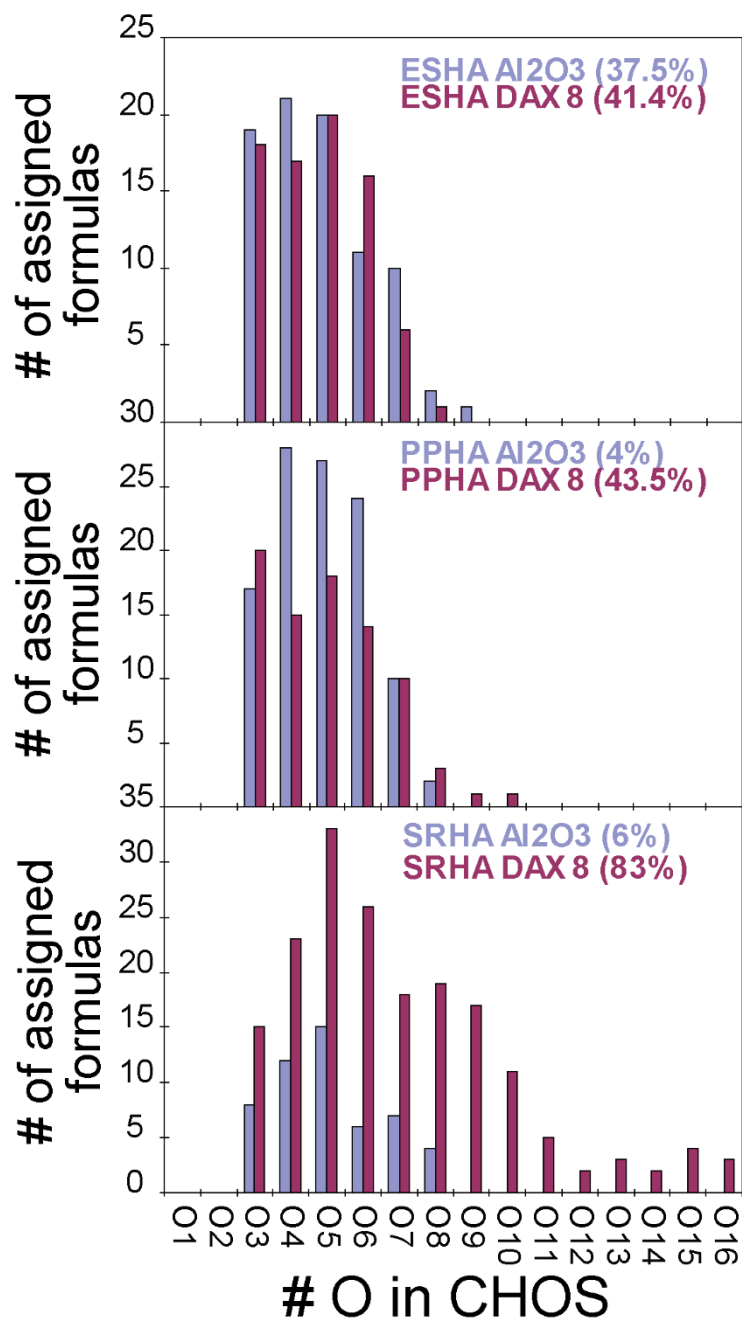
Figure SI16. Counts of oxygen atoms involved in non-sorbed CHOS-molecules when comparing pairs of samples separately.
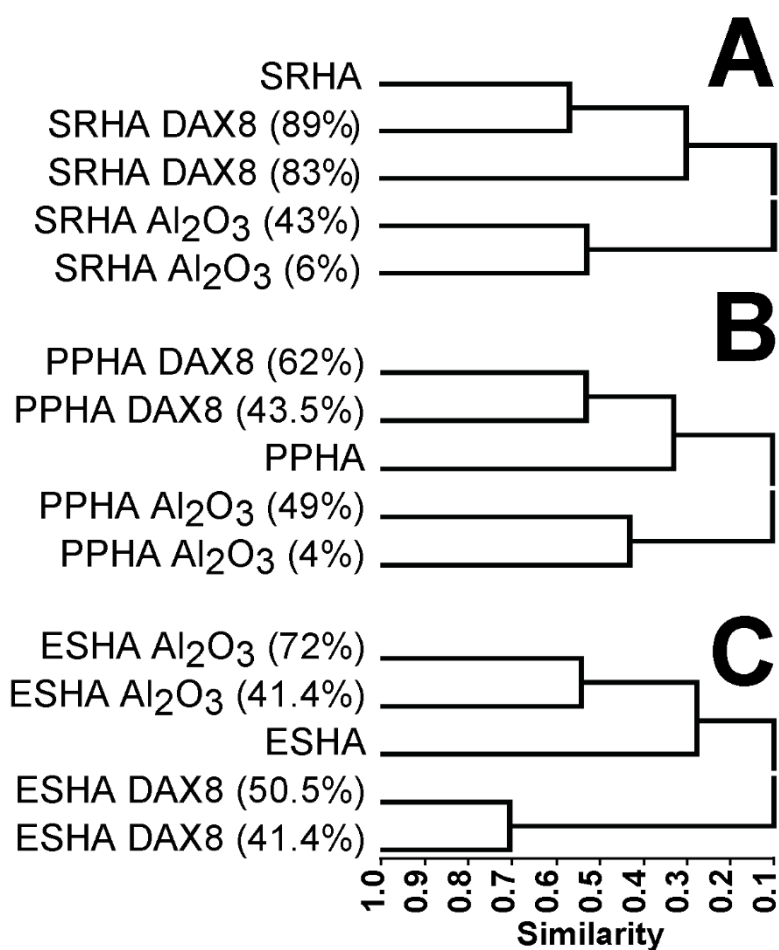
Figure SI17. Negative electrospray 12T-FTICR mass spectra of the original samples and non-sorbed molecular compositions for Suwannee River Humic Acid (SRHA), Pahokee Peat Hunic acid (PPHA) and Elliott Soil Humic acid (ESHA) samples using DAX8, Al_2O_3. The Clustering diagram based on the similarity values between the spectra of the samples using Pearson's correlation coefficient.

Chapter 4. Electron Exchange Capacities of Humic Acid Sorbed to Redox Active Clays.
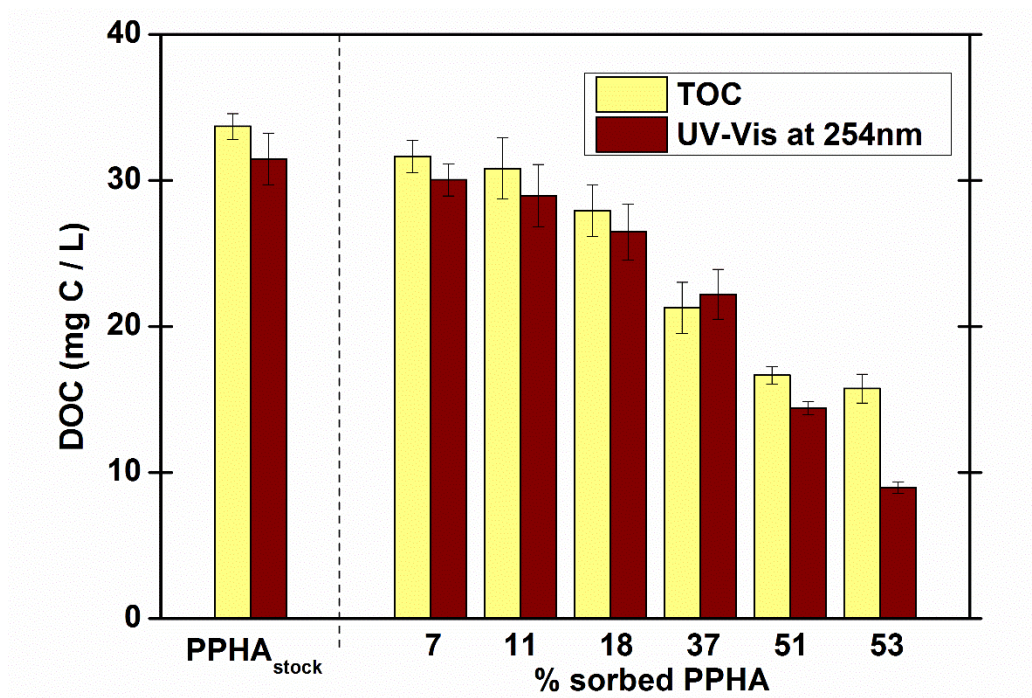

Figure SI18. Dissolved Organic Carbon (DOC) results for PPHA stock solution (PPHA$_{stock}$) and PPHA filtrates (0.45 µm filtered HA fraction after sorption) using with TOC analyzer and UV-Vis spectroscopy at 254 nm. For PPHA filtrates, data was arranged is ascending sorption level.
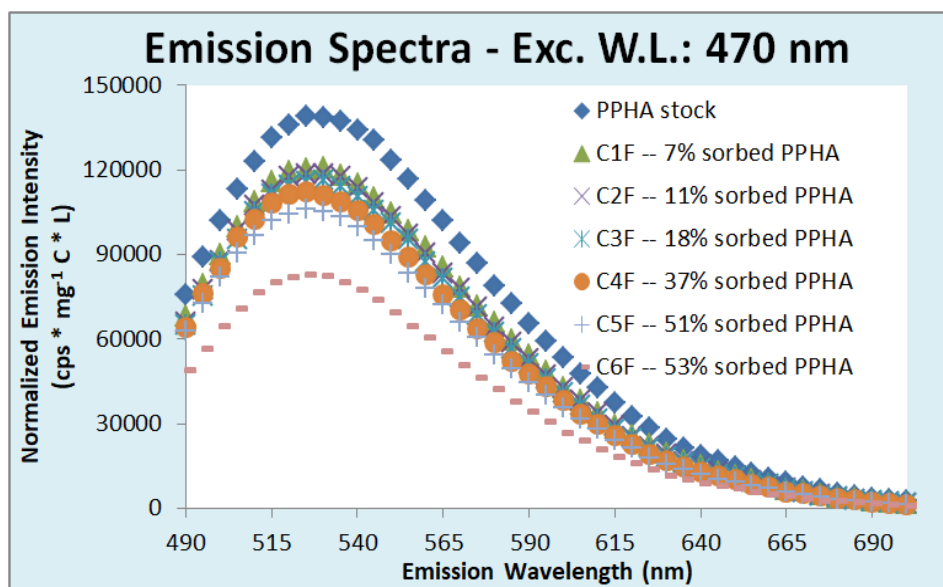
Figure SI19. DOC normalized Emission Intensity at set excitation wavelength (470 nm) of Pahokee Peat humic acid solution (PPHA$_{stock}$) and PPHA left in aqueous phase after sorption to Na-montmorillonite.
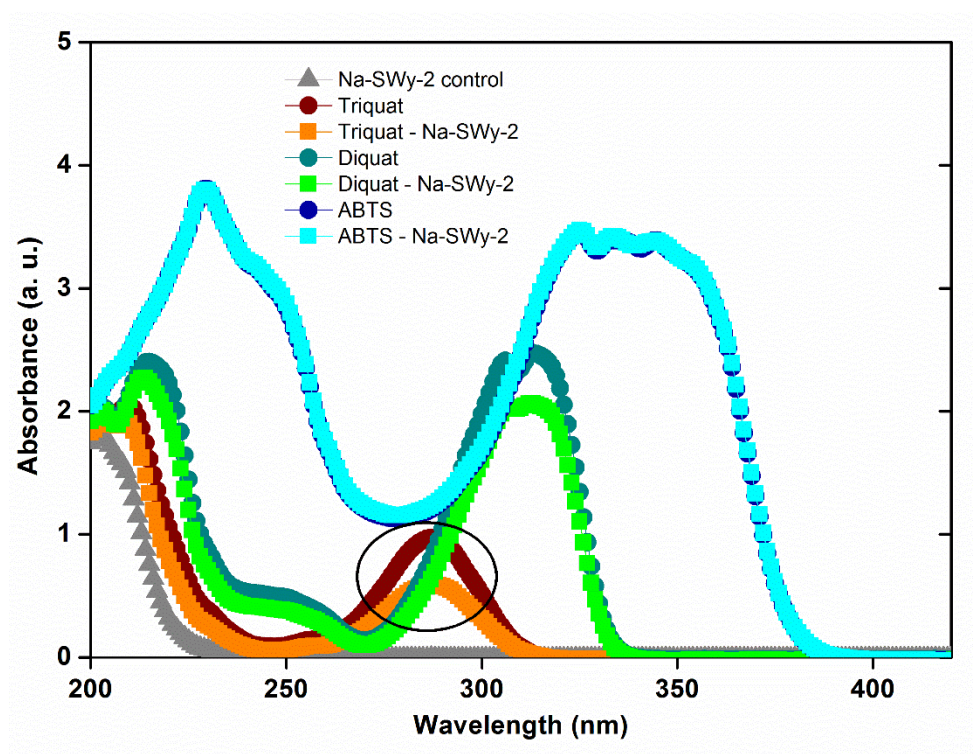

Figure SI20. UV-Vis absorption spectra of the electron transfer mediators used in the presence and absence of NA-montmorillonite (Na-SWy-2) to evaluate the degree of adsorption of the mediators using similar conditions as in mediated electrochemical reduction (MER) and oxidation (MEO) techniques.
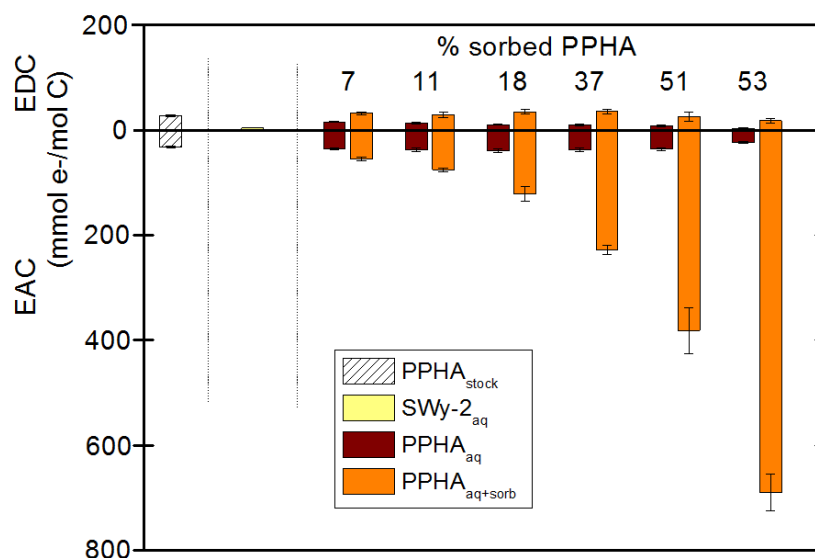
Figure SI21. Electron Donating Capacities (EDC, E_H(pH 7) = 0.61 V vs. SHE.) and Electron Accepting Capacities (EAC, E_H(pH 7) = - 0.49 V vs. SHE.) normalized to organic carbon content as a function of percentage of sorbed humic acid of Pahokee Peat Humic Acid (PPHA) upon sorption to Na-rich Montmorillonite (SWy-2). PPHA stock solutions (PPHA$_{stock}$, white crossed-lined bars), 0.45 µm filtrate of Na-SWy-2 suspension (SWy-2$_{aq}$, light yellow bars), aqueous PPHA fraction after sorption equilibrium (PPHA$_{aq}$; 0.45 µm filtrate of the suspension containing; dark red bars) and the whole suspensions containing Na-SWy-2 and PPHA (PPHA$_{aq+sorb}$, orange bars).
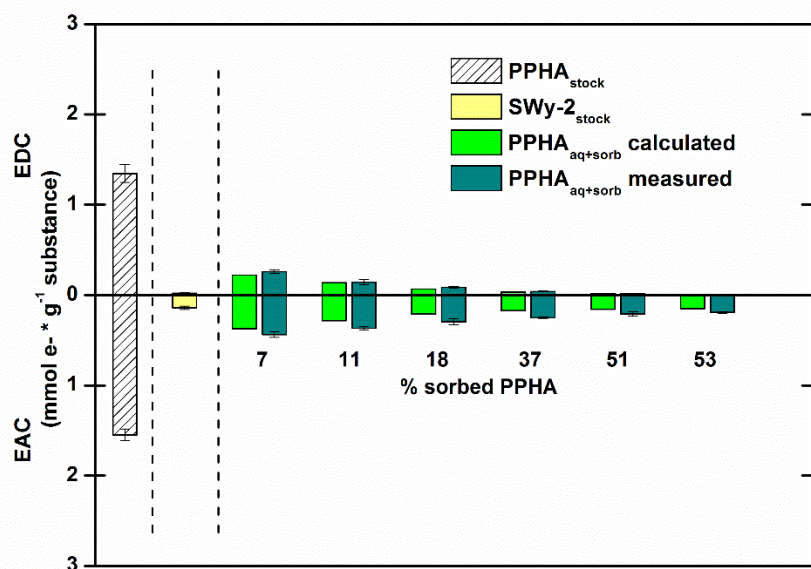

Figure SI22. Electron Donating Capacities (EDC, E_H(pH 7) = 0.61 V vs. SHE.) and Electron Accepting Capacities (EAC, E_H(pH 7) = - 0.49 V vs. SHE.) of PPHA stock solutions (PPHA$_{stock}$), Na-SWy-2 stock suspension (SWy-2$_{stock}$), measured for whole suspensions containing Na-SWy-2 and PPHA (PPHA$_{aq+sorb}$ measured); and calculated for whole suspensions (PPHA$_{aq+sorb}$ calculated) from individual contributions from PPHA and SWy-2 in the sorption batch (without accounting for electron transfer reactions or other effects upon sorption) and measured with mediated electrochemical oxidation and reduction.

Statement of personal contribution

In Chapter 2, the experiments were designed and organized by ES, OS and SH. Occasional advice was given by MS. Experiments and detailed data analysis was conducted by ES. Discussion of results was performed by ES, OS and SH. The manuscript was prepared by ES, together with OS and SH. MS provided useful review of the manuscript.

In Chapter 3, the sorption experiments were designed and organized by ES, OS and SH. ES and SH. Sorption Experiments and detailed data analysis was conducted by ES. Discussion of sorption results was performed by ES, OS and SH. Dr. Mourad Harir (MH, Helmholtz Zentrum München) and ES carried out solid phase extractions for FT-ICRMS measurements. MH performed FT-ICRMS acquisitions. Detailed FT-ICTMS data analysis and discussion was performed by MH and ES. The manuscript was prepared by ES, together with MH, OS and SH. Dr. Norberth Hertkorn (NH, Helmholtz Zentrum München) provided useful review of the manuscript.

In Chapter 4, the experiments were designed and organized by ES, OS and SH. Occasional advice was given by MS. Experiments and detailed data analysis were conducted by ES. Discussion of results was performed by ES, OS and SH. The manuscript was prepared by ES, together with OS and SH.

Curriculum vitae

Personal information

Family Name, Given Name	Subdiaga Rondon, Edisson Reinaldo
Birth place / Date	Tovar, Venezuela / March 25th, 1988
Current Address	Holbeinweg 2 - UG, 72076 - Tübingen
E-mail address	edissonsubdiaga@yahoo.com
Phone number	+4915776445424

Education Experience

Since 10.2014	PhD Candidate Eberhard Karls Universität Tübingen Center for Applied Geosciences Environmental Mineralogy and Chemistry Research Group Tübingen - Germany
07.2011 - 08.2014	Product Researcher Female Care Department. Procter & Gamble S.A. Caracas - Venezuela
09.2006 – 07.2012	Licenciado en Química (Roughly equivalent to Degree in Chemistry) University of Los Andes, Faculty of Sciences Merida - Venezuela

Scientific Publications

Hagemann, N.; **Subdiaga, E.**, Orsetti, S.; de la Rosa, J. M.; Knicker, H.; Schmidt, H. P.; Kappler, A.; Behrens, S. Effect of biochar amendment on compost organic matter composition following aerobic compositing of manure. *Sci. Total Environ*, **2018**, 613-614, 20-29.

Hagemann, N.; Joseph, S.; Schmidt, H.P.; Kammann, C.I.; Harter, J.; Borch, T.; Young, R.B.; Varga, K.; Taherymoosavi, S.; Elliott, K.W.; McKenna, A.; Albu, M.; Mayrhofer, C.; Obst, M.; Conte, P.; Dieguez-Alonso, A.; Orsetti, S.; **Subdiaga, E.**; Behrens, S.; Kappler, A. Organic coating on biochar explains its nutrient retention and stimulation of soil fertility. *Nat. Commun.*, **2017**, 8, 1089.

Conferences Attended

2018	Goldschmidt conference, Boston, August 2018 (Oral) Gordon Research Conference: Organic Geochemistry, New Hampshire, July 2018 (Poster) Interfaces Against Pollutants, June 2018 (Oral)
2017	Goldschmidt conference, Paris, August 2017 (Poster) ICCE, Oslo, June 2017 (Oral)
2016	International Conference of International Humic Substances Society. Kanazawa, September, 2016 (Oral) - **Student Travel Award** European Geoscience Union, April 2016 (PICO)